Conceptual Design of a Thermal Control System for an Inflatable Lunar Habitat Module

Submitted to:

John Thornborrow
Thermal Systems Engineer

NATIONAL AERONAUTICS AND SPACE ADMINISTRATION
UNIVERSITIES SPACE RESEARCH ASSOCIATION

Prepared by:

Ketan Gadkari
Sanjay K. Goyal
Joseph Vanniasinkam, Team Leader

Mechanical Engineering Design Projects Program
THE UNIVERSITY OF TEXAS AT AUSTIN
Austin, Texas

Fall, 1991

Acknowledgements

The design team would like to thank Mr. John Thornborrow for providing advice and material for this project. We would also like to thank our faculty advisor, Dr. John Howell, for his technical guidance throughout the semester. The team also thanks Mr. Hank Kleespies, our teaching assistant, for helping us keep up with this course. Thanks also goes to Mr Bert Herigstad for his administrative help. We would also like to thank Mr. Wendell Deen, for helping us improve our graphics. Finally, the design team would like to thank Dr. Steven Nichols for giving us the opportunity to work as a team on this project.

Executive Summary

Conceptual Design of a Thermal Control System for an Inflatable Lunar Habitat Module

NASA is considering the establishment of a manned lunar base within the next few decades. To house and protect the crew from the harsh lunar environment, a habitat is required. A proposed habitat is an spherical, inflatable module. Heat generated in the module must be rejected to maintain a temperature suitable for human habitation. This report presents a conceptual design of a thermal control system for an inflatable lunar module. The design solution includes heat acquisition, heat transport, and heat rejection subsystems.

The report discusses alternative designs and design solutions for each of the three subsystems mentioned above. Alternative subsystems for heat acquisition include a single water-loop, a single air-loop, and a double water-loop. The vapor compression cycle, vapor absorption cycle, and metal hydride adsorption cycle are the three alternative transport subsystems. Alternative rejection subsystems include flat plate radiators, the liquid droplet radiator, and reflux boiler radiators. Feasibility studies on alternatives of each subsystem showed that the single water-loop, the vapor compression cycle, and the reflux boiler radiator were the most feasible alternatives.

The design team combined the three subsystems to come up with an overall system design. Methods of controlling the system to adapt it for varying conditions within the module and in the environment are presented. Finally, the report gives conclusions and recommendations for further study of thermal control systems for lunar applications.

Table of Contents

List of Figures

List of Figures (continued)

List of Tables

I. Introduction

Following the success of the manned space flight program, one of the next goals of the National Aeronautics and Space Administration (NASA) is to establish a manned lunar base. To achieve this goal, NASA has tasked space system contractors and consultants to investigate various scenarios for the establishment of this base. The Universities Space Research Association (USRA) is one such consultant.

USRA is a consortium of 45 universities established by the National Academy of Sciences [1]. In conjunction with NASA, USRA has established the NASA/USRA University Advanced Design Program. There are three primary goals of this program. First, to foster engineering design education in US universities. Second, to supplement NASA's in-house advanced mission efforts. Finally, to promote interest among engineering students in the space program.

Through the Mechanical Engineering Design Projects Program at The University of Texas at Austin, USRA and NASA have suggested several design projects for the manned lunar base. One suggested project for the Fall 1991 semester is the design of a Thermal Control System (TCS) for an Inflatable Lunar Habitat Module. This report presents a conceptual design of this system.

This report contains four main sections. First, background information on the lunar mission and design problems associated with

thermal control on the lunar surface are discussed. The design criteria, project requirements, and design methodology are also presented in this section. In the second section, alternative designs for subsystems of the TCS are presented. The third section contains the feasibility study and decision matrices employed to select the best alternative design for each component of the TCS. In the final section of the report, a conceptual design solution of the TCS is presented .

1.1 Background Information

1.1.1 Manned Lunar Base Mission. NASA has a long range goal of constructing a fully equipped, manned lunar base on the near side of the moon by the year 2015. The proposed lunar outpost mission will consist of three phases: emplacement, consolidation, and utilization. The emplacement phase, to be completed by the year 2003, places a habitat with one year life support capabilities on the moon. Along with the initial habitat, the emplacement phase delivers laboratories, airlocks, and any required life support systems. The consolidation phase, to be completed by 2010, will expand the existing habitat. The expanded habitat will contain crew quarters, science laboratories, medical facilities, and other facilities necessary for long duration missions. Finally, in the utilization phase, crew members will conduct experiments on the moon [2].

NASA has proposed the use of a spherical, inflatable module for the habitat [3]. Various designs for this module have been suggested. One such design is shown in Figure 1. This module is divided into five levels. Each level is designated for specific activities. About one-third of the

module is buried in the lunar surface and the rest is covered with a radiation shield. The radiation shield is made of lunar soil called regolith [2]. Apart from protecting the inhabitants from harmful cosmic radiation, the shield acts as a means of passive thermal control. Heat transfer between the module and the environment is minimized by the shield. Consequently, a TCS is required to reject the heat generated within the module by crew and equipment.

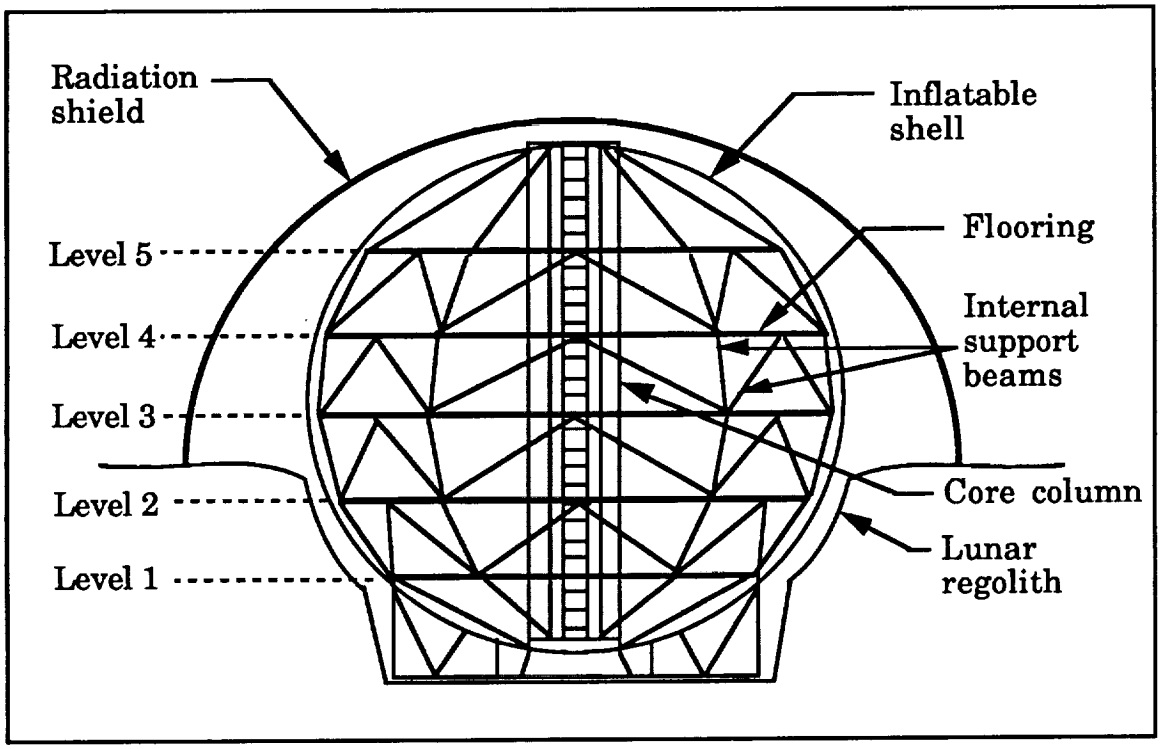

Figure 1. Inflatable Lunar Habitat Module [3].

1.1.2 Lunar Environment. The conditions of the lunar environment are more extreme than the conditions on earth. Some of the major characteristics of the lunar environment that hinder the design of a TCS

are presented below. Most sites of interest for the location of the base are located near the equator. Therefore, these characteristics are for sites close to the lunar equator [4].

1. The diurnal cycle of the moon is about 29.5 earth days.
2. The temperature of the lunar surface is about 111°C at midday and -171°C at night.
3. There exists a rarified atmosphere (200,000 atoms per cubic centimeter) on the moon whereas a dense atmosphere rich in oxygen exists on the earth. Due to this rarified atmosphere, the maximum solar irradiation on the lunar surface is 1371 W/m^2, as compared to 1000 W/m^2 on the surface of the earth.
4. The albedo (the percentage of solar irradiation reflected) of the lunar surface is about 7% whereas the albedo of the earth is about 34%.
5. The gravity on the moon is 1/6 of the gravity on earth.
6. The lunar soil (regolith) has very low thermal conductivity (between 0.7 and 1.5 mW/mK) and it is in the form of a fine powder for the first 3 centimeters of the lunar surface. Due to these fine regolith particles, there is a constant presence of lunar dust.
7. The lunar surface is subjected to micrometeorite impacts.

1.2 Design Problems

The characteristics of the lunar environment place some unique demands on a thermal control system for a lunar habitat. During the 14

earth-day-long lunar day, heat rejection to the environment is a major problem. Conduction to the lunar soil is one possible method of rejecting the heat. However, due to the low thermal conductivity of the lunar soil, conduction is an inefficient process of heat rejection. Due to the presence of a vacuum, heat rejection by convection is impossible. Thus, thermal radiation is the only mode of heat transfer to the environment. However, radiation to the environment is also a problem. On the moon the radiator must face either the sun, the lunar surface, or both. Consequently, the temperature of the thermal sink is higher than the temperature of the heat to be rejected. Moreover, due to extreme variation in lunar temperature, the thermal system must reject heat to a sink with a widely varying temperature.

Another major concern is the lunar dust kicked up during engine blasts and surface operations. The dust coats radiator surfaces and seriously degrades their emissive properties [4]. Also, the design of the radiators is affected by micrometeorite activity.

Due to the high cost of transporting equipment to the moon, the TCS must be designed such that its mass, volume, and power consumption are minimized. The criteria for designing the TCS in a manned area are significantly more stringent than those for unmanned modules or payloads. There are strict redundancy, health, and safety requirements that must be observed. For example, ammonia is not an acceptable working fluid for the manned areas because it is toxic. Water is the only known working fluid acceptable for manned areas [4].

1.3 Project Requirements

The design of the TCS is divided into three subsystems based on function: heat acquisition, heat transport, and heat rejection. The first project requirement is the design of a subsystem that acquires the excess heat load. Alternative mediums of heat removal must be investigated. The next requirement is the design of a subsystem that transports the heat load to a location where it can be rejected. Finally, a subsystem to reject the heat to either the environment or the lunar surface is required.

1.4 Design Criteria

1. The TCS must remove a heat load that varies with time.
2. The mass, volume, and power consumption of the TCS must be minimized.
3. The TCS must be designed for peak thermal loads coincident with end-of-life radiator properties. End-of-life radiator properties refer to the absorptivity and emissivity of the radiator after a specified period of time.
4. The TCS must be designed to reject low temperature waste heat generated within the module to a thermal sink at a temperature of up to 111°C.
5. The working fluids used in manned areas must be non-toxic.
6. The components of the TCS exposed to the lunar environment must be adaptable to lunar dust and micrometeorite impacts.

1.5 Proposed Design Methodology

After defining the problem and identifying the project requirements, the next step in the design process was to select a methodology to meet the project requirements. First, the design team did background research on the problem in order to generate a specification list. Next, the team divided the design into several functions. To satisfy each function, alternative designs of subsystems were created. Along with the alternative designs, a feasibility study was performed on each alternative design. Using the design criteria mentioned earlier as a basis for comparison of the alternatives, decision matrices were used to select the most feasible design of each subsystem. Next, the selected subsystems were combined to satisfy the overall function. Finally, a conceptual design solution was created for the overall system.

1.5.1 Specification List. Since there have been many proposed designs for the inflatable lunar habitat module, the team designed the TCS for a specific module. For example, the size and shape of the module, the power system available, the number of inhabitants, and the type of equipment within the module were determined. Such information was obtained from NASA engineers and references 2 and 5. A thermal energy balance was performed on the module to determine the total heat load to be supplied or removed such that a specified temperature is maintained within the module. Based on this information and the project requirements, a list of specifications was developed. The specification list is presented in Appendix A1.

1.5.2 Function Diagram. A function diagram for the TCS was developed next. The function diagram divides the overall function of the TCS into sub-functions. The functional division of the TCS is shown in Figure 2.

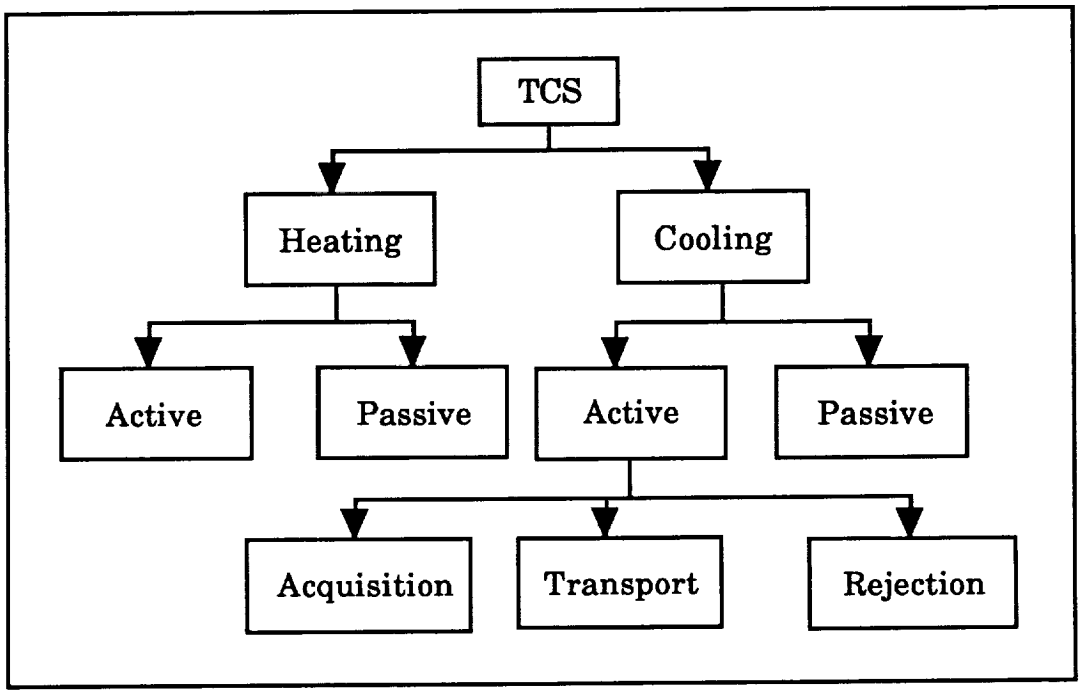

Figure 2. Functional Division of the TCS

1.5.3 Alternative Designs. Alternative designs to satisfy each sub-function were developed next. First, thermal control using passive means was analyzed. Using this analysis, it was possible to estimate the requirements of the active control system.

Alternative designs to satisfy the function of active control were developed next. As shown in Figure 2, active control is divided into two functions - heating and cooling. The cooling function is divided into three

sub-functions - heat acquisition, heat transport, and heat rejection. To achieve heat acquisition and transport, several thermodynamic cycles were investigated. To accomplish the function of heat rejection, radiation to the environment and conduction to the lunar soil were researched.

Next, alternative designs to satisfy each sub-function were developed. By combining the individual designs for each sub-function, alternative designs to satisfy the overall function will be developed. A decision matrix will be used to select the best alternative design.

1.5.4 Design Solution. A conceptual design solution for the chosen alternative design was created next. Detailed calculations were done to specify the performance of the TCS for a wide range of operating conditions. Further aspects of the design, such as the design of a back-up system, were discussed. Finally, recommendations for further work on the design of the TCS were made.

II. Alternative Designs

2.1 Introduction

Before beginning the alternative designs, a specification list was developed. These specifications provide a basis for all calculations performed on the alternative designs. It is assumed that the module is a sphere of diameter 16 m, with eight crew members [2]. For such a module, it was determined that the internal heat load varies from 25 to 50 kW [6]. Since the team is designing for worst case conditions, it is also assumed that the module is located at the lunar equator. Moreover, the TCS is assumed to operate at lunar noon. For these conditions, the thermal control system will be required to remove 50 kW of heat in order to maintain the temperature within the module at 21°C [6].

The design team investigated two means of controlling the temperature: active and passive thermal control. First, the team analyzed passive control. A two meter shield of regolith is to be used to protect the crew from cosmic radiation. As shown in Appendix A2, a two meter radiation shield allows only 0.39 kW of heat out of the module during the lunar night. Since this heat loss is negligible compared to the internal heat load of 50 kW, it was determined that no heating is required. During the lunar noon, the shield only allows 0.18 kW of heat into the module. Therefore, no further passive control was required. Next, the design team investigated active thermal control. As shown in Figure 3, active thermal

control systems are divided into three subsystems: heat acquisition, heat transport, and heat rejection.

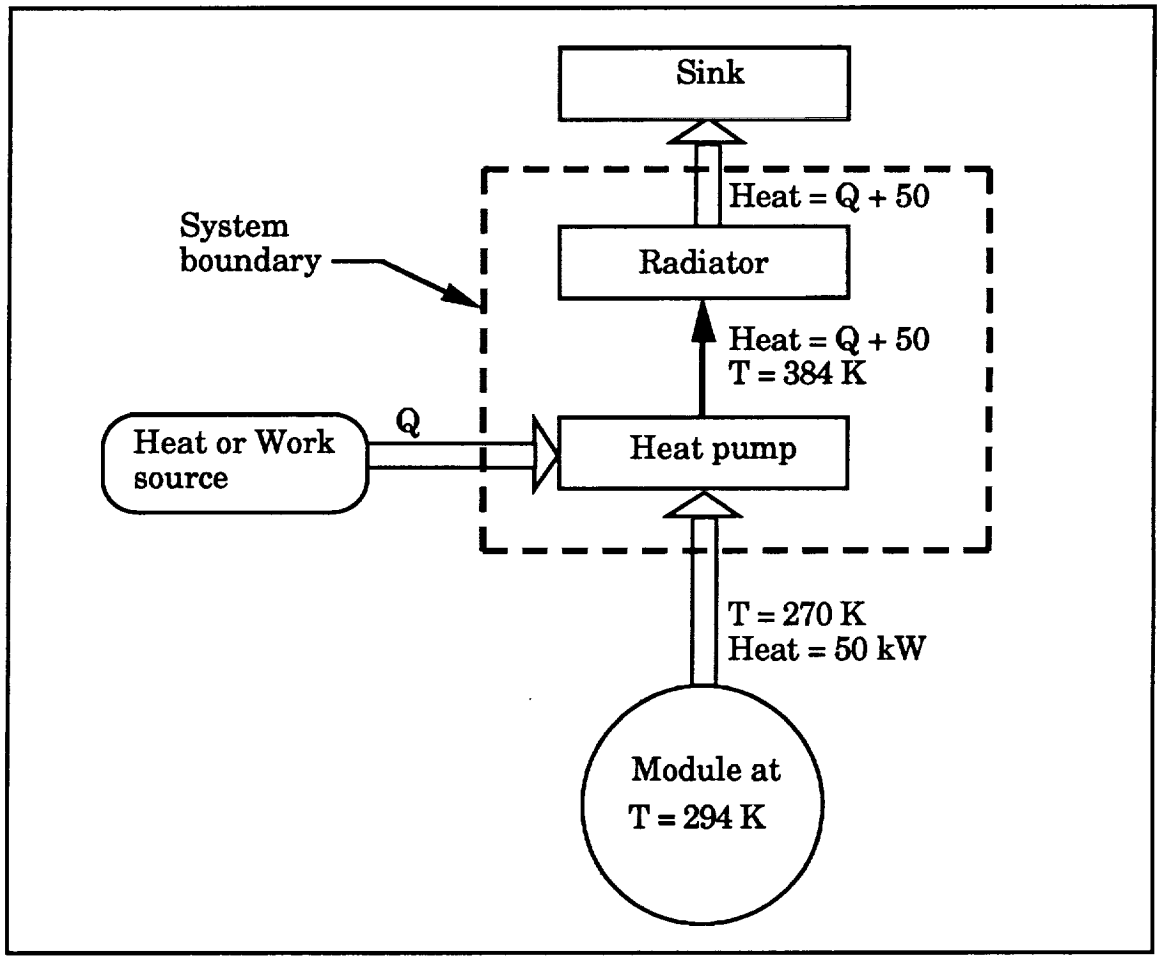

Figure 3. Heat Flow Through the TCS

2.2 Heat Acquisition Systems

The function of the heat acquisition is to absorb the heat generated within the module such that a temperature of 21°C is maintained. This heat must then be transferred to the transport system. A means of

controlling the humidity inside the module is also required. The design team investigated three concepts for acquiring the heat generated by the module and the crew.

2.2.1 Single Air-Loop System. As shown in Figure 4, the single air-loop system consists of an air loop which is used to remove heat directly from the equipment. The air loop is also used to dehumidify the air in the module. To remove heat from the equipment, air is sucked through the equipment racks. The duct carrying this air joins the main duct carrying the return air from the module. The air in the main duct leaves the module and enters a heat exchanger, transferring heat to the working fluid of the transport system. Due to the humidity in the air, some condensation will occur. The condensed water is directed to a storage tank.

The main advantage of this system is that no heat exchangers are required for the purpose of heat acquisiton. However, the mass of this system is very high because a considerably longer network of pipes is required to acquire the same heat load as compared to a water loop. The working fluid of the transport system is toxic and hence cannot be circulated inside the module. Therefore, to transfer heat to the transport system, the air must be transported out of the module. Hence, the power required to operate the blowers is high. It is also difficult to make the system redundant, since the additional set of ducts will greatly increase the mass and volume of the system.

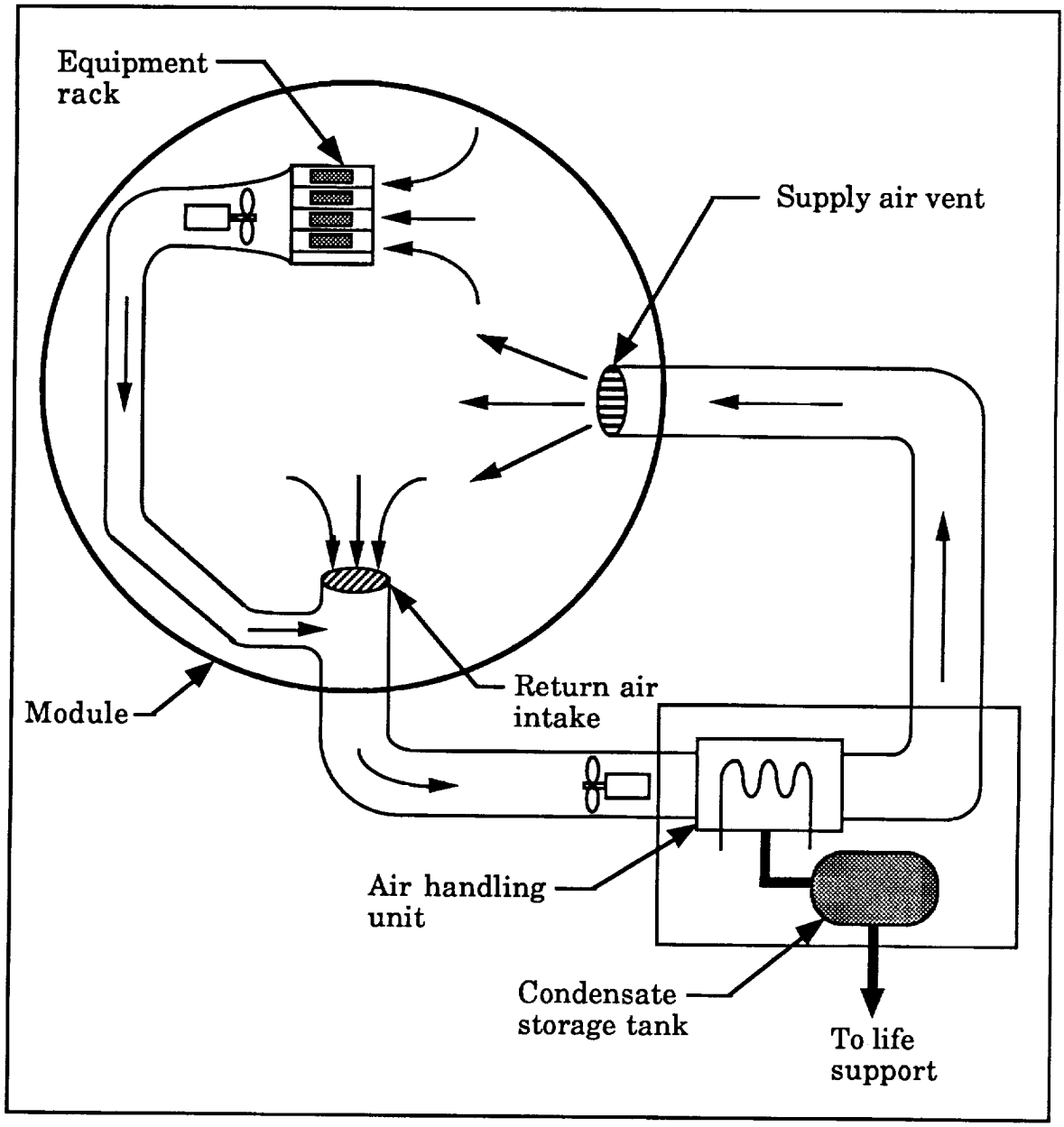

Figure 4. Single Air-Loop Concept

2.2.2 Double Water-Loop System. This system consists of two water loops, as shown in Figure 5. One loop is used to cool and dehumidify the air within the module. The other loop removes heat from the equipment by passing water through cold plates. The cold plates are stainless steel plates

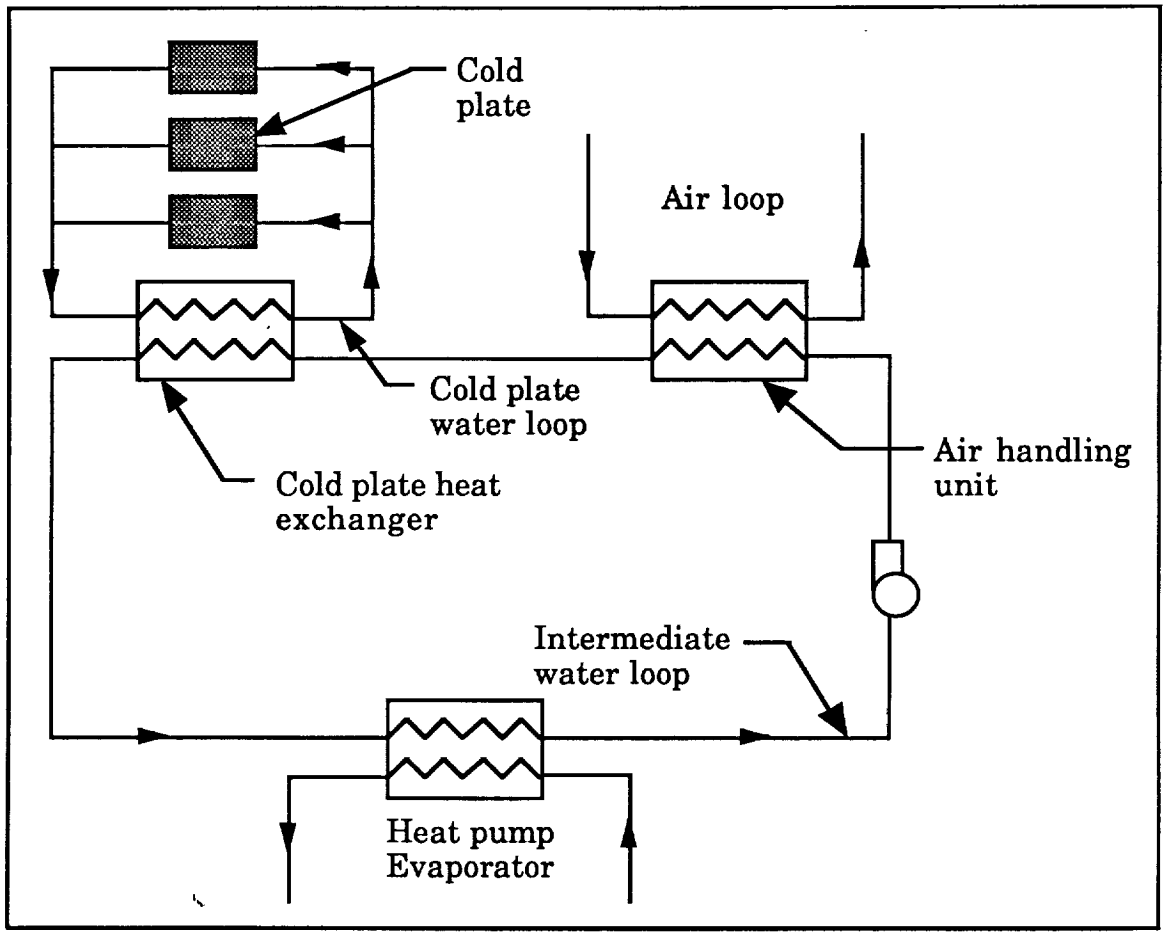

Figure 5. Double Water-Loop Concept

with a thickness of about 0.7 cm. Electronic equipment is mounted on top of these plates, so that the heat generated by the equipment is absorbed by the cold plates. Cold water is passed through the plates and removes the heat absorbed by the cold plates. An intermediate water loop collects heat from the condensing heat exchanger and the cold plate heat exchanger. The heat is then transferred to the working fluid of the transport system. The two-loop system has been proposed for Space Station Freedom. The two loops are at 21°C and 2°C. The 21°C loop cools the equipment, while the 2°C

loop cools the air in the module. Two heat exchangers are required to transfer the heat from the two loops to the working fluid of the transport system.

An advantage of this system is that the heat load is distributed over two loops. If a leak were to occur in one of the loops, part of the heat load will still be removed. However, if the intermediate loop fails, none of the heat load will be removed. Another disadvantage of the system is that its mass is high, because an additional heat exchanger is needed to remove heat from the cold plate loop.

2.2.3 Single Water-Loop System. This system consists of a single pumped water loop travelling through the module, as shown in Figure 6. Chilled water is used to first cool and dehumidify the air and is then pumped through cold plates to remove heat from the equipment. After leaving the cold plates, the heat gained by the water is transferred to the working fluid of the transport system. In a typical single-loop system, water cools the air at 2°C. While cooling the air, the temperature of the water increases. The water is then passed through the cold plates, where it gains more heat. The temperature of the water leaving the module is typically 20°C.

The main advantage of this system is its low mass, compared to the two-loop system. The only heat exchanger required in this system is the heat exchanger linking the acquisition system to the transport system. Another advantage of this system is that the working fluid of the transport system absorbs heat from water at a higher temperature than the double-loop system. Hence, the temperature lift of the transport system will be lower if a double-loop system is used. A disadvantage of the system is that

the entire heat load is collected by a single loop and a malfunction in this loop will cause the entire heat acquisition system to stop functioning.

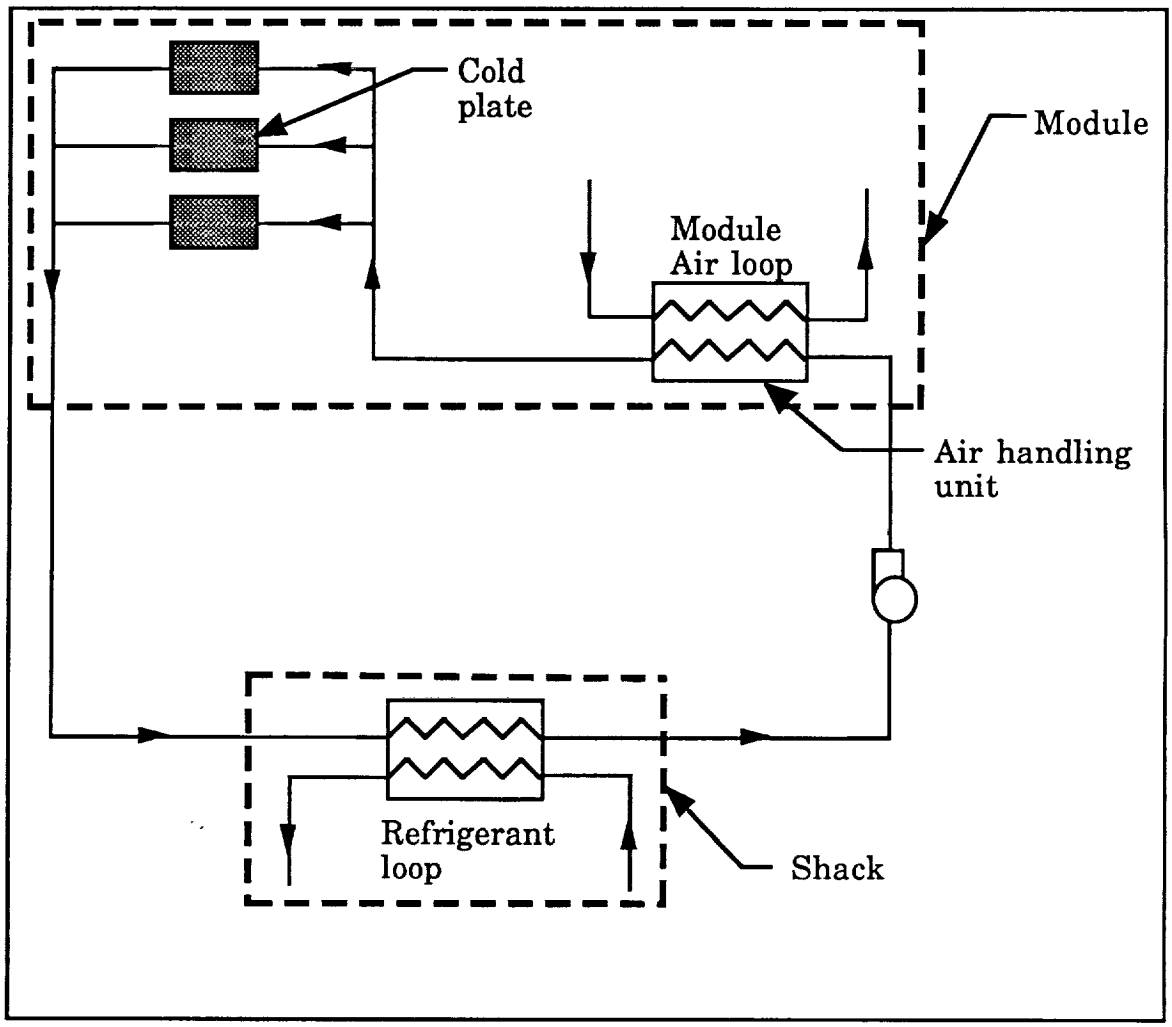

Figure 6. Single Water-Loop Concept

2.3 Heat Transport Systems

The function of the heat transport system is to make the acquired heat available at a suitable location and temperature where it can be rejected. The team developed three alternative heat transport system designs. These alternative designs are the vapor compression system, the vapor absorption system, and the metal hydride adsorption system. These designs utilize either work or heat inputs to drive the thermodynamic cycles.

The alternative heat transport systems are designed to transport 50 kW of heat from a temperature of -3°C to 111°C. The specified temperature range is the worst possible case that the transport system has to operate under. The low temperature of -3°C is due to the 2°C loop undergoing a 5°C temperature drop at the heat exchanger linking the acquisition system to the transport system. The high temperature of 111°C is the maximum possible temperature to which the heat will be rejected. For each alternative, operating conditions, mass and power requirements, advantages, and disadvantages are presented in this section.

2.3.1 Vapor Compression Systems. A vapor compression cycle is the most widely used method by which a refrigeration effect is achieved [7]. The most basic form of a vapor compression cycle is a single stage cycle, as shown in Figure 7.

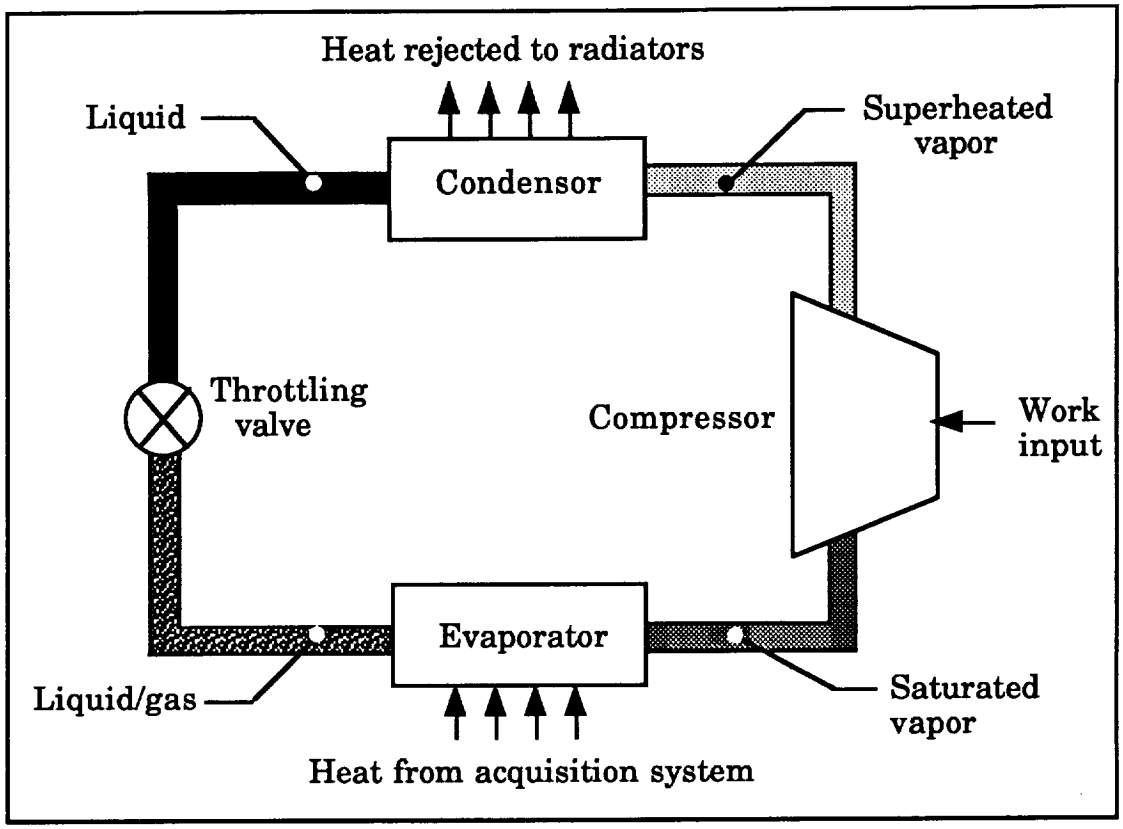

Figure 7. Single Stage Vapor Compression Cycle

This cycle comprises an evaporator, compressor, condenser, and expansion device. The refrigerant enters the evaporator as a two phase liquid vapor mixture. In the evaporator, the refrigerant changes phase from liquid to vapor as a result of heat transfer from the internal heat load to the refrigerant. During the phase change of a fluid, high rates of heat transfer occur between the fluid and the heat source at relatively low flow rates. Furthermore, heat transfer during the phase change of a fluid occurs at an almost constant fluid temperature [8]. The refrigerant is then compressed adiabatically to a higher temperature and pressure at which condensation occurs. As the refrigerant condenses, heat is transferred from the refrigerant to the cooler surroundings. Since the refrigerant

changes phase, a large heat load is transferred to the surroundings at low flow rates and constant temperature. The refrigerant then enters an expansion valve and expands to the evaporator temperature and pressure.

The performance of a single stage vapor compression system using Refrigerant 11 as the working fluid is evaluated in Appendix B1. To transport a 50 kW heat load from -3°C to 111°C, external work of 33.3 kW is required. The mass of the system is 176 kg for 50 kW of heat transported. The Coefficient of Performance (COP), a measure of the cooling capacity per unit external energy required, is 1.5.

Due to its high COP, the vapor compression system is the most widely used refrigeration system for terrestrial applications. Therefore, its performance in lunar applications can be more accurately predicted than any other cycle. Furthermore, the system is easy to maintain and repair. Maintenance and repair become important factors as the life of a system increases. The vapor compression system easily meets redundancy requirements. In case of a power failure, an entire backup system is not required. The only component requiring a backup is the compressor. Hence, employing a backup system will not greatly affect system mass. The components of this system are compact and occupy limited volume. These systems usually have higher COPs than heat driven refrigeration cycles.

The main disadvantage of vapor compression systems is the high power requirement. Furthermore, operating this system requires the use of rotating machinery. Such components will have to be replaced more frequently than components having no moving parts.

Since a wide temperature range must be spanned, the use of a single working fluid will cause extremes in pressure. Such extremes in pressure

can be avoided if two fluids are chosen for reasonable evaporation and condensation pressures in two temperature ranges. A major advantage of a two stage system is that the working fluids in the two stages need not be the same. Such a system is shown in Figure 8.

As shown in Appendix B1, an example calculation was performed using Refrigerant-11 and Refrigerant-12 as the working fluids. To transport a 50 kW heat load, 23.3 kW of external work is required. The mass of the system is 275 kg for 50 kW of heat transported. The COP of this system is 2.15.

The advantages and disadvantages discussed for single stage vapor compression systems apply for two stage systems. The primary advantage of the two stage cycle is that it requires 30% less power than the single stage cycle. An added advantage is that the system can operate at two levels. Hence, if the system is required to cool a smaller load, one of the compressors can be turned off. Thus, power can be conserved. Due to the lower power input, the total heat to be rejected is lower than for a single stage system. Consequently, the radiator mass will be lower. The two stage system has more moving parts than the single stage system. Therefore, the two stage system has a higher mass, is less reliable, more complex, and requires more maintenance than the single stage system.

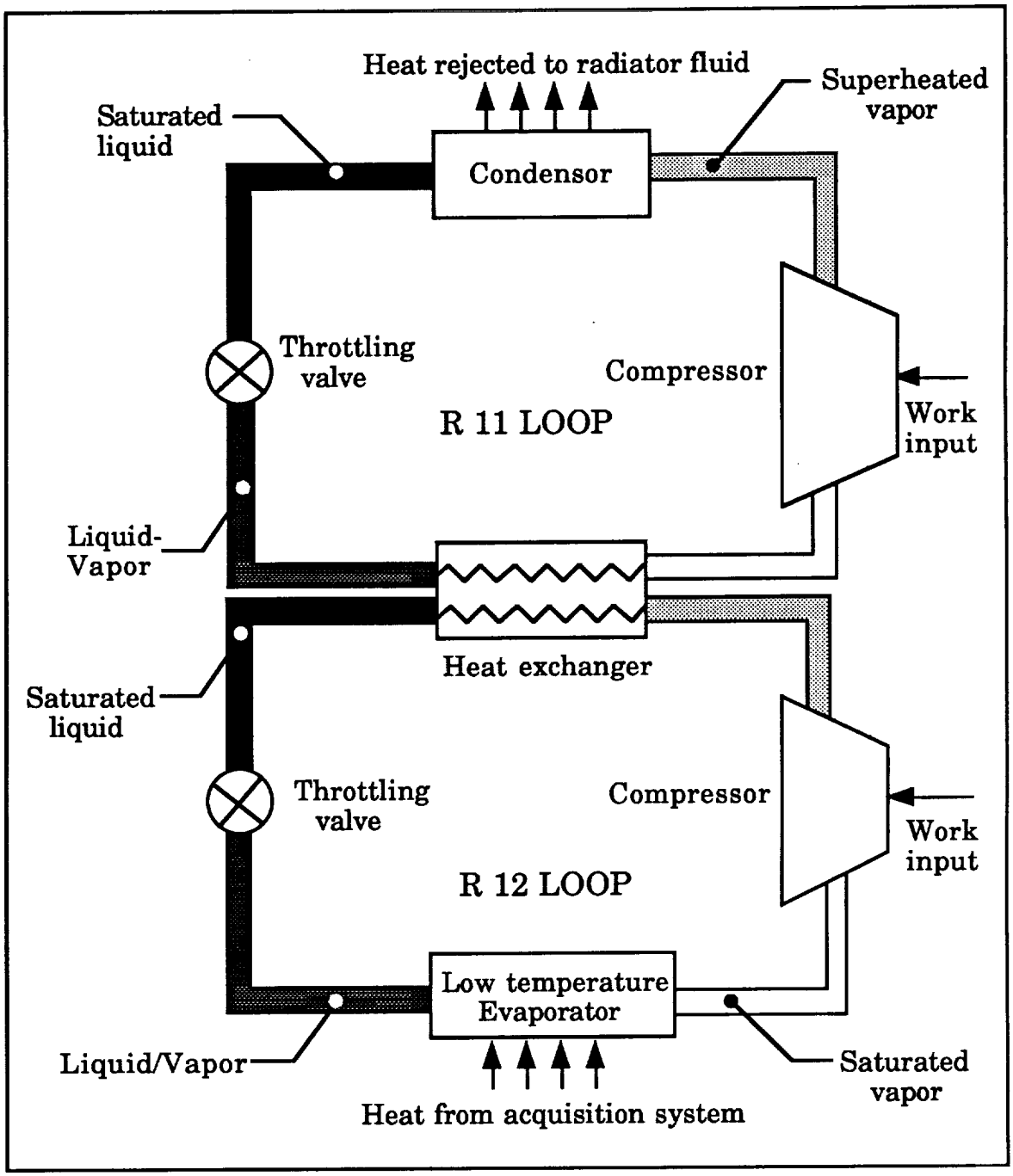

Figure 8. Two Stage Vapor Compression Cycle

2.3.2 Vapor Absorption Systems. One method of transporting heat from a low temperature to a high temperature is to drive a thermodynamic cycle with external heat. The most common heat driven cycle is the

absorption cycle. The basic elements of a vapor absorption system are a condenser, evaporator, absorber, desorber, and generator, as shown in Figure 9.

An absorption cycle uses two working fluids - a refrigerant and an absorbant. The cycle is based on the principle that less power is required to compress a liquid solution than a vapor. The evaporator and condenser function in the same manner as in the vapor compression cycle. However, the compressor is replaced by the absorber, liquid pump, and generator.

The refrigerant enters the evaporator as a liquid. Heat is transferred from the acquisition system to the refrigerant. Due to this heat transfer, the refrigerant evaporates at constant temperature. The refrigerant then enters the absorber, where it condenses and reacts with the absorbant to form a solution. In the process, the heat of reaction and heat of condensation are given off. Hence, the radiator must reject this additional load. The solution is then raised to a higher temperature and pressure by using a pump. The solution then passes through a heat exchanger to the generator. In the generator, the temperature of the solution is increased by energy supplied by an external heat source. The solute refrigerant is vaporized, producing a weak liquid solution. A two phase flow of refrigerant and solute leaves the generator and the two phases are separated by gravity. The weak solution is returned to the absorber through a heat exchanger. The weak solution returning from the generator transfers heat to the strong solution travelling to the generator. The refrigerant vapor is condensed, causing the heat to be transferred out of the system at a high temperature. The condensed vapor returns to the

evaporator through an expansion valve, and heat transport process is repeated.

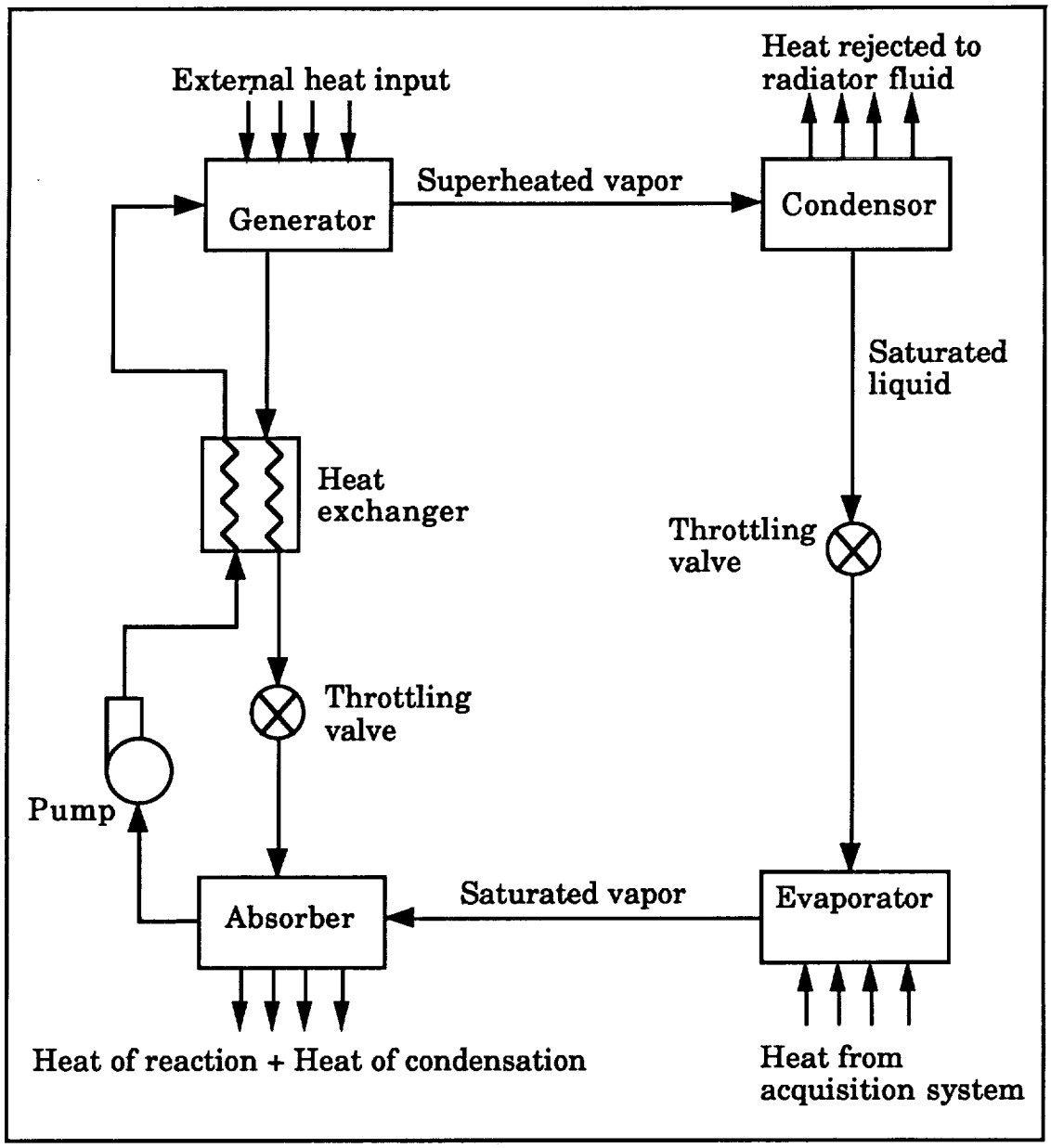

Figure 9. Vapor Absorption Cycle

An analysis of the performance of the vapor absorption cycle is presented in Appendix B2. To transport a 50 kW heat load from -3°C to 111° C, an external heat input of 86 kW is required. The mass of the system is about 500 kg. The COP of this system is 0.86.

The primary advantage of a vapor absorption is that it is heat driven. If waste heat from a nuclear plant is available, the system can be run without any added mass or power. A further advantage of this system is the absence of moving parts, increasing the life of the system. A disadvantage of this system is its high mass, since the absorber, generator, and heat exchanger are considerably heavier than a compressor in a vapor compression cycle [9]. A further disadvantage of this cycle is its low COP. Low COP implies that the radiator must reject a high load and thus have a large area. If a redundant system is required, the entire system will have to be replaced. Another problem is the separation of the vapor and liquid phase in low gravity.

2.3.3 Metal Hydride Heat Pump Systems. Certain metals and alloys can store large quantities of hydrogen. The hydrogen is stored within the intermetallic lattice structure. Within this structure, a maximum of six moles of atomic hydrogen can be stored in each mole of alloy. The concentration of stored hydrogen depends on the temperature and pressure of the metal hydride systems [7]. Over a wide range of hydrogen concentrations, pressure remains constant. This effect is similar to a phase change of a solid or fluid. As in the case of a solid or fluid, an energy change is associated with the transition of an alloy free of hydrogen to an alloy rich in hydrogen. This energy change is the heat of adsorption. For a given mass, the energy change associated with the heat of adsorption is up

to nine times greater than the energy change associated with the vaporization of water [7].

The ability of a metal to adsorb large quantities of hydrogen and the associated heat of adsorption can be exploited to construct a heat pump. A schematic of the metal hydride system is shown in Figure 10. Two vessels containing different metal hydride alloys are connected by a pipe. Initially, all the hydrogen is stored in vessel A. As shown in Figure 11, the cycle consists of four stages. In the first stage, a high temperature source of external heat is applied to vessel A with valve closed. During this stage, the temperature of vessel A increases. In the next stage, the heat is still applied to vessel A, but the valve is now opened. Hydrogen desorbs from vessel A and flows to vessel B where it is adsorbed. As vessel B adsorbs hydrogen, it is heated to a temperature at which the pressure of vessels A and B are equal. In stage three, vessel A is cooled to its original temperature by transferring energy to a heat sink. In the final stage stage, the valve is opened and hydrogen desorbs from vessel B and flows to vessel A. The removal of hydrogen from vessel B causes a pressure difference between the two vessels. To maintain pressure equilibrium, vessel B is cooled. At this point, energy is delivered to the low temperature source to complete the desorption process. This energy removed from the low temperature source is the refrigeration effect.

An example calculation was performed on this system, as shown in Appendix B3. It was determined that if the system is at an initial temperature of 27°C, 417 kW of external heat is required to transport a 50 kW load from 3°C to 111°C. The mass of the system is estimated to be 1475 kg. The COP of this system is 0.24.

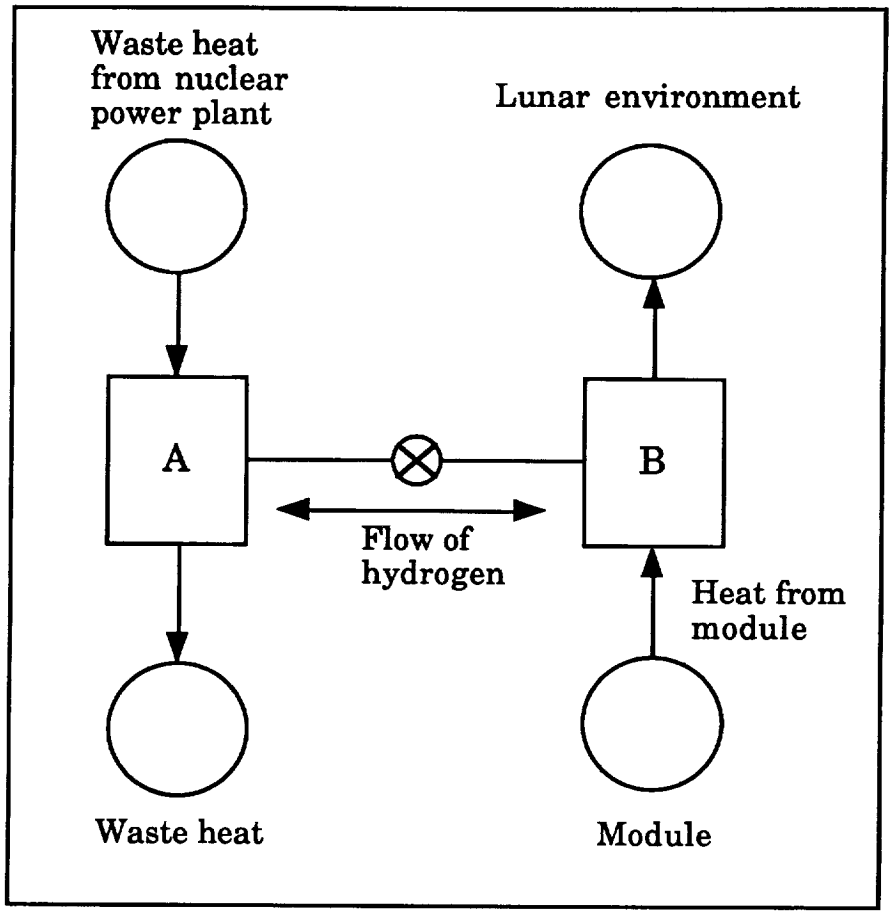

Figure 10. Schematic of a Metal Hydride Cycle

The primary advantage of this system is that it is a heat driven cycle. If waste heat from a power plant is available, the system can be operated without work input. Therefore, no rotating machinery is used in this system. Hence, the life of the system is longer than a cycle with components having rotating machinery.

The main disadvantage is that the technology of metal hydride systems is not fully developed and is still in the experimental stage [7]. Predicting the operation of a metal hydride system under lunar environmental conditions is very difficult. A further disadvantage is the low COP of the system. Hence, a large quantity of heat is required to

remove 50 kW of heat. Consequently, the total heat to be rejected is higher, resulting in an increase in radiator area. Finally, the entire process is not continuous. Therefore, at least two metal hydride systems will be required to operate in parallel.

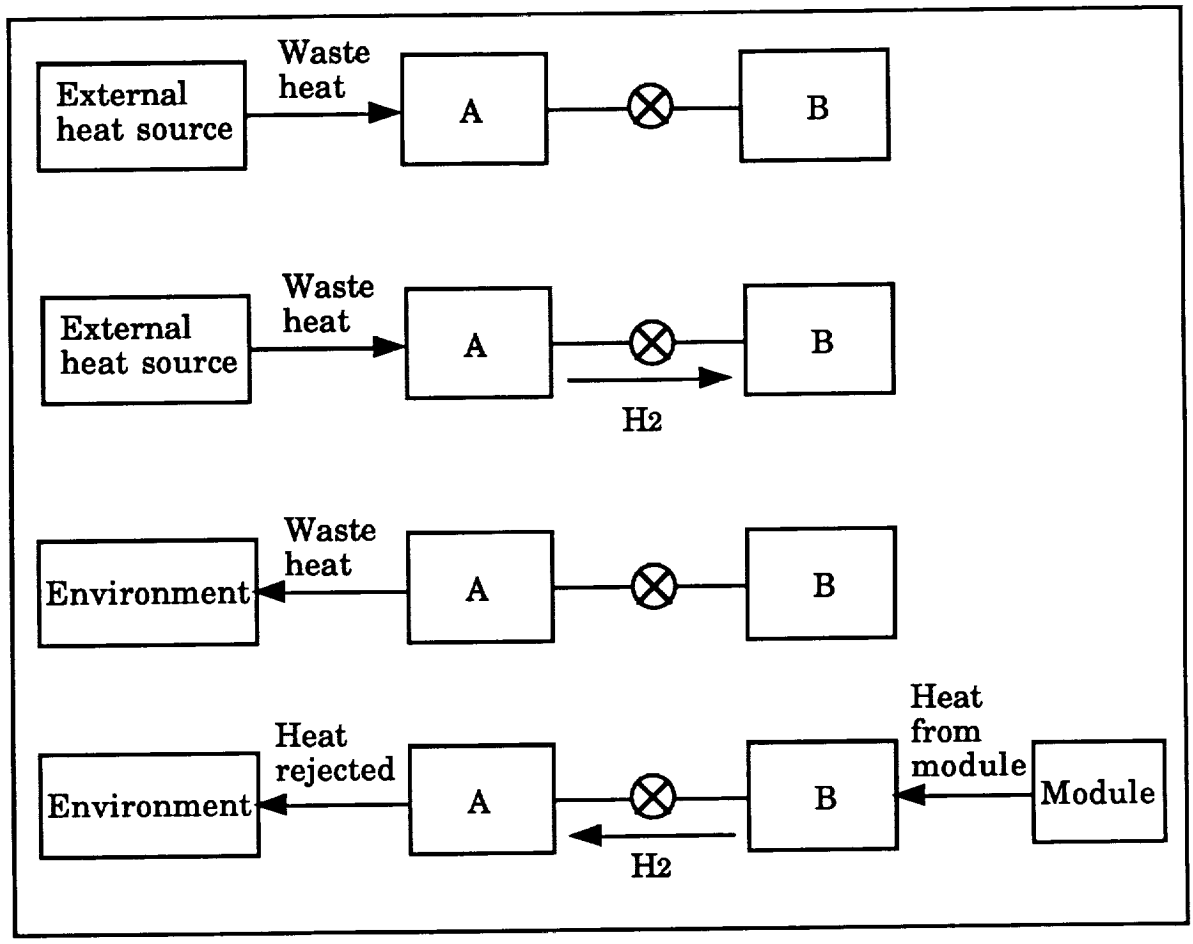

Figure 11. Four Stages of a Metal Hydride Cycle

2.4 Heat Rejection Systems

Heat acquired from the module by the transport system can either be conducted to the lunar soil or radiated to space. Due to the extremely low thermal conductivity of the lunar soil, heat rejection to the soil is not a feasible solution [6]. Therefore, alternative ways of heat rejection to the environment were considered.

The lunar environment places some unique demands on the design of a heat rejection system. The radiator must be designed to reject heat to a high effective sink temperature created by high solar irradiation and infrared (IR) flux from the hot lunar surface. Furthermore, the radiator must be adaptable to micrometeorite impacts and lunar dust. Finally, the weight of the radiator must be minimized.

In accordance with these functional and structural constraints, the design team investigated four types of radiator designs. These alternative designs include the flat plate radiator, parallel plate radiator, liquid droplet radiator, and reflux boiler radiator. These alternatives are described in this section of the report. For each alternative, the operating principle and the extent to which it meets the design criteria are discussed. The effective sink temperature, heat rejection capability, and radiator mass are also presented for each alternative. To analyze the performance of each radiator, certain assumptions were made. First, it is assumed that the heat transport system transfers 50 kW of heat from the module to the radiator. It is also assumed that the heat load is raised to a temperature such that the radiator surface temperature is 111°C.

2.4.1 Flat Plate Radiators. The flat plate radiator uses a flat surface to reject heat to the environment. A fluid is passed through the radiator. In doing so, heat is transferred from the fluid to the radiator by forced convection. Two possible orientations of the flat plate were investigated - horizontal and vertical. Figure 12 and Figure 13 show these orientations. The bottom surface of the horizontal plate is insulated from the lunar surface. Therefore, the radiator surface only intercepts the solar irradiation. The radiating surface of the vertically oriented plate is aligned east-west. As a result, the radiator surface receives minimal solar

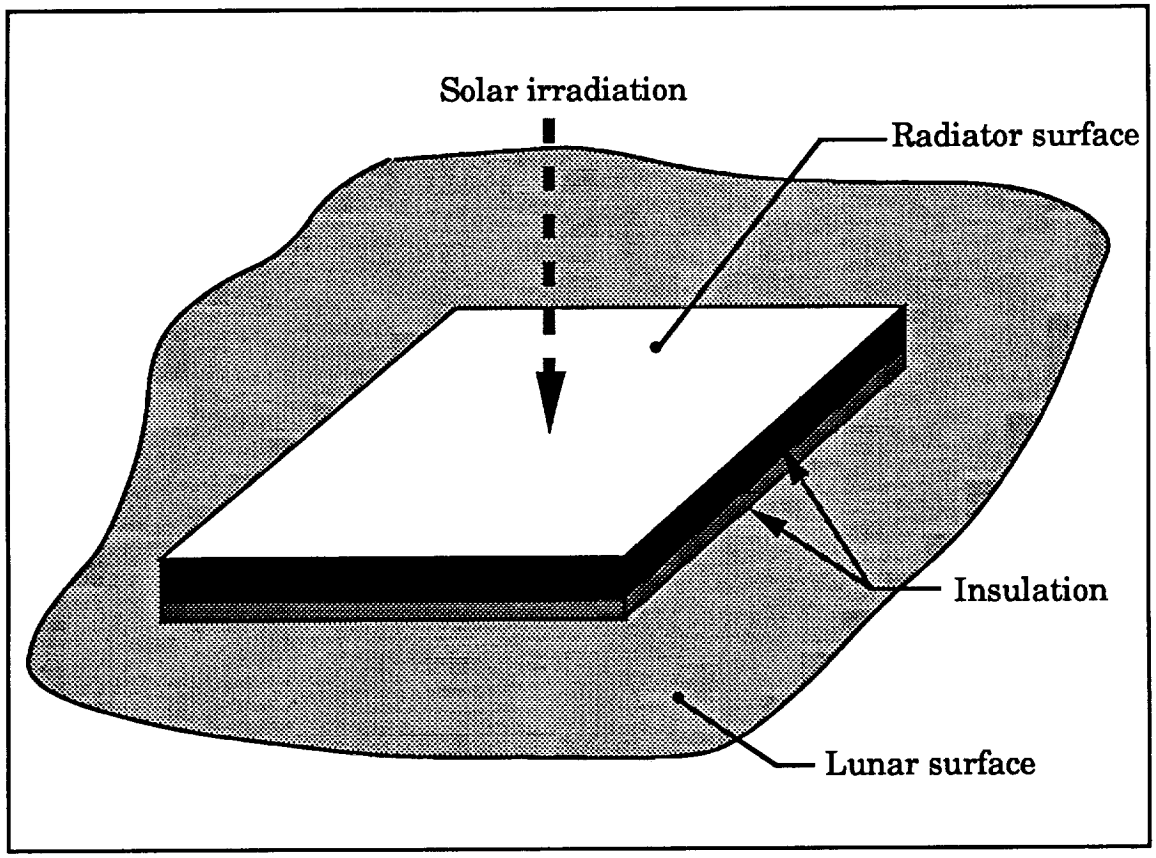

Figure 12. Horizontal Flat Plate Radiator

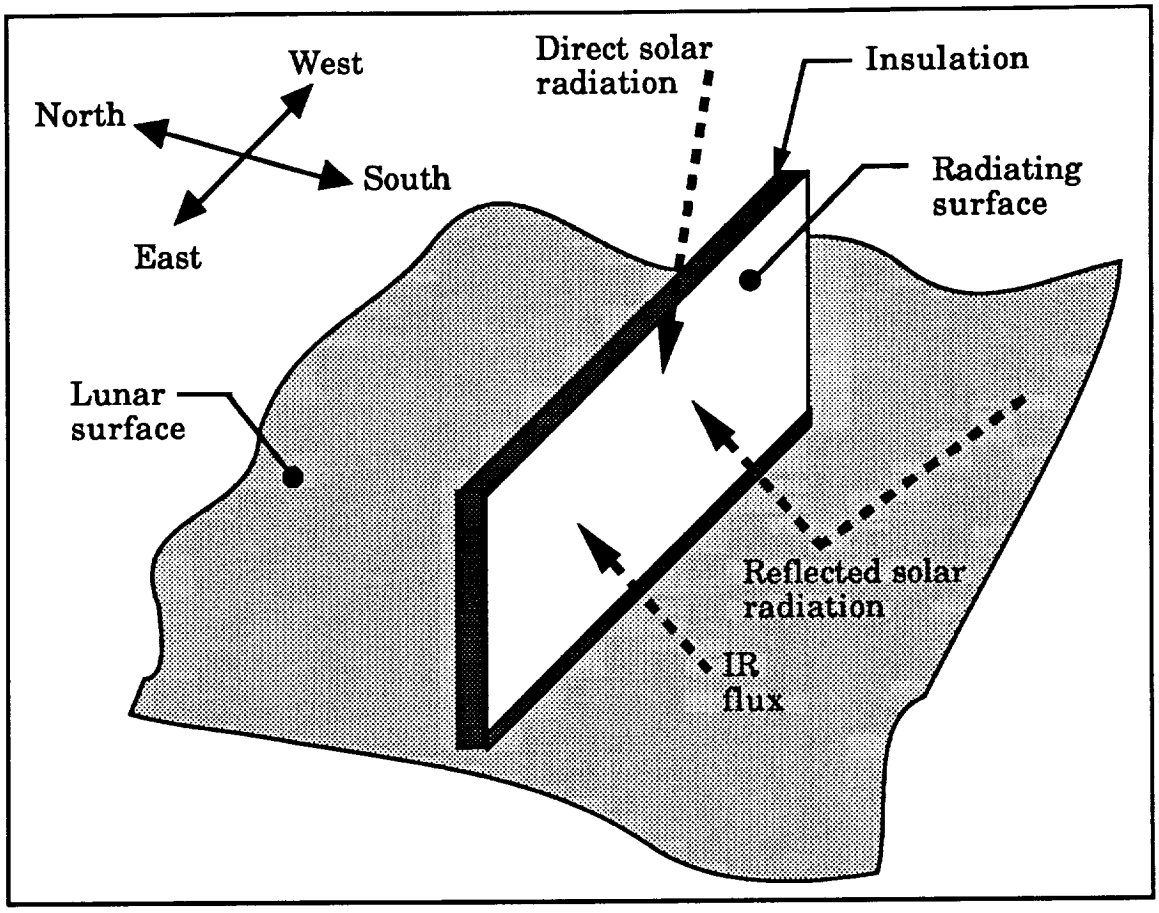

Figure 13. Vertical Flat Plate Radiator

irradiation. However, the vertical plate is partially exposed to radiation from the lunar surface. Hence, it receives IR flux emitted by the lunar surface and the solar irradiation reflected from the lunar surface.

Because each radiator orientation is subjected to different incident radiation, the effective sink temperature varies with orientation. In addition, the effective sink temperature varies with time because the intensity of incident radiation varies with time of day. Figure 14 shows the variation of effective sink temperature with time for both orientations of the flat plate. Because the effective sink temperature varies with time, heat rejected by the plates will also vary with time. Figure 15 shows the

variation of heat rejected per unit area of radiator surface. Furthermore, this variation is shown for two different radiator temperatures. The high and low temperatures refer to the operation of the radiator with and without a transport system respectively. Appendix C1 contains the assumptions made and equations used to generate the graphs in Figures 14 and 15. Appendix C1 also contains the mass calculations for both types of flat plate radiators

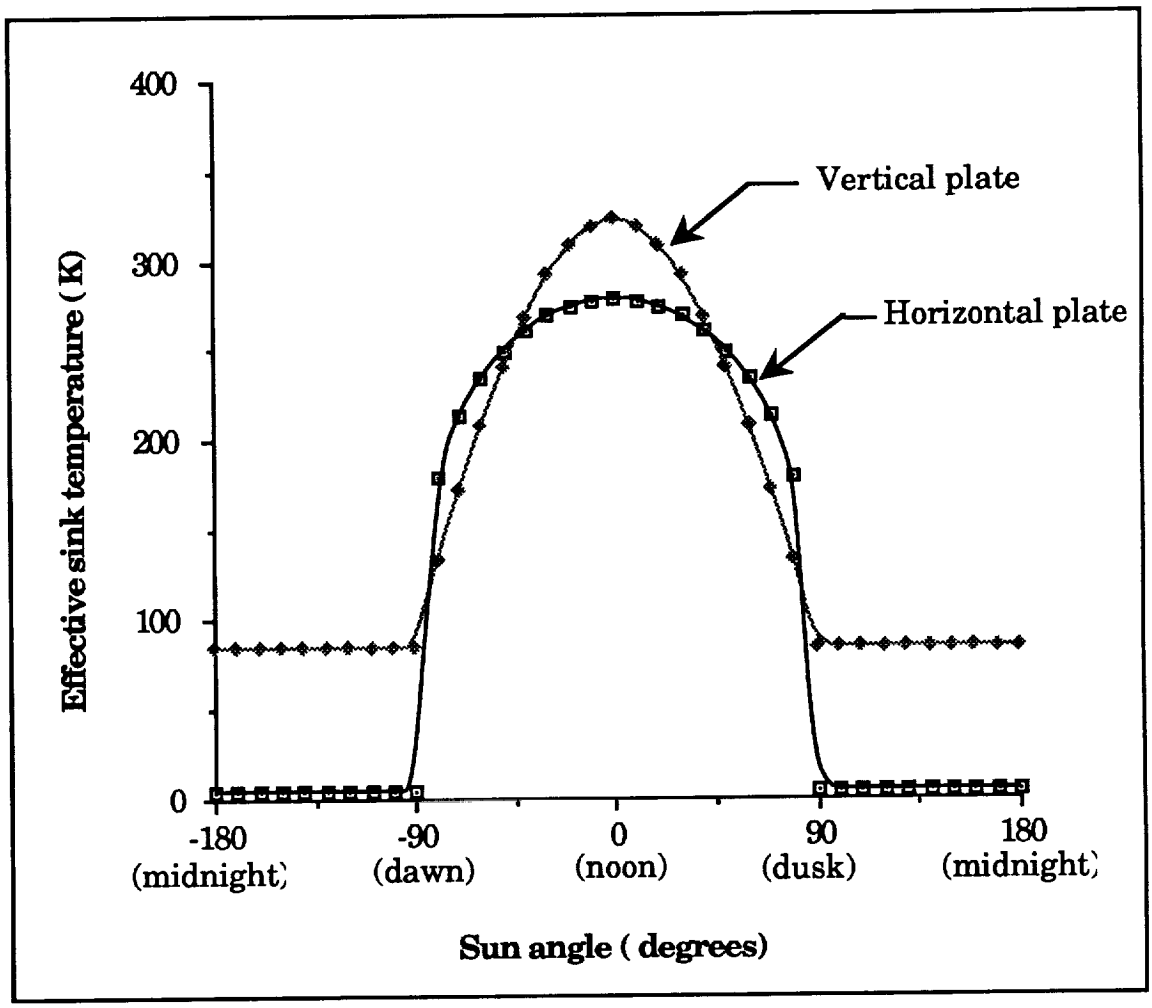

Figure 14. Effective Sink Temperature .Vs. Time of Lunar Day

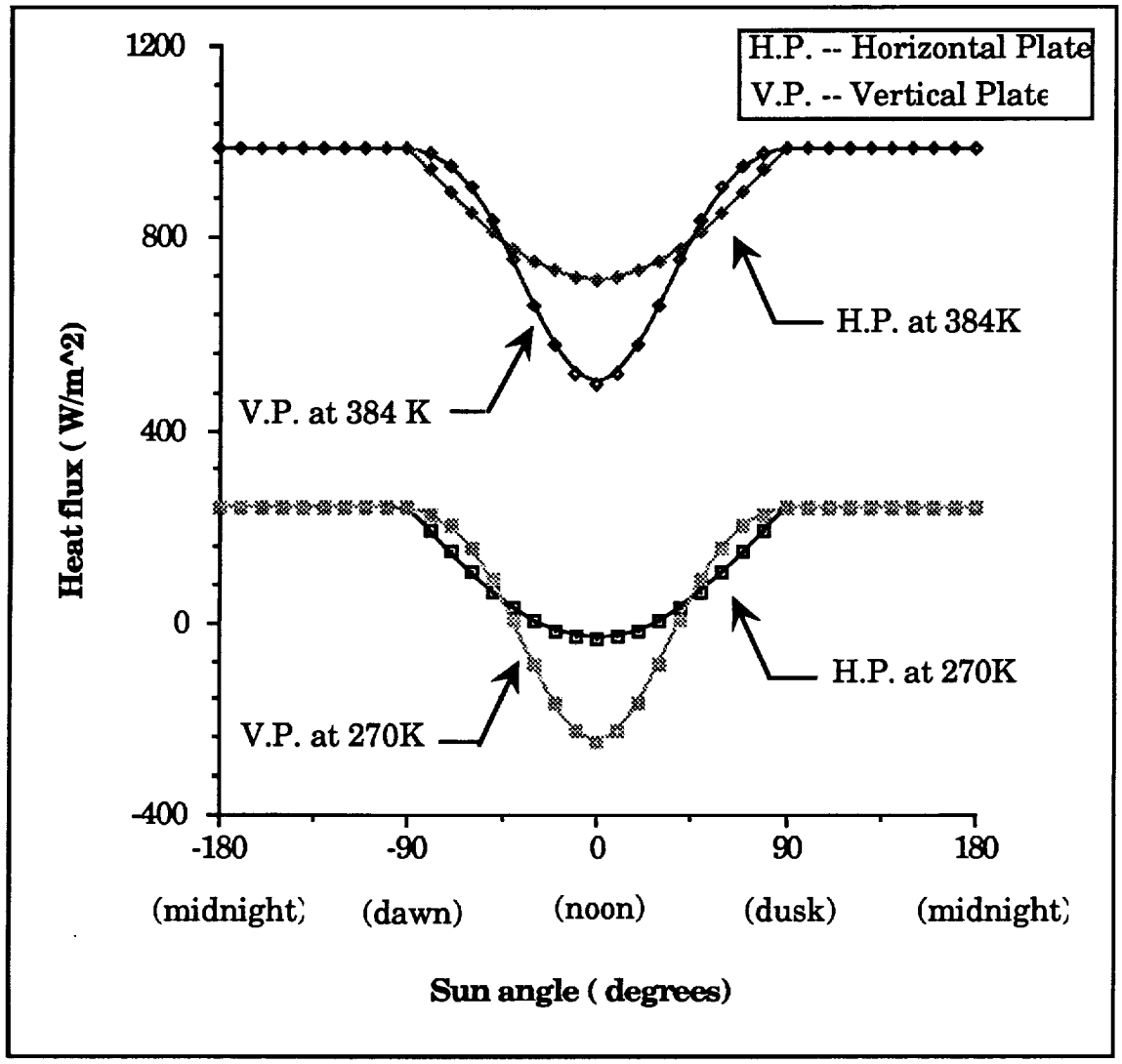

Figure 15. Heat Flux Radiated .Vs. Time of Day

Flat plate radiators have several advantages and disadvantages. The horizontal radiator has a low sink temperature of 5°C at lunar noon. The corresponding sink temperature of the vertical radiator is 49°C. Consequently, the horizontal radiator can reject more heat per unit area than vertical radiators. However, the vertical radiator provides twice the

area for heat transfer as compared to horizontal radiators for a given mass and volume. Vertical radiators also have a lower specific mass (14.4 kg per kW rejected) than horizontal radiators (20 kg per kW rejected).

Heat is gained by flat plate radiators when operating at -3°C at lunar noon, as shown in Figure 12. Therefore, flat plate radiators require the use of a heat transport system to raise the temperature of the heat load at the radiator. Because the fluid undergoes a temperature drop, the radiator surface will not be isothermal. Therefore, such radiators have a low fin efficiency of about 70%. The fin efficiency decreases with increasing length of radiator. Other disadvantages of these radiators include the degradation of radiator surface due to lunar dust and the possibility of failure due to micrometeorite impact. An important advantage of these radiators is the simplicity of their design.

2.4.2 Parallel Plate Radiator. The parallel plate radiator consists of two flat horizontal plates separated by a specified distance, as shown in Figure 16. The bottom plate is a horizontal flat plate radiator. The top plate is aligned horizontally to completely shade the radiator from solar irradiation.

Figure 17 shows the various heat fluxes incident on the two plates. The upper surface of the top plate absorbs a large portion of the solar irradiation. The bottom surface absorbs most of the IR flux and the reflected solar irradiation from the lunar surface. Due to the presence of the top plate, the radiator surface is subjected only to radiation emission from the lower surface of the top plate. As a result, the effective sink temperature for the radiator is reduced significantly.

In addition to shading the radiator, the top plate also acts as a heat collector. Preliminary calculations showed that up to 1100 W/m^2 of heat can be collected from the top plate. These calculations are presented in Appendix C2. This appendix also contains calculations performed to find the effective sink temperature, heat rejection capacity, and mass of this design.

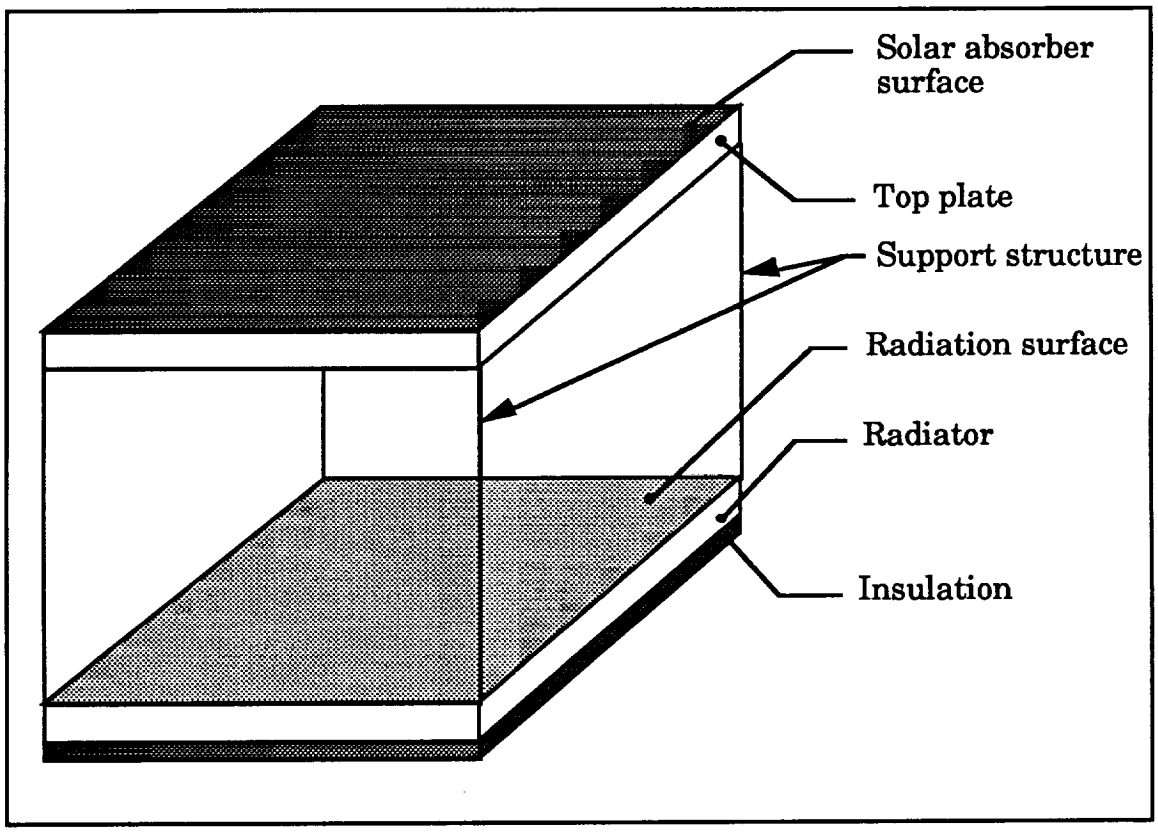

Figure 16. Three Dimensional View of the Parallel Plate Radiator

This alternative has many advantages. The effective sink temperature is -103°C, which is significantly lower than for flat plate radiators. Because the sink temperature is lower than -3°C, this radiator

can be used without the aid of a heat transport system. Furthermore, the presence of the top plate reduces the probability of a meteorite striking the radiator and exposure of the radiating surface to lunar dust. Finally, the top plate acts as a heat collector. The heat acquired can be used to drive a heat transport system, thus decreasing the power requirements of the TCS.

The primary disadvantage of this system is that the top plate significantly increases the mass of the radiator. The specific mass was found to be 30 kg per kW of heat rejected, including the mass of the top plate. This value is about twice the specific mass of a flat plate radiator. Another disadvantage of parallel plate radiators is that they are more complex to design than a flat plate radiator.

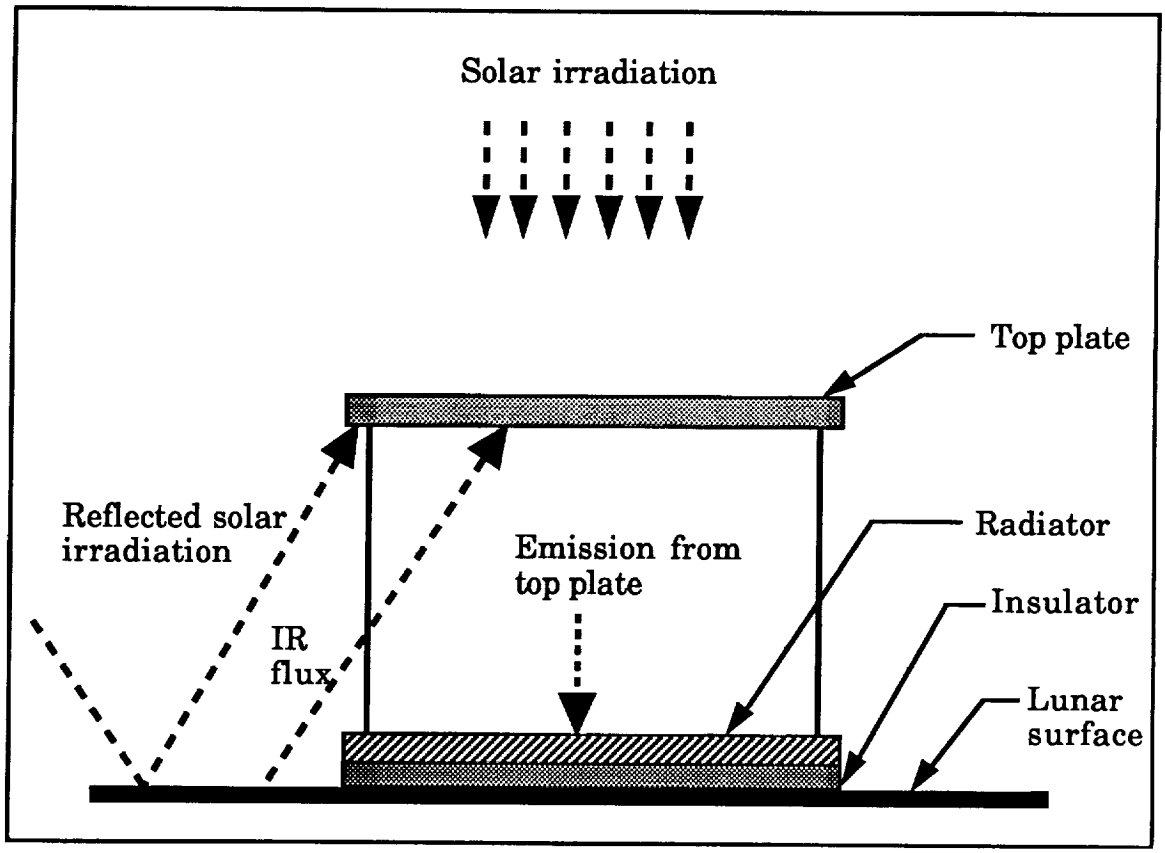

Figure 17. Heat Fluxes on the Parallel Plate Radiator

2.4.3 Reflux Boiler Radiator. A reflux boiler is an evaporation-condensation device used for transferring and rejecting heat. A reflux boiler is a closed tube or chamber, with a fixed volume of working fluid. The tube consists of three sections - the evaporator, the adiabatic region, and the condenser (see Figure 18).

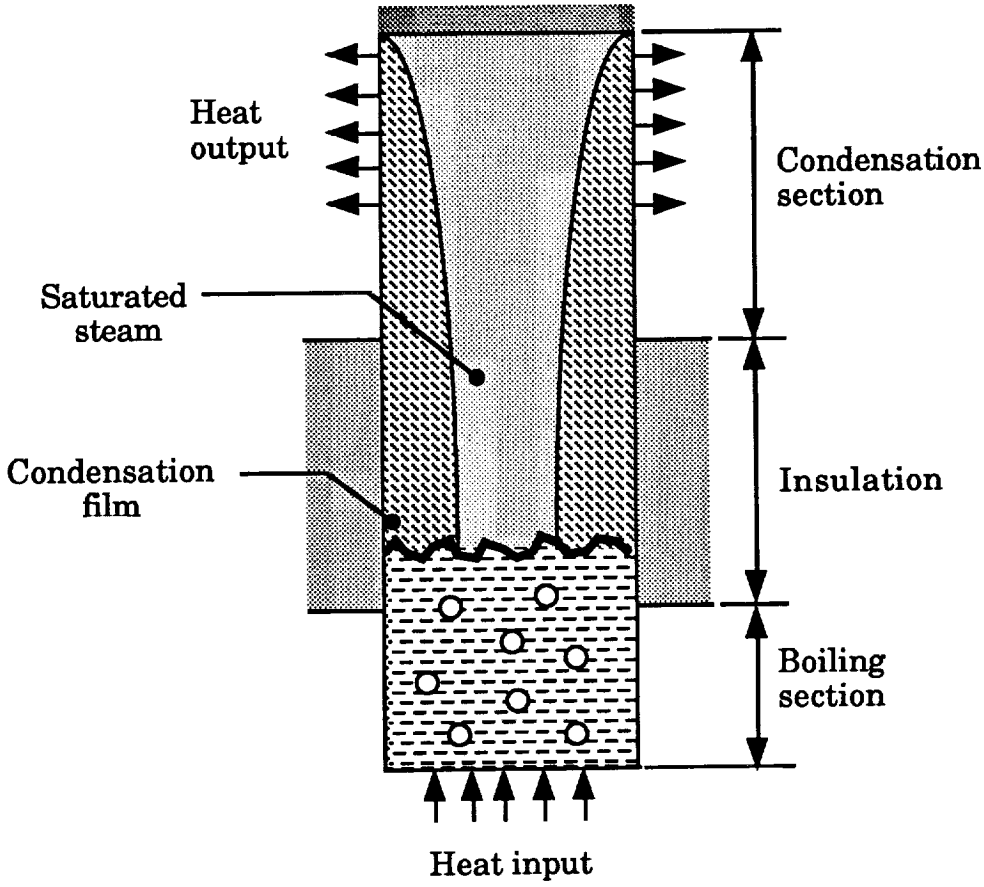

Figure 18. A Typical Reflux Boiler Radiator [8]

Heat removed from the module by the transport system is applied at the evaporator section. The heat transfer to the fluid vaporizes the fluid in the evaporator section. The resulting difference in pressure drives vapor

from the evaporator to the condenser. The fluid condenses, releasing the latent heat of vaporization to the walls of the tube. Aided by gravity, the condensed liquid falls back to the evaporator along the sides of the tube. Hence, the reflux boiler continuously transports the latent heat of vaporization from the evaporator to the condenser.

An analysis of the reflux boiler radiator was performed, as detailed in Appendix C3. The specific mass of this radiator is 10.6 kg per kW of heat rejected. The effective sink temperature of this radiator is 49°C, assuming the reflux boiler tubes are embedded in a vertical flat plate.

Since condensation is a constant temperature process, the walls of the reflux boiler tube are nearly isothermal. An isothermal surface ensures that the efficiency of the radiator is maximized. A typical efficiency of this radiator is about 95%. Furthermore, the efficiency decreases by a small amount as the radiator length increases. Another advantage of condensation is that heat transfer through a fluid is much higher. The amount of heat that can be transported in a reflux boiler is usually several orders of magnitude higher than that which can be transported as sensible heat by conduction or convection. The reflux boiler can therefore transfer a large amount of heat with a small unit size.

The performance of the reflux boiler radiator is limited by the dry-out limit. If the liquid in the reflux boiler is too small for the heat input, the condensate returning to the evaporator will dry out before reaching the evaporator. Hence, the process becomes discontinuous. A further disadvantage is the difficulty of starting the evaporation process. The velocity of the vapor is also limited by the sonic limit and the entrainment limit. The sonic limit must not be exceeded in order to ensure that thermal

gradients do not occur along the tube walls. The entrainment limit must be avoided to ensure that the vapor does not exert too much drag on the condensate. If the entrainment limit is exceeded, the condensate will be unable to return to the boiling section.

2.4.4 Liquid Droplet Radiator. Unlike the three types of radiators discussed, the liquid droplet radiator (LDR) uses a liquid surface to radiate heat to the environment. The heat to be rejected is first transferred to a liquid. The liquid is then injected into the environment as a stream of small droplets. The droplets are then exposed to the environment for a specific time, during which they are cooled by radiating heat to the environment. The cooled droplets are collected and re-used for the same purpose. Figure 19 shows the layout of an LDR.

The most important components of an LDR are the generator, liquid sheet, and collector. The generator is a pressurized plenum with an array of nozzles. Liquid jets form at the exit of the nozzles. Due to surface tension instabilities , the jets disintegrate into small droplets. This process of droplet formation is shown in Figure 20. A similar concept is used in ink-jet printers [10].

Although wider spacing between droplets improves the heat transfer rate, droplets formed by the generator are closely packed to minimize the size of the generator. Consequently, droplets travel as a sheet of liquid which is almost opaque (see Figure 21). By orienting the droplets as a sheet, the emissivity of the liquid sheet differs from that of an individual droplet. The emissivity of the sheet is a function of the liquid properties, the size of the droplets, and the spacing between droplets. Furthermore, the surface area available for radiation is the surface area of the sheet.

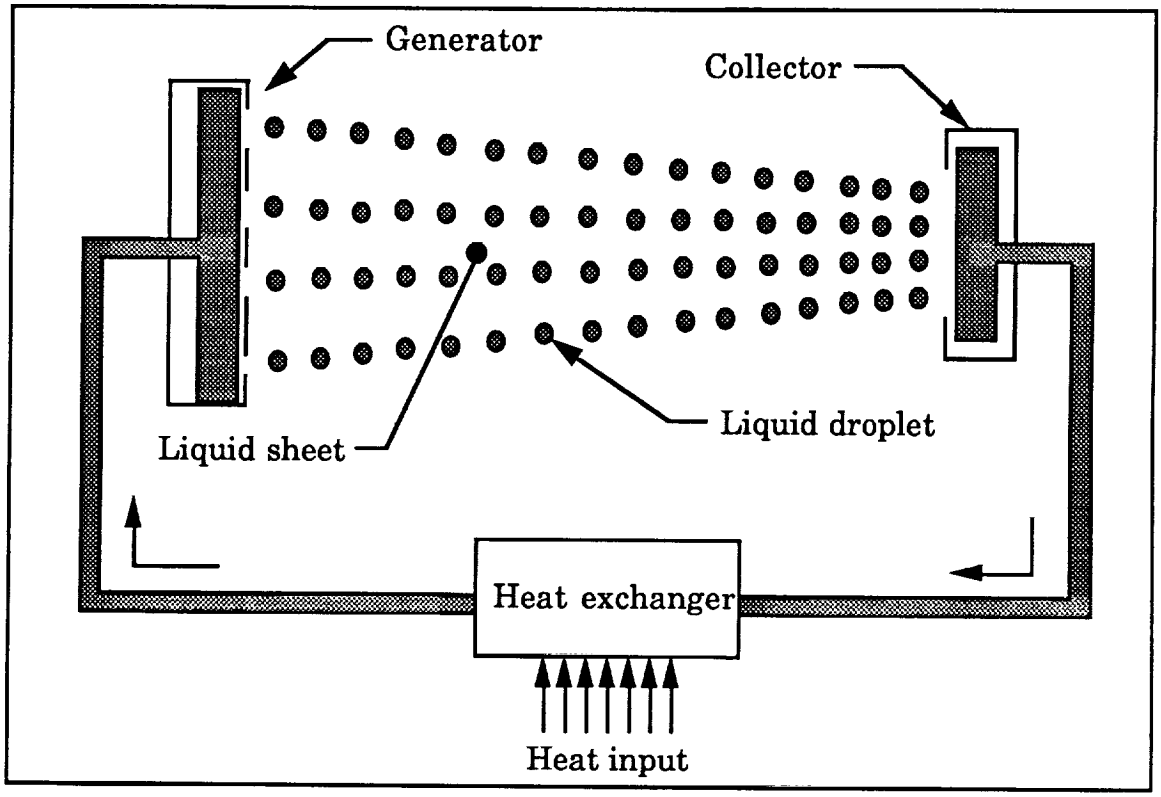

Figure 19. Layout of an LDR

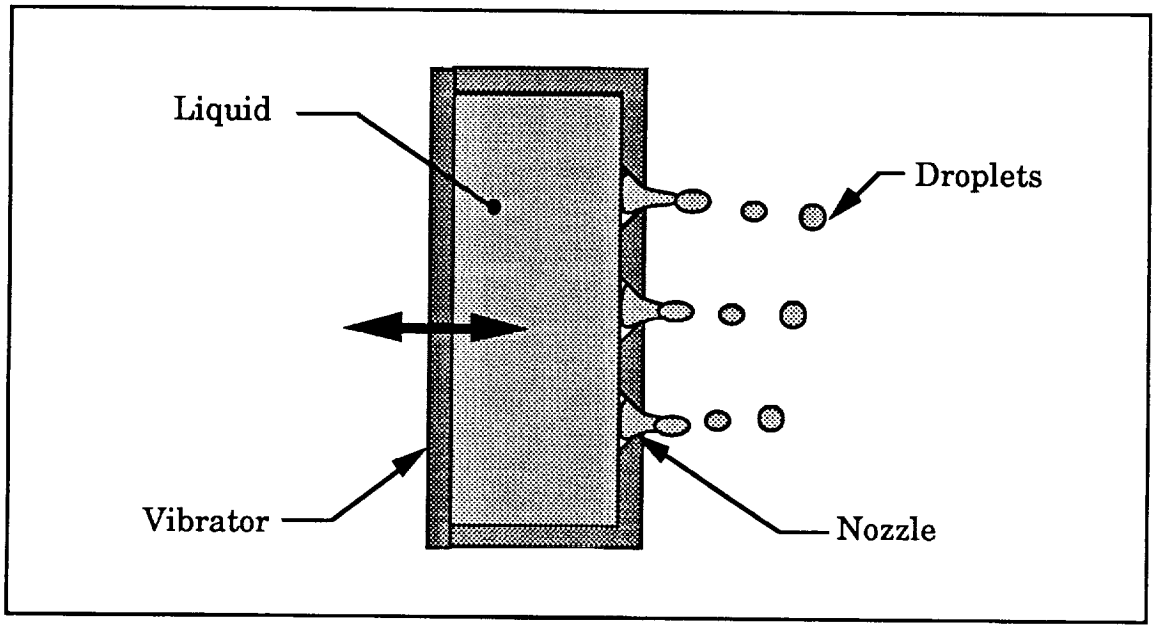

Figure 20. The Liquid Droplet Generator [10]

The sheet has a rectangular cross-section as opposed to a more obvious circular cross-section. This geometry is selected to reduce the effective sink temperature. Moreover, the sheet converges as it approaches the collector. This sheet orientation is chosen to keep the size of the collector small. The collector is a rotating drum, which forms the droplet stream into a continuous liquid by centrifugal acceleration [10].

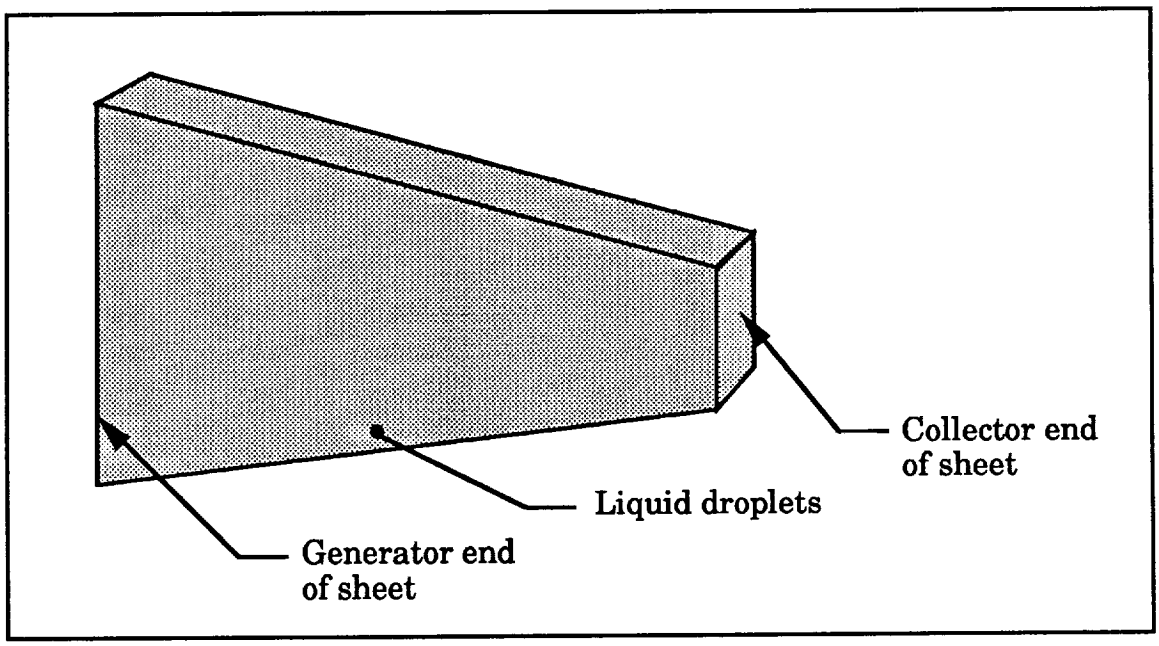

Figure 21. Profile of the Liquid Sheet

Preliminary calculations were done to estimate the heat rejection capability of this design. First, the effective emissivity of the liquid sheet was determined [11]. Next, an energy balance was performed on the sheet to calculate the effective sink temperature of the radiator. The next step involved the assessment of the time that the sheet should be exposed to the environment to cool from 111°C to 87°C [8,10]. Using this transit time, sink

temperature, and emissivity of the sheet, the area of liquid sheet required to reject 50 kW of heat at 111°C was calculated. Next, the sheet area was used to find the width of the sheet at the generator and collector. These widths were used to estimate the size of the generator and collector. Finally, using the size of the liquid sheet, generator, and collector, the mass of the LDR was determined. The specific mass of the LDR is 6.2 kg per kW rejected. These calculations are summarized in Appendix C4.

The greatest advantage of the LDR is its low specific weight. The use of liquid droplets as the radiation medium provides a large surface to mass ratio. Moreover, it is easier to transport an LDR to space than a flat plate or parallel plate radiator. The 212 m^2 required to reject 50 kW of heat can be stored in 0.07 m^3 of liquid plus the volume of the generator and the collector. Finally, the LDR is less vulnerable to damage caused by micrometeorite impacts than solid surface radiators. The LDR possesses immunity from single point failure due to micrometeorite impact. A study was conducted by Mattuk and Hertzberg to evaluate the mass lost by the liquid sheet when struck by a micrometeorite. Mass loss due to deflection and evaporation of droplets was considered. The study concluded that the mass loss due to meteorite impacts is negligible [11].

Apart from its many advantages, the LDR has many disadvantages. Loss of mass of the liquid due to vaporization over time is significant. Another disadvantage is the effect of gravity on the droplets. To account for this problem, the collector will have to be placed below the generator. Furthermore, the liquid is susceptible to contamination by lunar dust. Other disadvantages include complexity of design and operation.

2.5 Summary of alternative designs

The single air-loop system requires no heat exchangers within the module for the purpose of heat acquisition. The mass of this system is high, due to the long network of ducts required. The single water-loop system has the lowest mass and power requirements. However, a redundant system is difficult to incorporate. In a double water-loop system, the heat load is distributed over two loops. The mass of this system is high, since an additional heat exchanger is required inside the module.

Important results of the alternative heat transport systems are presented in Table I. The vapor compression cycle has the lowest power requirement and is the lightest in weight. The absorption and the metal hydride cycles have the advantage of being driven by heat.

Table I

Summary of Heat Transport Systems

	Vapor Compression		Vapor Absorption	Metal Hydride
	Single stage	Two stage		
Mass (Kg)	175	275	500	1450
Heat Input (kW)	0	0	86	450
Work Input (kW)	33.3	23.3	0	0
COP	1.5	2.15	0.58	0.22

Table II presents a summary of the important results of the alternative heat rejection systems. The parallel plate radiator has the lowest sink temperature, but possesses the maximum mass. The liquid droplet radiator has the lowest mass. However, the design and operation of a LDR is complicated. Reflux boilers have a relatively low mass but also involve complex design. The flat plate radiators are the simplest to design and construct. However, flat plate radiators are heavier than LDRs and reflux boilers.

Table II

Summary of Heat Rejection Systems

	Flat Plate		Parallel Plate	Reflux Boiler	Liquid Droplet
	Horizontal	Vertical			
Sink Temperature (in Celcius)	5	49	-103	49	49
Specific mass (in Kg / kW)	20	14.4	30	10.6	6.2

III. Feasibility Study

After completing the alternative designs, the team determined the the feasibility of each alternative. With the use of a decision matrix, the team compared the alternative designs in an organized and logical fashion. The decision matrices use the design criteria as a basis for comparing alternative designs. Appendix D contains the decision matrices for each of the alternative subsystems. The team determined the order of importance of the design criteria based on a literature review of the design of systems for space applications. After the order of importance was established, weighting factors were assigned to each criterion. Next, the team rated each of the alternative according to how well the alternatives fulfilled the design considerations. Numerical values were assigned based on how well each alternative satisifies the design criteria. The numerical values ranged from zero to a hundred, where hundred is the highest rating. These ratings were based on both qualitative and quantitative comparisons. The rating scale is shown in Appendix D.

Table III gives a summary of the decision matrices results. The single water loop system was ranked the highest of the heat acquisition system alternatives. This system has a low mass and power requirement. Furthermore, this system enables a lower temperature lift of the transport system. The two stage vapor compression cycle was ranked the highest of the transport system alternatives. This alternative has a low power

requirement, reasonably low mass, and is the most adaptable to temperature control. The highest ranked heat rejection system was the reflux boiler radiator. This alternative has a low mass and volume due to its high fin efficiency.

Table III

Results of Feasibility Study

Acquisition System		Transport System		Rejection System	
Alternative	Rating	Alternative	Rating	Alternative	Rating
Air loop	64	Single stage vapor compression	86.6	Horizontal plate	71
Single water loop	**84.75**	Two stage vapor compression	**88.6**	Vertical plate	75.8
Double water loop	76.5	Vapor absorption	72.6	Parallel plate	65
*****	*****	Metal hydride	58.4	Reflux boiler	**79.3**
*****	*****	*****	*****	Liquid droplet	75.5

IV. Design Solution

After completing the feasibility studies for each alternative subsystem, the team began creating a design solution. The thermal control system solution consists of a single water-loop acquisition system, a two stage vapor compression transport system, and a reflux boiler radiator heat rejection system. This section of the report presents a conceptual design solution of each of these subsystems. In addition, these subsystems are combined such that the overall function of the TCS is satisfied.

This section of the report is divided into five subsections. First, the overall design process is explained. The next three sections discuss the design solution for the acquisition, transport, and rejection systems. Finally, the design issues of the overall system are presented.

4.1 Design Process for Overall System

A schematic of the overall TCS is shown in Figure 22. The methodology used to design the subsystems of the TCS for the varying conditions within the module and of the environment is presented below. First, the design team identified the heat energy producing components within the module. From such heat producing components, the maximum and minimum heat loads to be removed by the acquisition system were calculated. The sensible and latent heat loads were also calculated. Hence,

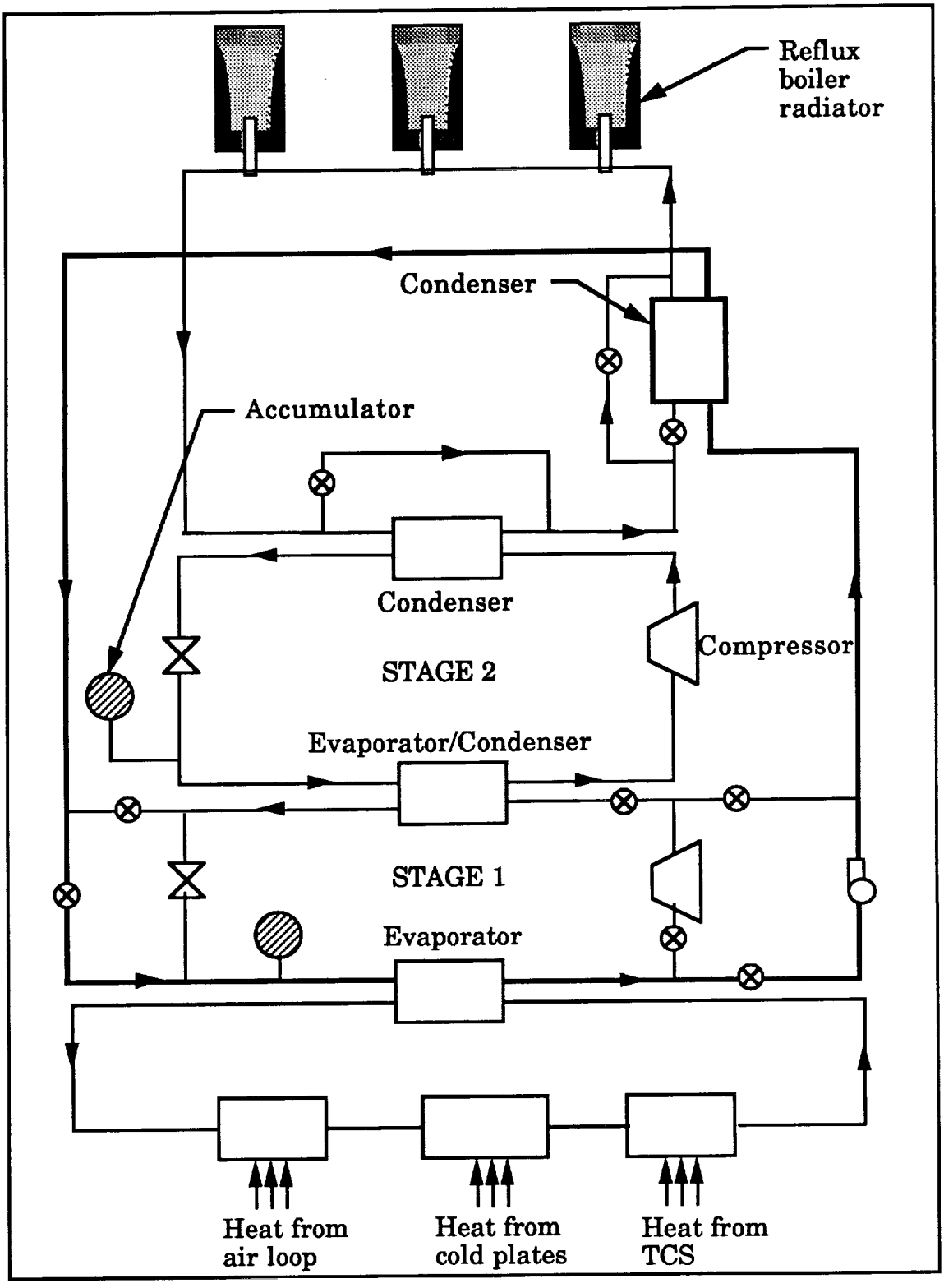

Figure 22. Layout of Overall TCS

amount of heat that must be removed by air and the amount to be removed by water were determined. Based on the maximum heat load, the air and water loops were designed such that the temperature within the module is maintained between 18°C and 24°C. The design team calculated that the temperature of the water from the heat acquisition system enters the heat exchanger linking the acquisition system to the transport system at 25°C and leaves at 7°C.

Next, the heat transport system was designed. To minimize power consumption, the team decided to use a stagewise operation. In a stagewise operation of a two stage vapor compression system, three operating conditions are possible. Either no stages, one stage, or two stages are operated at any given time.

Due to the stagewise operation of the vapor compression system, the radiator must operate at three different temperatures. After determining these temperatures, the radiators were designed to reject the maximum heat load at each of these temperatures.

A variable heat load or sink temperature will cause a thermal and fluid imbalance in the TCS. Moreover, the temperature in the module will fluctuate beyond the specified range. Hence, a means of controlling the system for variable operating conditions was considered next. The acquisition and transport systems were adapted for variable heat loads. Apart from being subjected to variable heat loads, the radiators are exposed to a varying sink temperature. A control system that accounts for these two variable conditions was designed. Finally, overall system design issues such as the adaptability of the TCS to the lunar environment and the placement of the TCS were addressed.

4.2 Acquisition System Design Solution

The function of the heat acquisition system is to collect the heat generated within the module and transport it to the evaporator of the transport system. Heat inside the module is generated by the crew and by equipment. This heat is generated in two forms: sensible and latent. Sensible heat is the heat produced by equipment and by humans, resulting in an increase in the air temperature. Latent heat is the heat added to the air due to the evaporation of water, resulting in an increase in the air humidity. The acquisition system must therefore remove both the sensible and latent heat loads, to ensure that a comfortable temperature and humidity is maintained within the module [12]. Furthermore, heat generated by the TCS must also be removed by the acquisition system.

This subsection of the design solution discusses four main aspects of the acquisition system design. First, the operating parameters of the system are defined. Next, the components of the acquisition system are designed. The operation and control of the system are discussed next. Finally, the mass and power requirements of the acquisition system are presented.

4.2.1 Operating Parameters

The primary heat energy producing elements are the mission control, science experiments, life support system, TCS, and humans. After the heat energy producing elements within the module were identified, it was determined that the acquisition system was required to collect a

maximum heat load of 89 kW. 74 kW of heat is generated within the module and the remaining 15 kW is generated as heat by the TCS when operating at full load. The minimum heat load was determined to be 12 kW, assuming that the entire crew is outside the module and only the mission control system and life support system are in operation. The detailed heat load calculations are presented in Appendix E1.

The acquisition system is designed such that part of the heat load is collected by the cold plates and part is collected by the internal air loop. To determine the fraction of the heat load that the air loop must collect, ventilation requirements were considered. For adequate ventilation of the module, five air changes per hour are required. To meet this requirement, the entire volume of air within the module must pass through the life support system and the air conditioning unit five times per hour. Based on this information, a volumetric flow rate of 3 m^3/s was calculated. From psychrometric charts, it was determined that the air must be cooled to 12.7°C to remove the latent and sensible heat loads. The heat rejected by the air to the chilled water is 37 kW. Thus, the cold plate water loop was designed to remove the remaining 37 kW, as shown in Appendix E2.

4.2.2 Design of Components

Figure 23 shows the entire heat acquisition system. The major components of the heat acquisition system are the water loop and the air loop. The design of the two loops is discussed in this section.

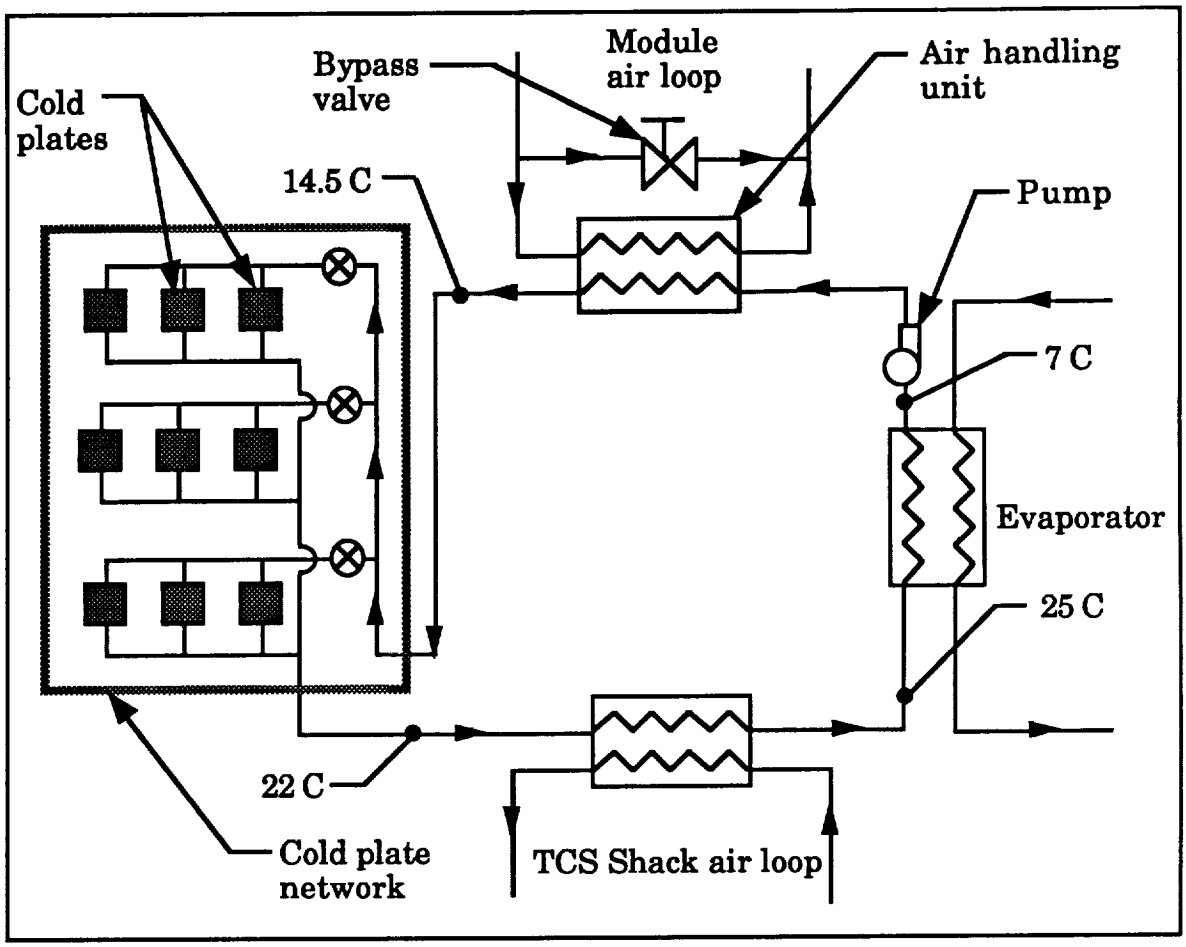

Figure 23. Overall Layout of Acquisition System

4.2.2.1 Water Loop. The heat acquisition system consists of a single pumped water loop which is first used to cool and dehumidify the air inside the module. The water is then passed through cold plates to absorb the heat generated by the equipment.

Cold plates are metallic plates attached directly to equipment inside the module. This equipment is placed on racks as shown in Figure 24. Cold plates are used because less energy is required to remove heat directly from its source than to remove heat after it has been dissipated into the air. In addition, to remove a given load, the power required to pump water

through the cold plates is less than the power required to circulate air through the equipment. The team assumed an average plate surface area of 1500 cm^2 and a thickness of 0.6 cm. The average heat flux from the electronic equipment is 1 W/cm^2 [13]. Therefore, each cold plate collects an average of 1.5 kW of heat. The cold plate network is arranged in parallel so that the temperature of the water entering the cold plates is fixed at 14.5°C and the temperature of the water leaving the cold plates is 22°C. This temperature range was selected to prevent the water vapor in the air within the module from condensing. The cold plates are placed on levels 0, 3, and 4, since it was assumed that most of the heat producing equipment will be placed on these levels. The calculations performed to design the components of the water loop are shown in Appendix E3.

Since equipment will be placed on the cold plates, the plates are required to have a high strength. Furthermore, the plates must have a high thermal conductivity because they remove heat from the equipment by conduction. Therefore, stainless steel was chosen as the material for the cold plates. The pipes of the water loop are made of a titanium alloy consisting of 6% aluminum and 4% vanadium [13]. This material is used because it is lighter than steel and has a higher strength. Another reason for using titanium is that its thermal conductivity is three times lower than steel. A low thermal conductivity is desirable in piping because the temperature of the fluid in the pipes must not be influenced by the surrounding temperatures.

4.2.2.2 Air Loop. The air loop consists of 3 main ducts. The main ducts extend from the air handling unit in level 0 to level 5, decreasing in diameter at every level, as shown in Figure 25. The diameter of each main

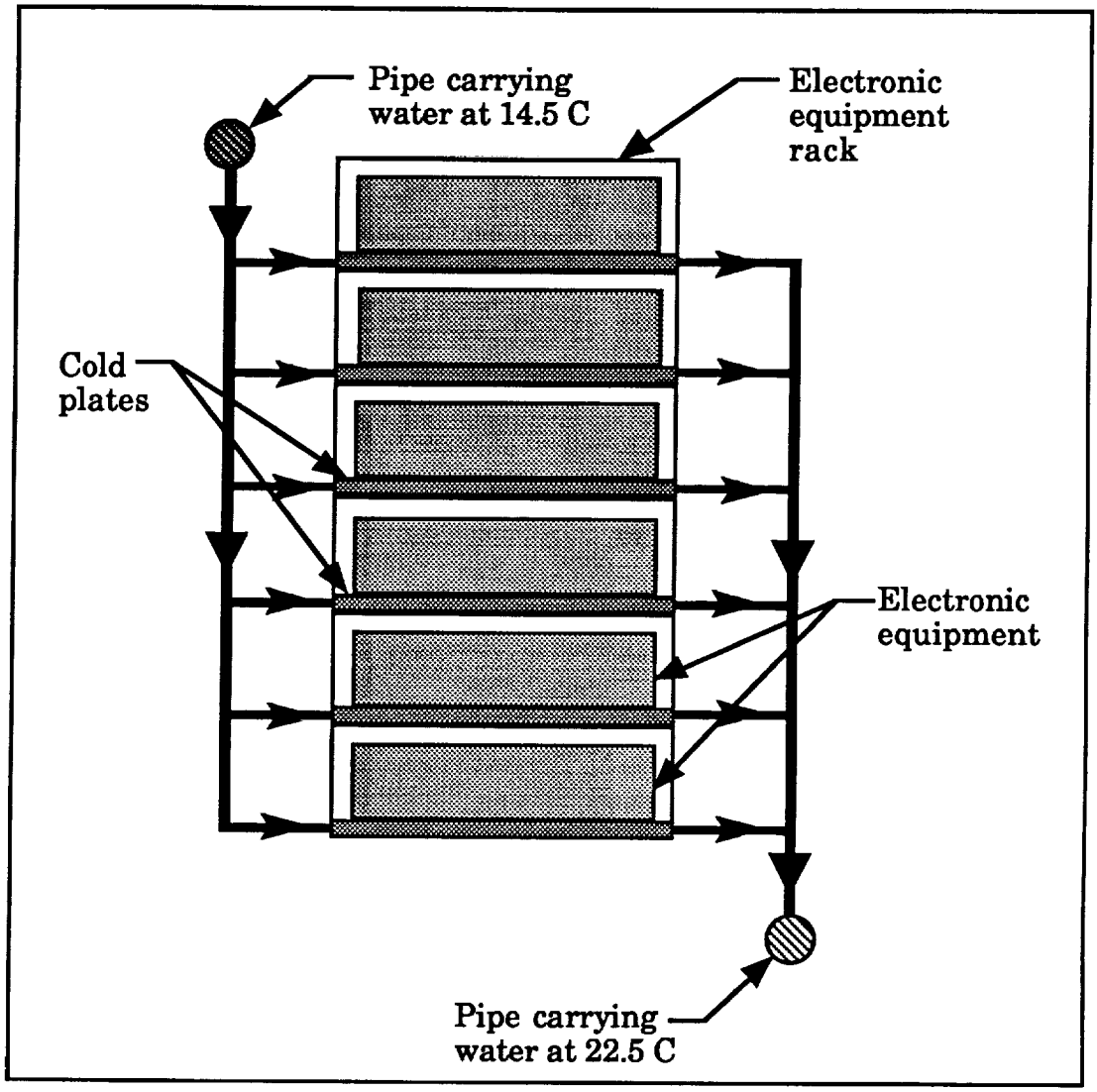

Figure 24. Cold Plate Network

duct at level 0 is 42 cm, decreasing to a diameter of 20 cm at level 5. This shape and size of the main ducts was selected to account for the reduction in volumetric flow rate of air from level 0 to level 5. At each level, two branch ducts are attached to each main duct, as shown in Figure 26. Therefore, six branch ducts are located on each level 60° apart. This configuration of the branch ducts was chosen such that air will be

circulated from the outer periphery into the core of the module. If air is passed through ducts at high velocities, the noise of the system increases. In order to keep the noise of the system low, an air velocity of 7.6 m/s was chosen for the main ducts and 6.1 m/s for the branch ducts [14]. Appendix E4 presents detailed calculations performed for the flow requirements and the duct sizes. This analysis was used to find the duct size and mass flow rate in every air duct within the module.

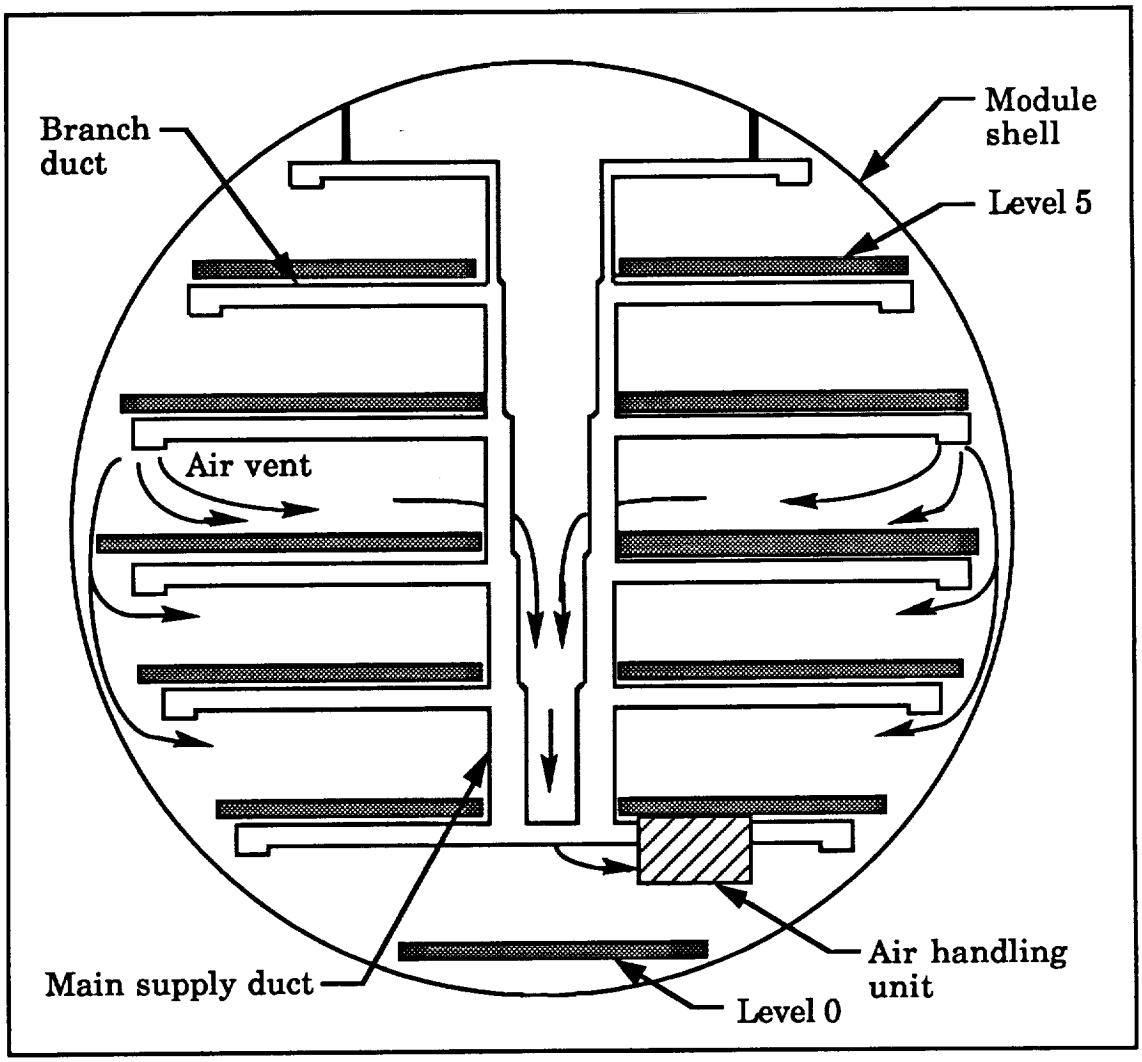

Figure 25. Side View of Ducting

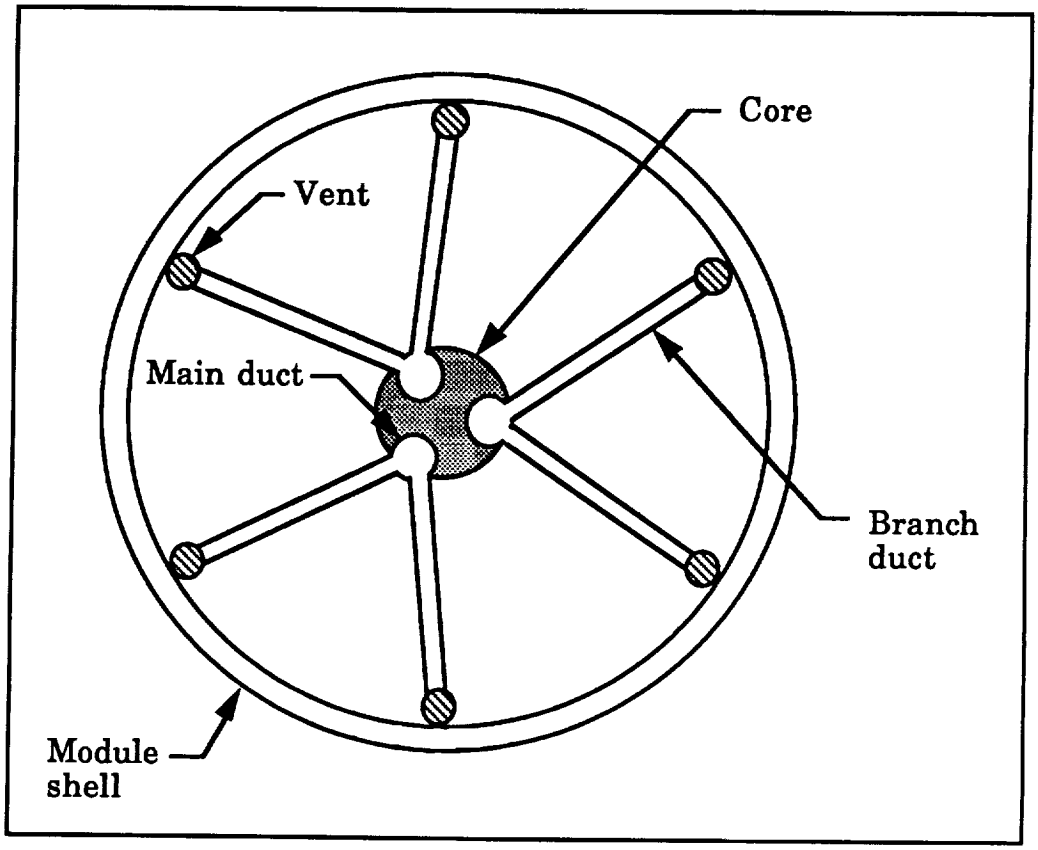

Figure 26. Top View of Ducting

4.2.3 System Operation and Control

4.2.3.1 Designing for Maximum Heat Load. At worst case operation, the acquisition system must collect 89 kW of heat. Chilled water leaves the evaporator of the transport system at 7°C and a mass flow rate of 1.18 kg/s. The water is passed through the air handling unit in the module. In this unit, air is blown over the chilled water coils. Air enters the unit at a temperature of 22.7°C and is cooled to a temperature of 12.7°C to remove the latent and sensible heat loads. Before the air enters the unit, it passes through the life support system. The life support system removes the carbon dioxide from the air and revitalizes it with oxygen. The sensible and

latent heat loads rejected by the air loop to the water loop are 34.8 and 2.15 kW respectively. The moisture in the air that condenses due to this cooling process is collected in a storage tank and returned to the life support system for purification and recirculation.

The heat transfer within the air handling unit increases the temperature of the water from 7°C to 14.5°C. The volumetric flow rate of air required to reject the latent and sensible heat loads was calculated to be 3.06 m^3/s.

After cooling and dehumidifying the air, the water at 14.5°C is then pumped through cold plates located on levels 0, 3, and 4 [15]. The mass flow rate of the water passing through each cold plates is 0.047 kg/s. The cold plates acquire 1.5 kW from the equipment which is mounted on top of the cold plates. During this process, the temperature of the water rises from 14.5°C to 22°C. The water at 22°C then leaves the module and enters the shack where the TCS is located. The air within the shack rejects 15 kW of heat to the water, increasing the temperature of the water to 25°C. Water at this temperature and a mass flow rate of 1.18 kg/s enters the evaporator of the transport system. Appendix E5 contains calculations done to determine the operation of the acquisition system.

4.2.3.2 Designing for Variable Heat Loads. To acquire the minimum heat load of 12 kW, the flow of water through the cold plates is shut off and only the air handling unit is operated. To acquire 12 kW of heat, the required air flow rate is 1.06 m^3/s. To maintain the temperature of the water entering the evaporator at 25°C, the mass flow rate of the water is reduced to 0.16 kg/s. The mass flow rate is varied by changing the speed of

the pump. Calculations to estimate the operation of the acquisition system for variable heat loads are also presented in Appendix E5.

To control the temperature within the module, a bypass valve is used. This valve is controlled by a thermostat located inside the module. When the heat load varies, so does the temperature within the module. The thermostat senses this change in temperature and adjusts the bypass valve such that a fraction of the air bypasses the air handling unit [16].

4.2.4 Mass and Power Requirements

The mass of the system was calculated by considering the air ducts, the cold plates, cold plate plumbing, and the working fluid. Based on the heat load that the system is required to acquire, the size of each major component was determined. The total mass of the acquisition system was estimated to be 1148 kg, as shown in Appendix E6. Table IV summarizes the results of the mass analysis of the acquisition system. As shown in Appendix E4, the power required to operate the acquisition system is 6.83 kW.

4.3 Transport System Design Solution

After designing the acquisition system to remove the internal heat load from the module and the TCS, the team identified the conditions under which the transport system is required to operate. Each component of the transport system was then designed to operate within such conditions. Next, working fluids that operate safely and efficiently under the specified

conditions were selected. Finally, the team calculated mass and power requirements for the transport system.

Table IV

Mass Estimate of Heat Acquisition System

Components	Mass (kg)
Ducting	797
Piping	76
Cold plates	169
Air handling unit	106
Total	**1148**

4.3.1 Operating Conditions

As mentioned in the design process, a stagewise operation of the vapor compression system is used as shown in Figure 27. During the lunar night, the sink temperature remains at -189°C. Since this temperature is much lower than the temperature of the waste heat to be rejected, heat can be rejected without the aid of the vapor compression system. Hence, the

system was designed such that both stages are bypassed during lunar night. If both stages are bypassed, the refrigerant leaves the first stage evaporator and transfers heat to the radiator fluid at 0°C. Therefore, the temperature of the radiator was determined to be -10°C. For this radiator temperature and a sink temperature of -189°C, the radiator area required to reject the maximum internal heat load was calculated using the radiation equation

$$q = \varepsilon\sigma A(T^4_{rad} - T^4_{sink})$$

where ε is the emissivity of the radiator surface, σ is the Stefan-Boltzmann constant, A is the radiator area, T_{rad} is the radiator temperature, and T_{sink} is the sink temperature. The calculated radiator area is 345 m^2. This area is the minimum area required for night operation without the aid of a vapor compression system. Since the radiator area must be minimized, the team decided to use the radiator area calculated for night operation.

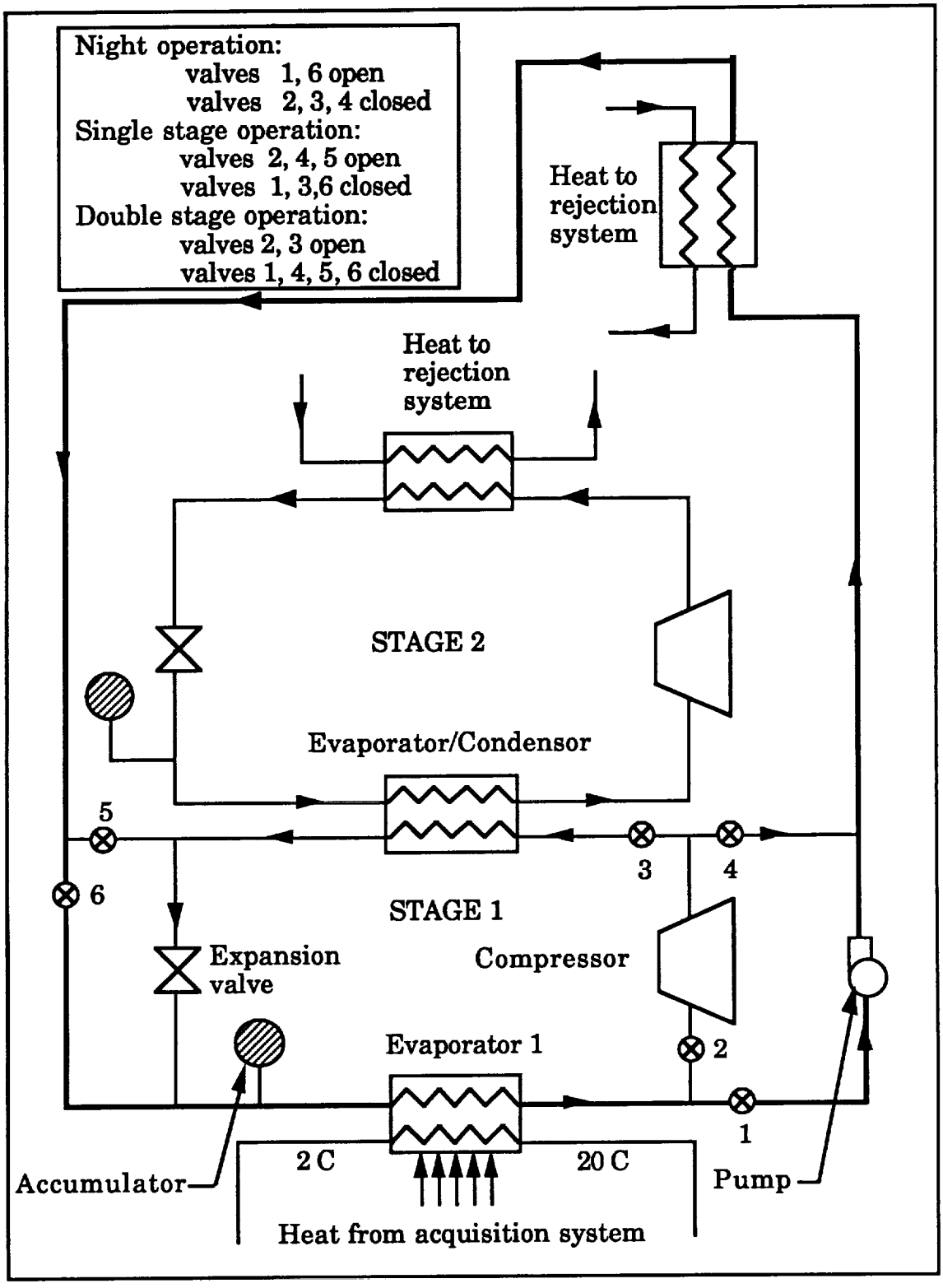

Figure 27. Overall Transport System

Using this area, the system operation at lunar noon was considered. At lunar noon, both stages of the vapor compression system will be operating. The total heat to be rejected is the sum of the internal heat load, the work done by the compressors on the refrigerant, and the heat generated by the TCS. Using the radiator area of 345 m^2, the sink temperature of 50°C at lunar noon, and the maximum heat load of 126 kW to be rejected, the temperature at which the radiator must operate at lunar noon is 98°C. To obtain this radiator temperature, the refrigerant must leave the second stage at 110°C. Hence, the maximum temperature lift of the heat transport system is 110°C. Since both the maximum and the minimum temperatures of the transport system were known, the corresponding pressures were determined. Using these pressures, the interstage pressure and temperature were calculated. Thus, the operating parameters of the transport system were defined, as shown in Appendix F1.

From the heat load calculations, it was determined that the vapor compression system must transport an internal heat load ranging from 12 to 74 kW. However, the system must also transport the work done on the fluid by the compressors and the heat generated by the compressors. Depending on the number of stages in operation, the heat generated by the compressors and the work done on the fluid vary. Therefore, the maximum and minimum heat loads to be transported depend on the number of stages in operation, as determined in Appendix F1. Figure 28 shows the maximum and minimum heat loads to be removed for stagewise operation. The maximum possible load that the vapor compression system is required to handle is 126 kW, when both stages are in operation and the

internal heat load is maximum. The minimum possible load is 12 kW, when no stages are in operation and the internal load is minimum.

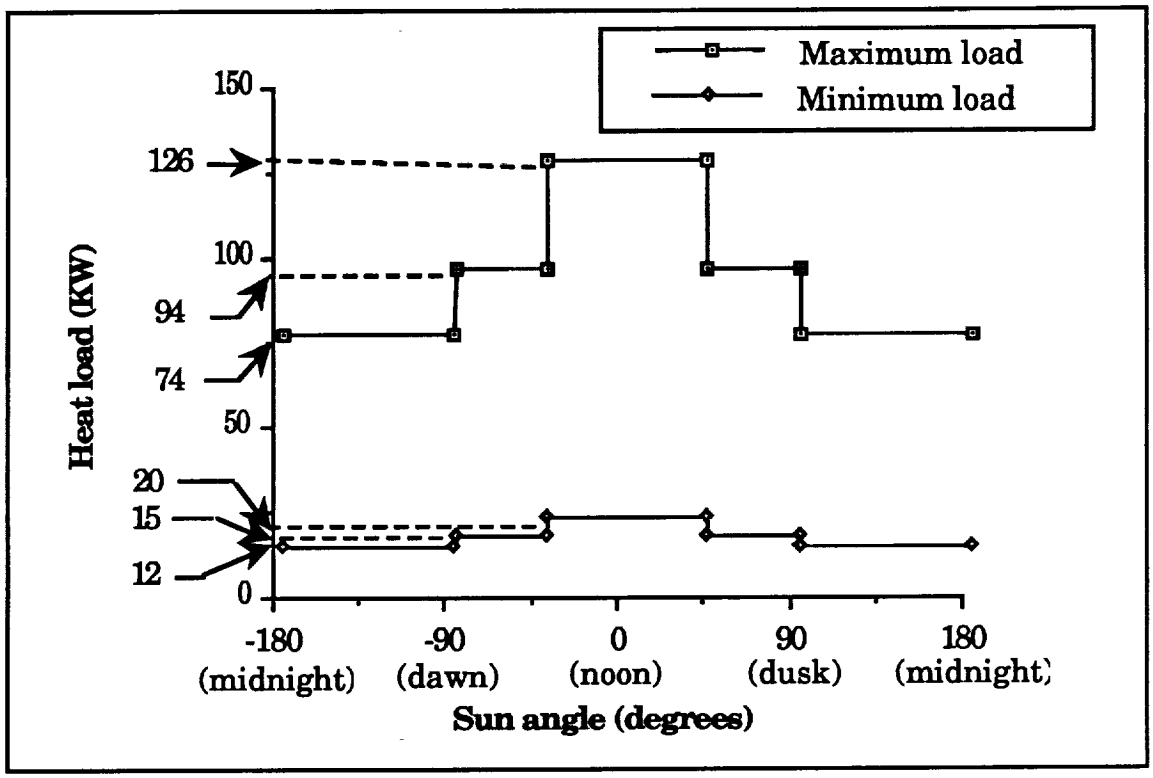

Figure 28..Heat Load for Stagewise Operation

4.3.2 Design of Components

The vapor compression system consists of evaporators, compressors, condensers, and expansion valves. The thermodynamic processes of the working fluid during a single stage of a vapor compression cycle are shown in Figure 29. Both an ideal cycle and an actual cycle, which contains non-ideal processes such as pressure drops in the evaporator and condenser, are shown. Each component is designed to enable the system to operate as

close to the ideal cycle as possible. The design of each component for the operating parameters mentioned earlier is given in Appendix F2.

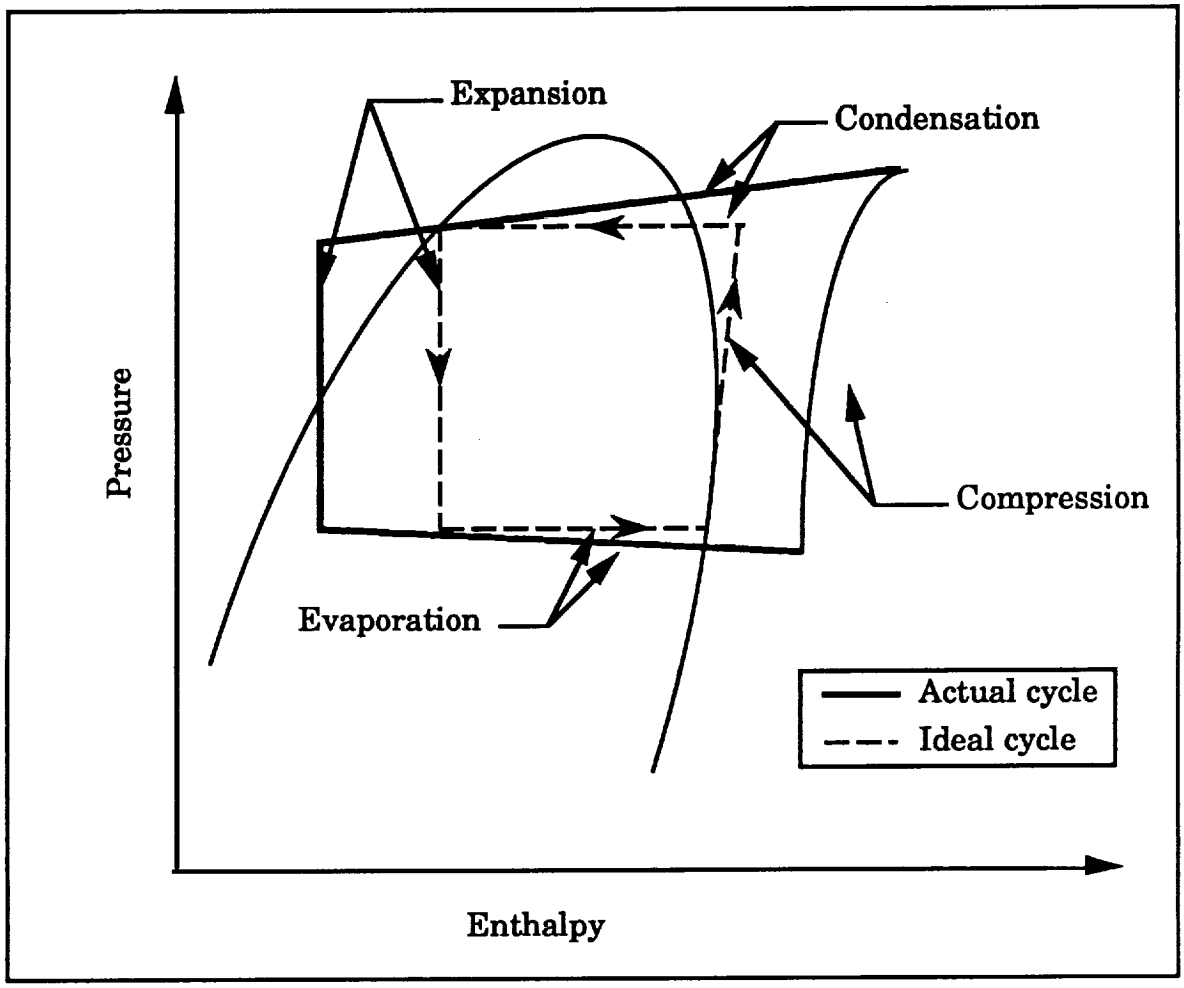

Figure 29. Actual and Ideal Vapor Compression Cycle

4.3.2.1 Design of Evaporator. The refrigerant flowing through an evaporator absorbs energy as it cools a fluid (usually water or air). The refrigeration effect is obtained by cooling this fluid. The temperature profiles as a function of position for a parallel flow arrangement are shown

in Figure 30. Because the state of the refrigerant in most of the evaporator is saturated, the pressure and temperature are linearly dependent. There is a drop in pressure in the evaporator, which accounts for the drop in temperature of the refrigerant, as shown in the figure. The drop in pressure is undesirable because as the evaporator pressure decreases, more specific compressor work is required. Thus, the COP of the system decreases. In order to minimize the drop in refrigerant pressure and temperature, a parallel flow heat exchanger was selected over a counterflow heat exchanger.

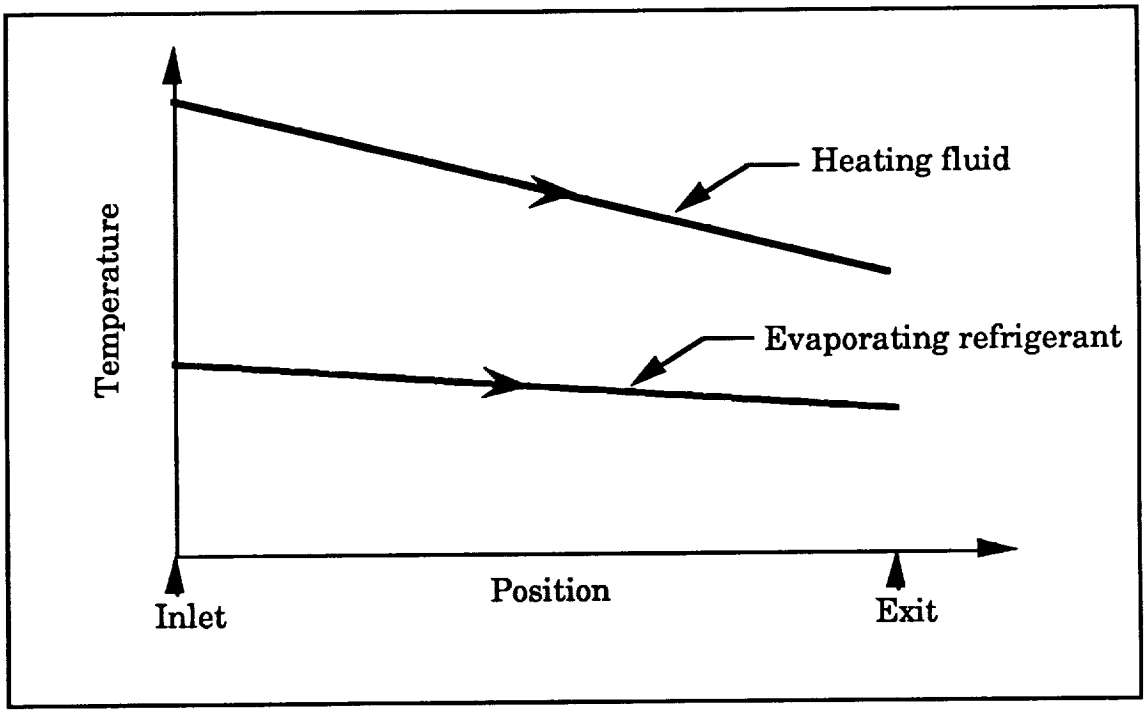

Figure 30. Heat Transfer in an Evaporator

4.3.2.2 Design of Condenser. A condenser is used to reject both the work of compression and the heat absorbed by the evaporator. To reject this

heat, the condenser's refrigerant temperature must be higher than that of the fluid cooling the condenser. As shown in Figure 31, the refrigerant exiting the compressor and entering the condenser is superheated. A short distance after entering the condenser, the refrigerant is cooled to the saturation point. Condensation then occurs over most of the heat exchanger length as the refrigerant goes from 100% to 0% quality. The temperature decrease in this two-phase region is due to the refrigerant pressure drop. Counterflow heat exchangers were chosen since they have higher heat exchanger performance than parallel flow.

4.3.2.3 Design of Compressor. A compressor is used to increase the pressure and temperature of the vapor exiting the evaporator. To select a suitable compressor for this application, various types of compressors such as reciprocating, rotary, and dynamic (centrifugal) compressors were investigated. After considering factors such as power requirements, reliability, and capacity control, it was determined that both reciprocating compressors and centrifugal compressors are suitable.

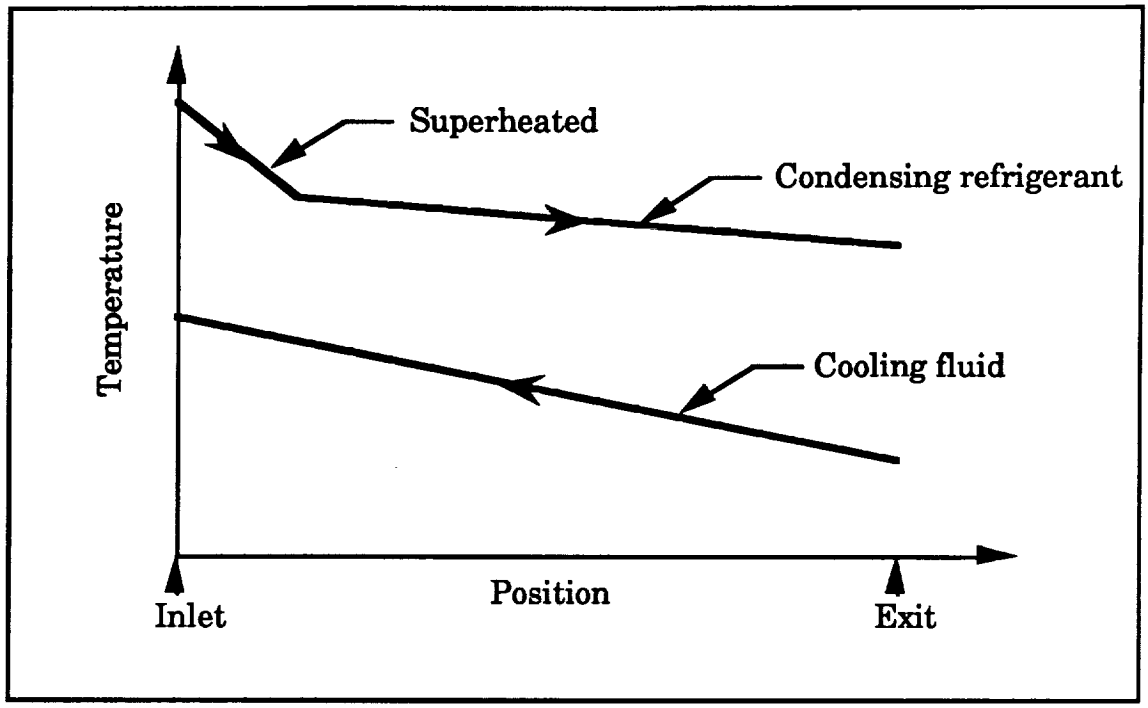

Figure 31. Heat Transfer in a Condenser

4.3.3 Selection of Working Fluid

There are a large number of working fluids which can serve as refrigerants for vapor compression cycles. An investigation of various working fluids revealed that very few can operate across a temperature range of 0°C to 100°C and remain below the critical point [17]. Hence, the design team decided to use a different working fluid in each of the two stages of the vapor compression system. An analysis of the compressor work required and the mass flow rate required was performed for various working fluids, as shown in Appendix F3. The evaluation was performed for temperature ranges of 0°C to 50°C and 50 °C to 100°C. From this study, it was determined that R12 is to be used for the first stage and R11 for the second stage.

4.3.4 System Operation and Control

This section discusses the operation of the system over a range of heat loads. The use of a stagewise operation to minimize power consumption is also discussed here. The system operation is analyzed in Appendix F2. The transport system is shown in Figure 27.

4.3.4.1 Designing for Maximum Heat Load. At worst case operation, the vapor compression system is required to transport 89 kW of internal heat from the module and TCS at temperature of 0°C to 110°C. Heat from the acquisition system is transferred to R12 in the evaporator. The R12 evaporates at 0°C and leaves the evaporator as a saturated vapor. The refrigerant then enters the compressor where it is superheated to a temperature of 60°C and a pressure of 1 MPa. The vapor enters the evaporator-condenser, where it condenses and transfers heat to R11. The R11 enters the evaporator section of the evaporator-condenser at 40°C and the heat transferred to it by the R12 enables R11 to evaporate at a pressure of 0.2 MPa and a temperature of 40°C. The R11 is then compressed to a temperature of 110°C and a pressure of 0.8 MPa. The superheated R11 vapor then enters a heat exchanger where it transfers heat to the radiator fluid at a temperature of 100°C.

4.3.4.2 Designing for Variable Heat Loads. The minimum heat load produced by the module is 12 kW. The vapor compression cycle is designed such that the temperatures and pressures at each state of the cycle remain constant, regardless of the heat load. To enable constant temperatures at each state, the mass flow rate in each loop is varied. The mass flow rate can be varied by using either an accumulator or a pump. Since the pressure of each state must be maintained at the specified value, it was

determined that an accumulator will be used to vary the mass flow rate. The maximum possible change in heat load is 77 kW, when the heat load drops from its maximum value to a minimum. In this case, the mass flow rate in the first stage loop is reduced from 0.8 kg/s to 0.1 kg/s and in the second stage loop from 0.9 to 0.1 kg/s. As shown in Appendix F4, it was determined that the accumulators will have to store a maximum of 9 kg in either loop. Since such a mass can be stored easily, the team decided to use accumulators in each loop to vary the mass flow rate.

4.3.4.3 Designing for Minimal Power Consumption. In order to minimize power consumption, the team decided to shut off the stages of the cycle at various times of the lunar day/night. One of the requirements was to have both compressors off at night. Under this operating condition, the R12 exits the first stage evaporator at 0°C and transfers heat to the radiator fluid. The temperature of the radiator is -10°C. At lunar night, the sink temperature remains at -189°C. In order to reject the maximum heat load of 74 kW, the radiator area required was determined to be 345 m^2. This is the minimum possible area required for the radiator to reject the maximum heat load at night with both stages of the cycle switched off.

Next, the design team investigated the time during which the single stage will be operated. During single stage operation, the vapor exiting the compressor is at a temperature of 60°C. The vapor exchanges heat with the radiator fluid, which gains heat at a temperature of 50°C. It was determined that for the calculated radiator area of 345 m^2, and a radiator temperature of 50°C, the maximum heat load for single stage operation of 94 kW will be rejected when the sink temperature becomes -8.7 °C. This sink temperature corresponds to a sun angle of ± 41.5°. Therefore, for any

sink temperature between -189°C and -8.7°C, a single stage operation is employed. Furthermore, for any sink temperature above -8.7°C, the radiators will not be able to reject the maximum heat load of 94 kW. Thus, two stage operation is employed for sink temperatures greater than -8.7°C. Based on the analysis presented in Appendix F5, the stagewise operation of the transport system for various sink temperatures is shown in Figure 32.

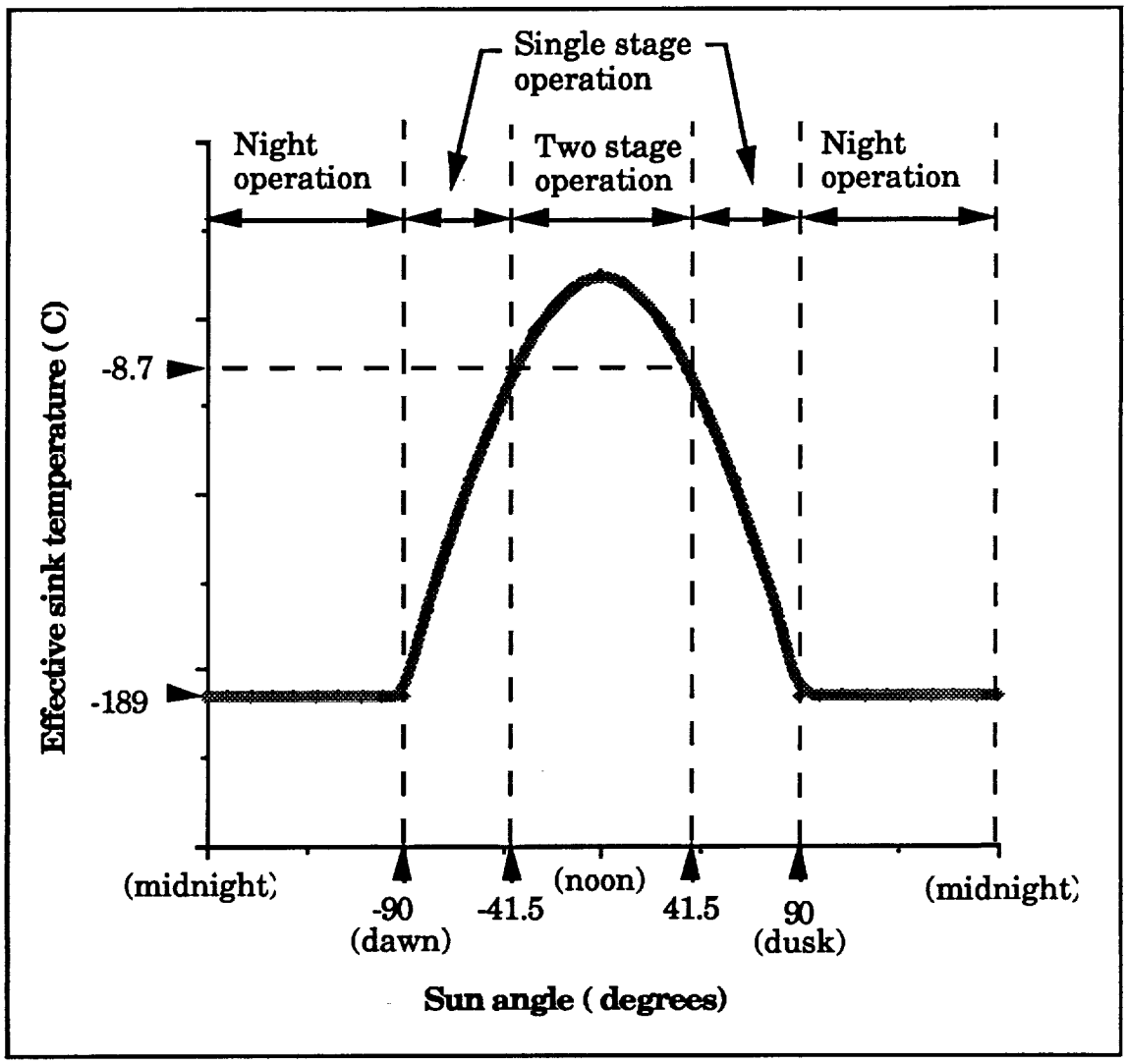

Figure 32. Stagewise Operation vs Sink Temperature

4.3.5 Mass and Power Requirements

The power consumed by the vapor compression system as a function of sun angle for maximum heat load is shown in Figure 33. The average power consumption is 17.8 kW.

The mass of each component of the vapor compression system was also calculated. For each heat exchanger, the temperature differences and the maximum heat transfer were used to calculate the UA parameter. The UA parameter is the product of the overall heat transfer coefficient and the surface area available for heat transfer. The objective in heat exchanger design is to provide as much surface area as possible between two fluids while also minimizing the pressure drop. The mass of the heat exchanger is thus dependent on both the area and the overall heat transfer coefficient. For each heat exchanger, the overall heat transfer coefficient and area were determined. Using a correlation from reference x, the mass of each heat exchanger was found from knowledge of the UA parameter. For each compressor and pump, the maximum power was calculated. The maximum power was related to the mass of compressor or pump. The mass of the piping was also estimated. The mass of the accumulators was estimated using the maximum mass it is required to hold. The mass and power estimates for the complete transport system are given in Appendix F6. Based on this analysis, the average power consumption is 18 kW and the mass of the transport system is 1413 kg. A summary of the mass estimate is given in Table V.

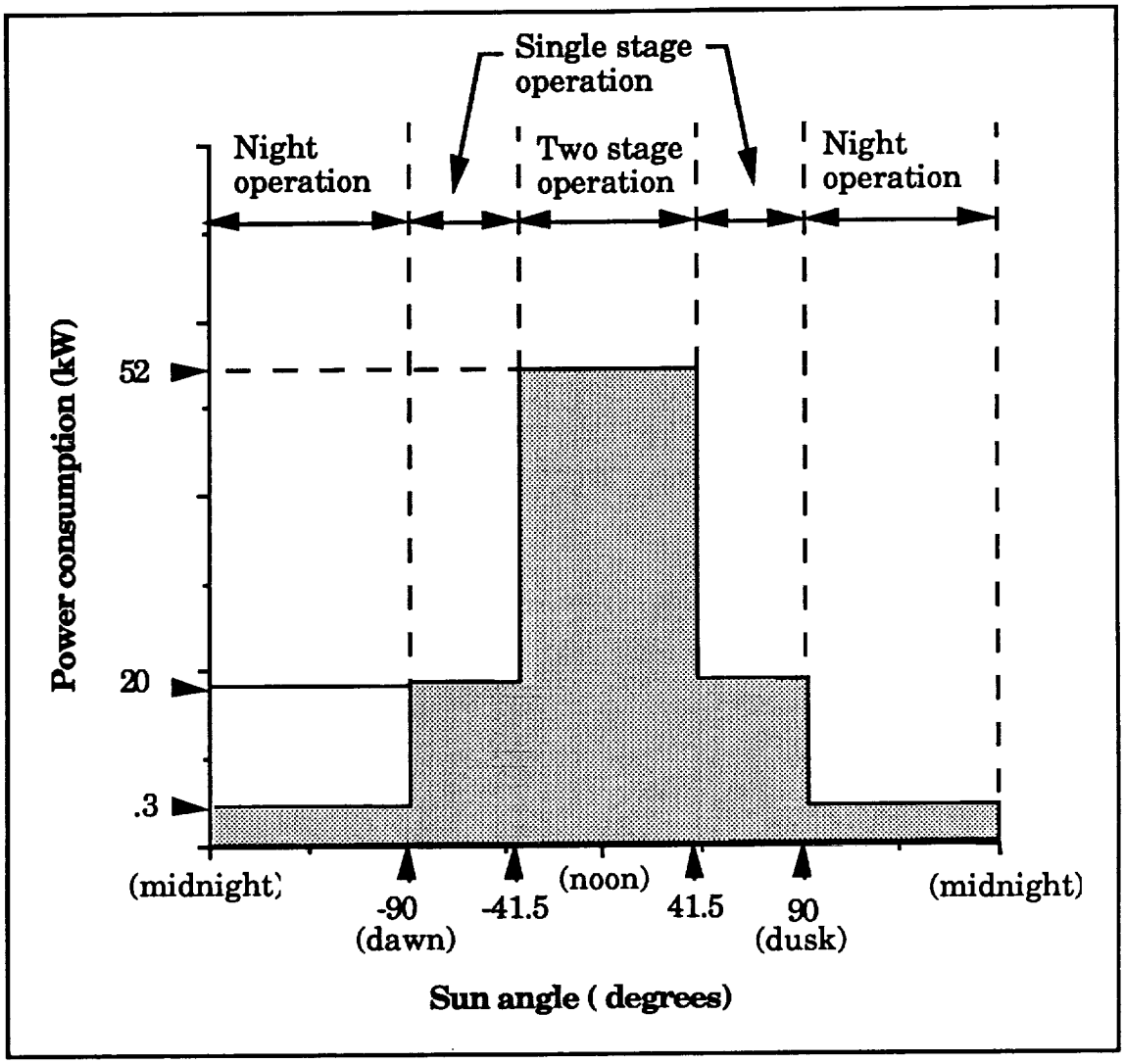

Figure 33. Power Consumption of Transport System

Table V

Mass Estimate of Heat Transport System System

Components	**Mass (kg)**
3 Evaporators	1090
Condenser	193
2 Compressors	40
Piping and working fluid	90
Total	**1413**

4.4 Heat Rejection System Solution

Following the design of the transport system, the heat rejection system was designed. The function of the heat rejection system is to reject the heat transported by the vapor compression system. This section discusses four topics. First, the operating conditions under which the reflux boiler radiator must operate are defined. Next, design of the components of the rejection system are discussed. The operation and control of the system for varying conditions are explained next. Finally, a mass estimate of the heat rejection system is presented.

4.4.1 Operating Conditions

At any given time, the radiator is required to reject the internal heat generated within the module, the heat generated by the TCS, and the work imparted by the compressors to the working fluid. The heat generated by the TCS and the compressor work done on the fluid depend on the internal heat load as well as the number of stages in operation. Hence, the maximum and minimum heat loads to be rejected depend on the number of stages in operation, as shown earlier in Figure 28. Furthermore, the system must be able to reject any intermediate heat load.

The system must be adaptable to reject the maximum and minimum heat loads. To accomplish this function while keeping the power consumption of the transport system low, the radiator must operate at three different temperatures corresponding to the number of stages operating.

The radiator fluid must therefore be a saturated vapor at three different temperatures. These radiator temperatures are summarized in Table VI.

Table VI

Operating Temperature of Radiators

Night operation	Single stage operation	Double stage operation
-10 C	50 C	100 C

The radiators are subjected to varying sink temperatures. Therefore, for a given radiator temperature, the heat rejection capability varies with time. The rejection capability of the radiator must therefore be controlled such that the radiator does not reject more heat than is transported by the vapor compression system.

4.4.2 Design of Components

4.4.2.1 Reflux Boiler Radiator Design. The original reflux boiler radiator concept consists of a closed vessel in which both boiling and condensation take place. However, the radiator fluid is required to evaporate and condense at -10°C, 50°C, and 100°C. In order to obtain a high quality saturated vapor at three different temperatures, the saturation pressure of the working fluid must be varied. The design team determined

that changing the pressure within a closed system is inefficient. Hence, the team decided to use a pump to increase the saturation pressure and a throttling valve to decrease the pressure of the working fluid. It was determined that the working fluid must be evaporated before entering the radiator. This modified reflux boiler concept is illustrated in Figure 34. The vapor enters the radiator through a pipe and condenses along the side walls of the radiator. The condensate collects at the bottom of the radiator and joins the return line.

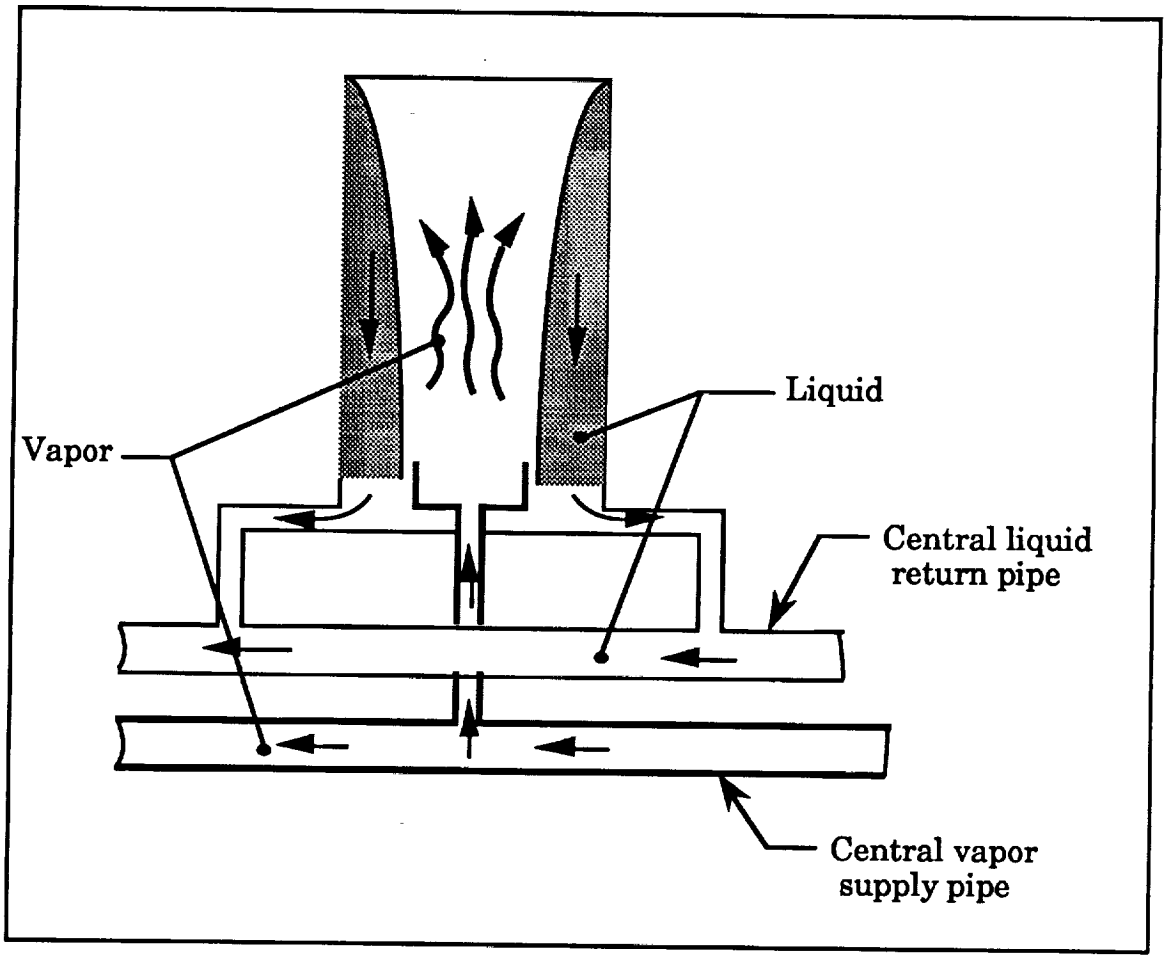

Figure 34. Modified Reflux Boiler

The operating temperature of the radiator working fluid varies from -10°C to 98°C. A fluid that can operate over this range of temperature without nearing the critical point is required. An investigation of various refrigerants showed that R114 is suitable for this application. This fluid was used in the reflux boiler analysis presented here.

The design team investigated radiator shapes of circular and rectangular cross-section. Cylindrical radiators have a higher surface area to volume ratio than rectangular radiators. However, the effective sink temperature for a rectangular vertical radiator is lower than the sink temperature for a cylindrical radiator. Furthermore, the effective area for radiation of aligned cylindrical radiators is much less than that of aligned rectangular radiators, due to radiative exchange between adjacent cylindrical surfaces. Hence, the design team selected rectangular radiators. These radiator surfaces are aligned east-west, and the non-radiating surfaces are insulated. The spacing between the radiator walls must be minimized so that the area of the non-radiating surfaces are minimized.

The design of the radiator involved determination of the length of the radiator and the spacing between the radiator walls. The reflux boiler must be designed such that the temperature difference between the vapor and the radiator wall must be minimized. To achieve these conditions, the film thickness and hence the length of the radiator must be minimized. However, a fixed radiator area of 345 m^2 is required. If the length is minimized, the width of the radiator will be too great. Due to various transport limits, constraints are placed on the minimum length and

minimum spacing between the radiator walls. These limits include the boiling limit, entrainment limit, and the sonic limit.

Since the vapor and liquid move in opposite directions, a shear force exists at the liquid-vapor interface. If the vapor velocity is sufficiently high, a limit can be reached at which the shear force is so high that the liquid cannot return to the bottom of the tube. This limit is the entrainment limit. When the entrainment limit is reached, part of the radiator wall becomes dry. Consequently, the radiator walls cease to be isothermal.

The critical vapor velocity at which entrainment occurs depends on the mass flow rate of both the vapor and the condensate [18]. For the maximum heat load, the mass flow rate of the vapor will be maximum. The mass flow rate of the condensate depends on the length of the tube. Hence, for the maximum heat load, the critical vapor velocity depends on the radiator length.

The mass flow rate of the vapor is also limited by the sonic limit [19]. The flow of vapor in the reflux boiler vapor core is similar to the flow characteristics encountered in a converging-diverging nozzle. For a given vapor core area, there is a maximum mass flow rate of vapor that can be transported up the tube. Any further increase in the heat load transported by the vapor will increase the mass flow rate, resulting in supersonic flow of the vapor. Since the mass flow rate of the vapor does not increase, the heat transfer along the tube does not increase. Hence, a large axial temperature gradient along the tube is formed and isothermal operation of the radiator is not possible. The radiator cross-sectional area must be designed such that for high heat loads, the area is sufficient to prevent sonic flow from occuring.

In accordance with these limits, the radiators were designed. Each side of the radiator was modelled as a vertical flat plate with vapor condensing along its sides, as shown in Figure 35. At steady state, the heat flux transferred from the condensate to the radiator wall must equal the heat flux radiated to the environment. Using this energy balance, the average convection heat transfer coefficient is related to the radiator temperature by

$$h = \varepsilon\sigma(T^4_{rad} - T^4_{sink}) / (T_{sat} - T_{rad})$$

where T_{sat} is the temperature of the saturated vapor, T_{sink} is the sink temperature, T_{rad} is the radiator temperature, ε is the emissivity, and σ is the Stefan-Boltzmann constant. For condensation along a vertical plate, the convection coefficient is also related to the film length by a correlation given in reference x. Combining the two relations, the radiator temperature as a function of radiator length was determined. The team found that the radiator temperature differed by a very small amount from the vapor temperature, even for very large lengths. As shown in Figure 36, for a length of 17 m, the radiator surface temperature is only 0.5°C less than the vapor temperature. Hence, the team assumed that the surface temperature was the same as the vapor temperature for the overall analysis of the TCS. This graph illustrates the high fin efficiency of the reflux boiler radiator. Furthermore, the graph shows that the fin efficiency decreases slightly for large increases in radiator length.

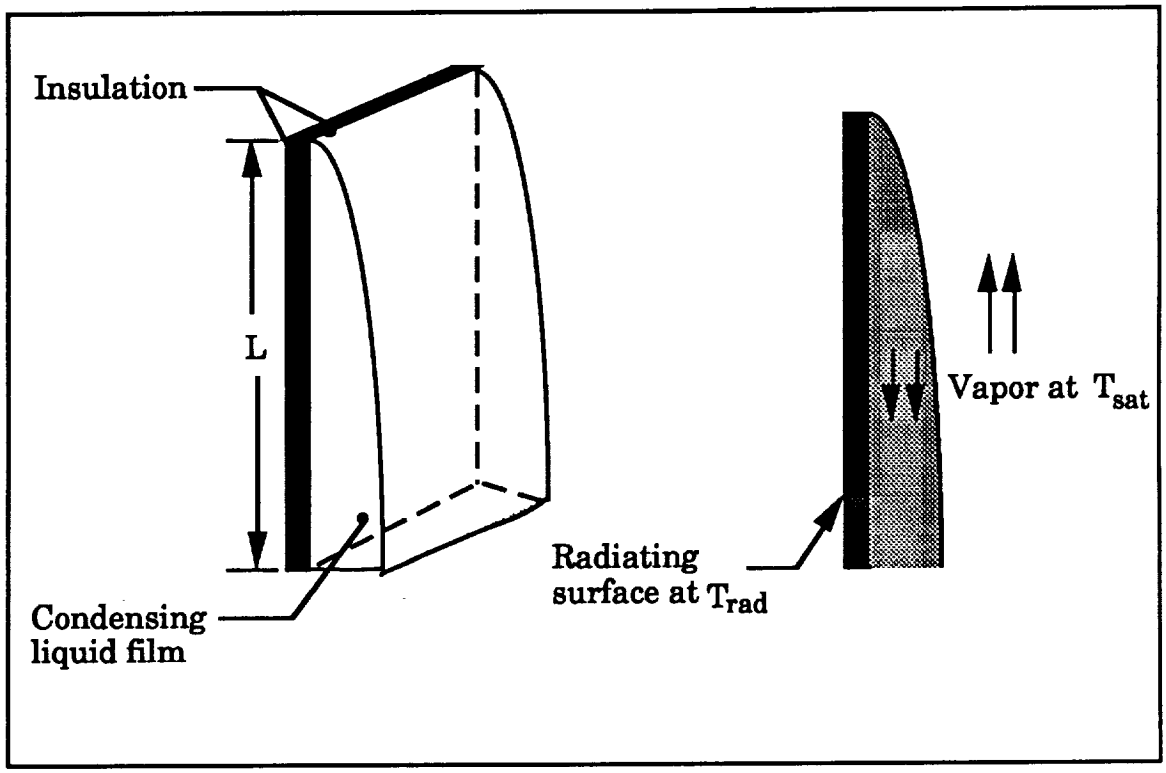

Figure 35. Reflux Boiler Modelled as Vertical Plate

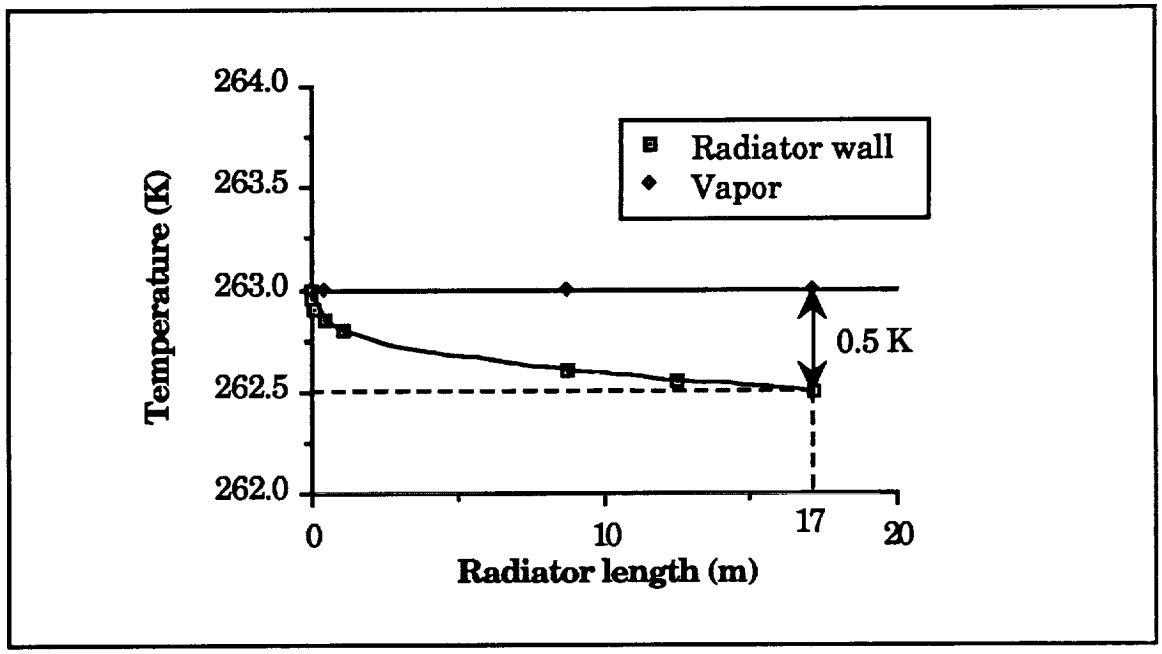

Figure 36. Radiator Temperature vs Length

Since the radiators must be modular, the team used twenty radiators. The team determined the critical flux at which the sonic limit is reached. For the maximum heat load, the minimum cross-sectional area to prevent the sonic limit from occuring was found. Each rectangular radiator is 17.25 m long and 0.5 m wide, providing a total radiator surface area of 345 m^2. For this length, the critical vapor velocity was found to be six times higher than the actual maximum vapor velocity. Hence, for the radiator dimensions selected, none of the transport limits will be exceeded. The calulations for the design of the reflux boilers is presented in Appendix G1.

4.4.2.2 Design of Pressure Control Subsystem. The function of the pressure control subsystem is to vary the pressure of the radiator fluid such that it will evaporate at the three different operating temperatures specified. The pressure control system consists of a pump and an expansion valve, as shown in Figure 37. The pump is required from dawn to noon, when the radiator temperature must be increased from -10°C to 50°C, and then from 50°C to 100°C. The pump is therefore required to operate only twice during the day. Just before the first stage is switched on, the fluid returning from the reflux boiler at a temperature of -10°C is pumped to a higher pressure. This pressure corresponds to a temperature of 50°C, enabling the radiator fluid to evaporate at this temperature. A similar process occurs just before the second stage is switched on, resulting in another increase in the pressure of the working fluid. From noon to dusk, the expansion valve is required twice to reduce the pressure of the radiator fluid.

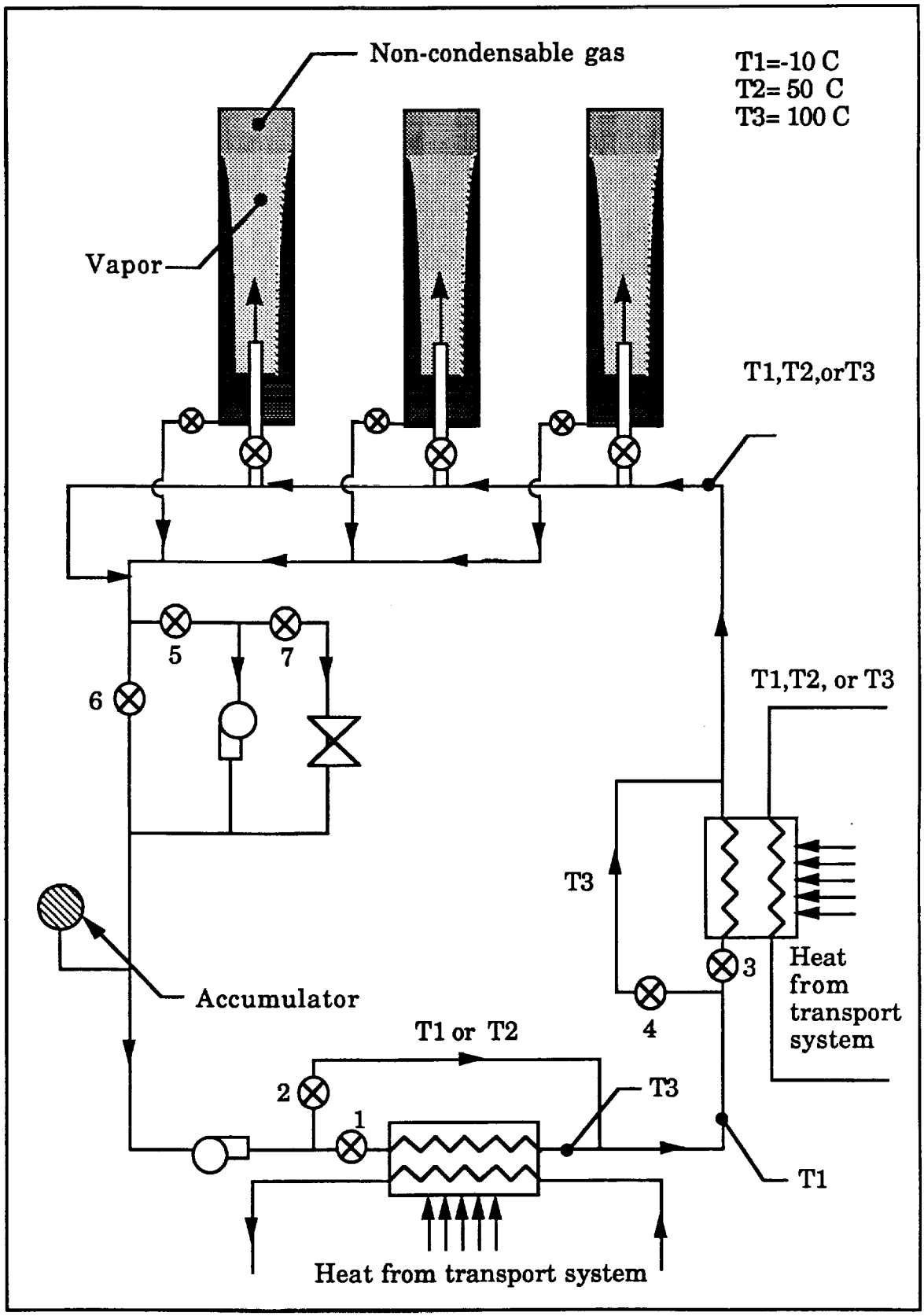

Figure 37. Overall Rejection System

4.4.3 System Operation and Control

For night operation, the radiator fluid takes the path shown in Figure 37. Valves 2 and 3 are open, while 1 and 4 are closed. As a result, the radiator fluid bypasses heat exchanger A and vaporizes in heat exchanger B. This vapor then enters the radiators where it condenses down the walls of the radiator. The condensate is collected at the bottom of the radiator where it joins the main liquid return line. The radiator fluid is designed to be at a pressure corresponding to a saturation temperature of -10°C.

The first stage is switched on around dawn, when the sink temperature is just above -189°C. Before the first stage is switched on, valves 6 and 7 are closed and valve 5 is opened. The pump is used to raise the pressure of the radiator fluid to a value corresponding to the saturation temperature of 50°C. When the first stage is switched on, the R12 exiting the compressor exchanges heat with the radiator fluid in heat exchanger B, which evaporates and enters the radiator. Before the second stage is switched on, the pump is again used to raise the pressure of the radiator fluid in order to evaporate it. When the second stage is switched on, valve 1 and 4 are open, and 2 and 3 are closed. The radiator fluid exchanges heat with R11 in heat exchanger A and bypasses heat exchanger B. Just before each stage is switched off, valve 5 and 6 are closed and valve 7 is opened. Thus, the radiator fluid is sent through the expansion valve to reduce its pressure so that it can be evaporated at a lower temperature.

4.4.3.1 Designing for Maximum Heat Loads and Maximum Sink Temperature.

The heat rejection capability of the radiators is given by the equation

$$q = \varepsilon\sigma A(T^4_{rad} - T^4_{sink})$$

where ε is the emissivity, σ is the Stefan-Boltzmann constant, A is the area, T_{rad} is the radiator temperature, and T_{sink} is the sink temperature. The variation of heat rejection capability and the maximum possible heat load with sun angle are shown in Figure 38. Based on the equation, the amount of heat rejected by the radiators can be controlled by varying the emissivity, area, or radiator temperature. For each stage of operation of the vapor compression cycle, the radiator temperature was designed such that it rejects the maximum heat load at the highest sink temperature during that stage. As illustrated in Figure 38, the maximum sink temperature at each stage occurs at points A, B, and C. However, if the sink temperature decreases, the radiators are capable of rejecting more heat than is required at maximum heat load.

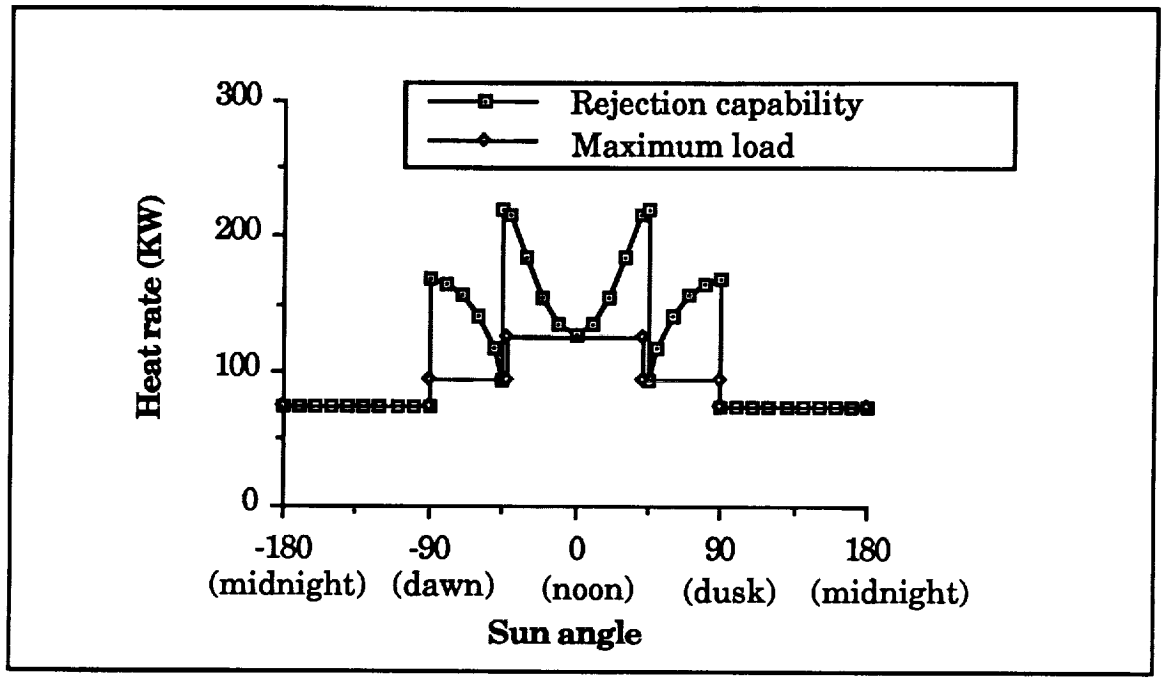

Figure 38. Rejection Capacity for Stagewise Operation

4.4.3.2 Designing for Maximum Heat Load and Varying Sink Temperature. In the previous section, the rejection system was initially designed for the highest sink temperature. Consequently, the system will always have a higher rejection capability than the heat load, except at the maximum sink temperature at each stage. The excess rejection capacity varies from 0 to 94 kW. Based on the radiation equation, there are three means of controlling the rejection capability of a radiator: control of emissivity, radiator temperature, and area.

Louvers are used used to change the absorptivity to emissivity ratio of the radiator. By opening or closing the louver blades over the radiator surface, the effective emittance of the radiator is varied. However, this concept was proved infeasible for lunar applications in a study done by NASA. Next, the team investigated control of radiator temperature. As the

the radiator temperature is fixed because of stagewise operation, this method of control could not be used without increasing the number of stages of the vapor compression system.

Finally, the team investigated ways to control the rejection capability of the radiators by controlling the radiator area. Two independent control techniques were used to solve the problem of excess rejection capability. The first technique used was to bypass radiators. To bypass a radiator, the valve connecting the radiator fluid loop to the radiator is closed. Hence, no vapor enters the radiator. All the vapor inside the radiator condenses down the walls and returns to the main loop. Therefore, the effective area for radiation decreases. Since twenty radiators are used, the area of each radiator is 17.25 m^2. By bypassing radiators, the radiator area can be varied from 0 to 345 m^2 in increments of 17.25 m^2.

For the twenty one possible discrete radiator areas, the sink temperature at which the rejection capacity equals the maximum heat load was found. Consequently, a sequence in which each radiator is bypassed was determined, as shown in Appendix G2. The excess rejection capacity varies from 0 to 10 kW, as shown in Figure 39. Using this technique, the excess rejection capability is greatly reduced. This effect is illustrated in Figure 40.

By providing discrete variations in area, the excess rejection capability can be reduced but not completely eliminated. Because the sink temperature is a continuous function of time, the area of the radiators must be varied continuously to completely eliminate the excess rejection capability. In order to do so, the variable conductance concept is suggested [20]. This concept involves using a noncondensable gas in a reservoir

attached to the reflux boiler radiator, as shown in Figure 41. The pressure in the gas reservoir is the same as the saturation vapor pressure of the radiator fluid. A decrease in the sink temperature will cause more heat to be lost momentarily by the radiator fluid, resulting in a small decrease in vapor temperature. Since the vapor is saturated, a small temperature decrease causes a large drop in vapor pressure. The change in vapor pressure causes the noncondensing gas from the gas reservoir to enter the radiator, resulting in a decrease in the area available for condensation. By decreasing the area, the heat rejection capability will decrease such that the heat rejected equals the heat load to be rejected.

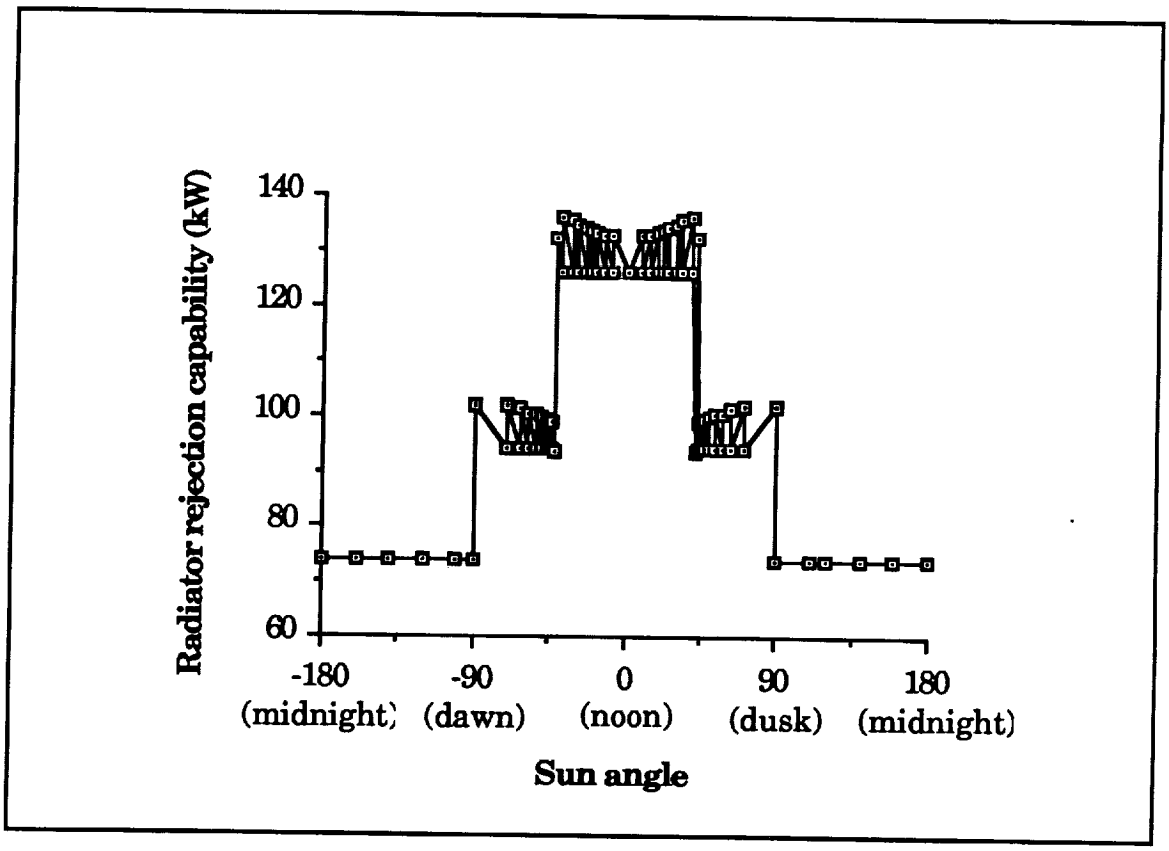

Figure 39. Rejection Capacity with Radiator Bypass

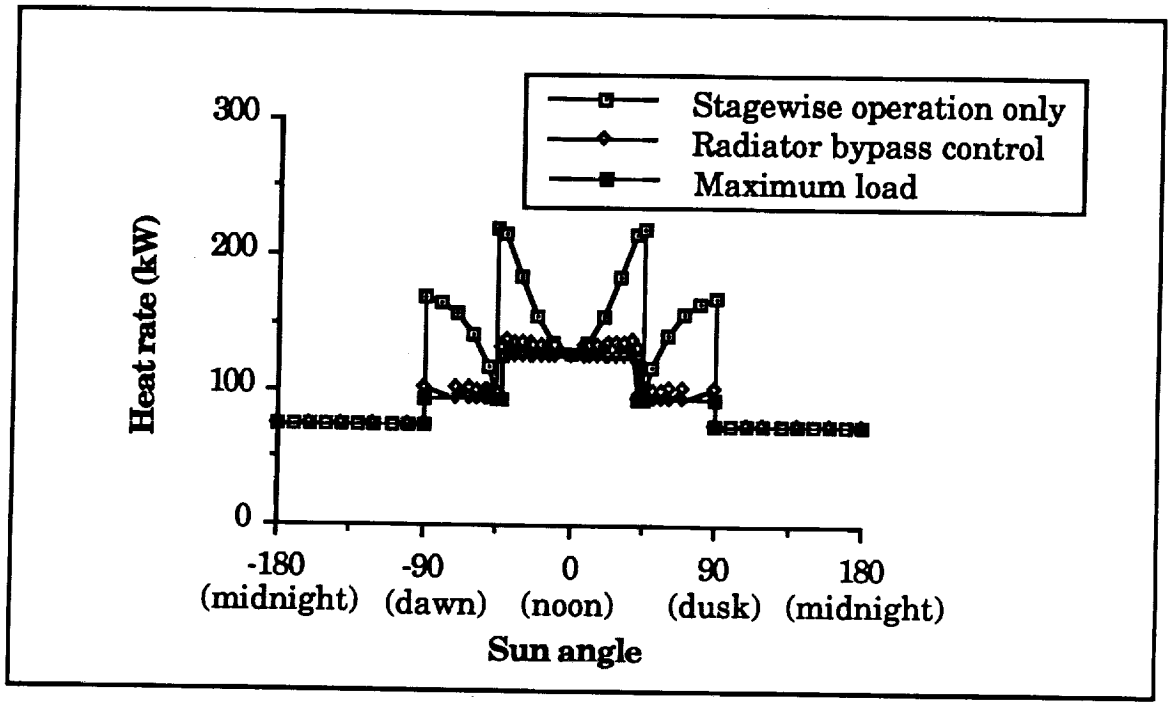

Figure 40. Effect of Bypassing Radiators

This concept may be used without bypassing radiators. The worst case occurs when the heat load is minimum (20 kW) and the sink temperature is -8.7°C, corresponding to point D on Figure 40. As can be seen, the heat rejection capability of the radiators is about 225 kW. For this case, the area change required of each radiator is 14.25 m^2. Due to the excess storage volume required, the mass of the radiator will greatly increase. However, if the radiators are bypassed, the heat rejection capability is about 132 kW. Therefore, the area of each radiator will have to be reduced by only 6.25 m^2. These calculations are also shown in Appendix G2.

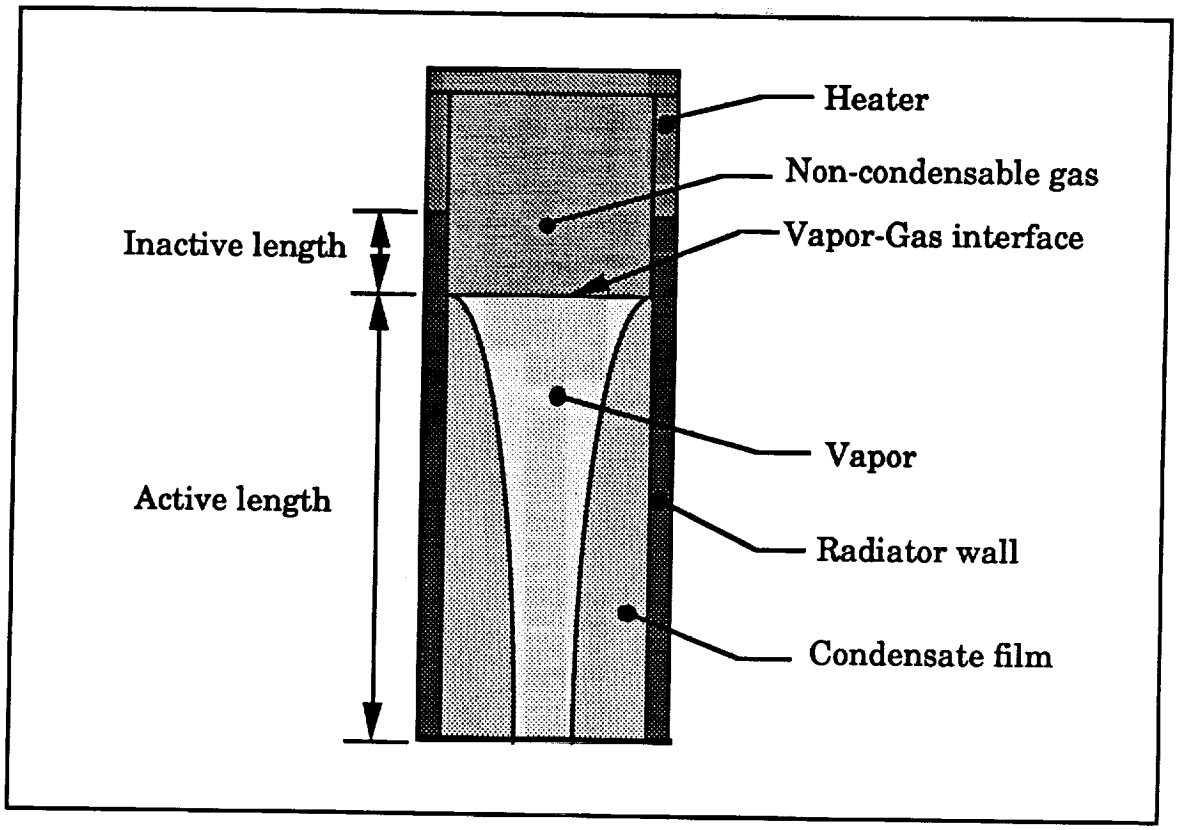

Figure 41. Variable Conductance Concept

4.4.3.3 Designing for Variable Sink Temperature and Variable Heat Load. In the two previous sections, the temperature control systems discussed were designed for the maximum heat load. However, the rejection system must account for variable heat loads. When the heat load decreases, the mass flow rate of the radiator fluid is decreased using an accumulator. Depending on the mass flow rate, the number of radiators to be used is determined by the relation

$$\text{Number of radiators used} = m_c / m_i,$$

where m_c is the current total mass flow rate in the loop and m_i is the mass flow rate into each radiator at design level. This system coupled with the variable conductance concept will enable the heat rejection capability to equal the heat load at any given time.

To control the system for varying sink temperature, the technique of bypassing radiators explained in the previous section is used. If the heat load and sink temperature vary simultaneously, the two independent control techniques are used. Using each technique, the number of radiators to be used is determined. The system selects the lower of the two values. The variable conductance concept superimposed on the above two control methods will ensure that the radiator area is adjusted for both the change in heat load and the change in sink temperature. Thus, the amount of heat rejected by the radiators will equal the heat load to be rejected.

4.4.4 Material for Radiator.

A material proposed for radiators to be used on Space Station Freedom is Advanced Ceramic Fabric (ACF) material. This composite material consists of lightweight ceramic fabrics bonded with thin metallic foils. The outer layer consists of the ceramic material. The inner layer is a metallic foil which acts as the pressure boundary to contain the working fluid [21].

ACF materials being studied include carbon fibers, fused silica, and silicon carbide. These materials have a higher strength to mass ratio than traditional metallic radiator surfaces. Furthermore, ACF materials are compatible with various working fluids.

Table VI

Mass Estimate of Heat Rejection System

Components	Mass (kg)
Radiators	1725
Piping	14
Working fluid	130
Total	**1869**

4.4.5 Effect of Lunar Environment. Since the transport system will be placed in a shack under the regolith, the radiators will be the only components of this system that are directly exposed to the lunar surface. The effect of lunar dust on radiators is a harmful one. The only means by which lunar dust can be kicked up is due to surface operations. Hence, surface operations must not be performed near the side of the module that the TCS is located. Furthermore, the radiators must be aligned such that the surfaces do not face the regolith covering the module. If the radiators face the module, the sink temperature seen by the radiator will be higher.

Conclusions

This report contains the conceptual design of a thermal control system for lunar applications. Alternative designs for heat acquisition, heat transport, and heat rejection were presented in this report. Feasibility studies on alternatives of each subsystem showed that the single water-loop, the vapor compression cycle, and the reflux boiler radiator were the most feasible alternatives. Combination of these subsystems yielded an overall system that satisfied the design criteria mentioned earlier in the report. The extent to which the overall system meets the most important design criteria is discussed below.

The mass of the system was kept low, since low mass was the most important design criterion. Mass estimates and power requirements for the TCS are given in Table VII. The design team did not optimize the mass of the overall system. The total system mass is about 4430 kg. This mass is comparable to a TCS of mass 1927 kg, with about half the cooling capacity of the TCS presented in this report [22].

The power requirements of the system were also considered. The team determined that the average power consumption can be decreased by using a stagewise operation. The use of a stagewise operation is especially feasible for lunar applications because the sink temperature at lunar night is extremely low and remains so for 14 earth-days.

Table VII

Mass and Power Estimates for TCS

Subsystem	Mass (kg)	Power (kW)
Acquisition	1148	6.8
Transport	1413	17.8
Rejection	1869	.3
Total	**4430**	**24.9**

Control of the system for variable heat loads and variable sink temperatures was another important design criterion. This criterion was met by using a stagewise operation, bypassing radiators, and by using the variable conductance concept.

The design team considered the adaptability of the system to the lunar environment. The placement of the system was discussed with respect to the lunar dust kicked up during surface operations. Although the effect of lunar dust is an important factor in the radiator design, the extent of its effect on radiator surfaces is unknown. However, the design team accounted for the fact that the emissivity of the radiator decreases with time. The effect of micrometeorites on the placement of the radiators was also not considered, since micrometeorite impacts on the lunar surface are considered to be random.

Various safety requirements were also considered. No toxic fluids were used inside the module. The radiators were designed to be modular, so that a failure in one radiator will not affect the performance of the other radiators. A redundant system was not designed in this study, although it was used as a criterion for comparing the alternative designs.

Recommendations for Future Study

The aim of this report was to design the three subsystems of the TCS to acquire, transport, and reject heat from the module to the lunar environment. Although the design team met this goal, much more work must be done on this project before prototypes can be built.

The heat load calculations performed in this report were based on equipment to be used on Space Station Freedom. To perform a detailed design of a TCS for lunar applications, more background information is needed regarding the lunar mission. To accurately determine the heat load, the designer must know exactly what equipment will be inside the module. The crew size must also be determined.

The mass estimates presented in this report were for components used for terrestrial applications. Mass estimates of components designed specifically for space applications must be determined. Furthermore, the mass of the TCS must be minimized. If the radiator area is reduced, the radiator temperature must increase. Hence, the temperature lift of the vapor compression system must increase. If the temperature lift of the vapor compression system increases, the mass and the power requirement increases. Hence, the radiator area and the temperature lift of the system must be varied such that the total mass of the system is minimized. The radiator must be operated at a temperature at which the total mass is minimum.

The analysis of reflux boilers presented in this report only demonstrates feasibility of the concept. Hence, it is at an elementary level. No correlation adequately estimates the thermal performance of a reflux boiler in a low-gravity environment. An analysis that accounts for the low-gravity effect is needed.

It is important to determine what the available power source will be for the lunar mission. If a nuclear power source is used, high temperature waste heat is available. Consequently, using a heat driven cycle instead of a work driven cycle will result in a large saving of power.

The upper plate of a parallel plate radiator functions as both a shading device and a solar collector. It was determined that the low temperature heat absorbed by a parallel plate radiator cannot be used to drive a heat driven cycle. However, if low temperature heat can be used for some other purpose, the parallel plate radiator concept must be investigated in more detail.

References

1. Alred, John, "NASA/USRA Advanced Engineering Design Program", paper submitted to SPACE 90, the second International Conference on Engineering, Constructions, and Operations in Space, (American Society of Civil Engineers, N.Y., 1989).

2. Cameron, Elizabeth A., Duston, John A., Lee, John D., "Design of Internal Support Structures for an Inflatable Lunar Habitat", (1990) report prepared for Universities Space Research Association.

3. Yin, Paul K., Ph.D., P.E. "A Preliminary Design of Interior Structure and Foundation of an Inflatable Lunar Habitat", paper submitted to SPACE 90, the second International Conference on Engineering, Construction, and Operations in Space, (American Society of Civil Engineers, New York, N.Y., 1989).

4. Costello, Frederick A., Mengers, David R., Moore, James S., Radermacher, Reinhard, Swanson, Theodore, "Low-Temperature Thermal Control for a Lunar Base", paper submitted to SAE conference on Advanced Environmental/Thermal Control and Life Support Systems.

5. NASA Document (November 1989) "Report of the 90 day Study on Human Exploration of Moon and Mars", Internal NASA report, prepared by NASA/JSC for the National Space Council.

6. DeBarro, Marc J., Farmer, Jeffrey T., Simonsen, Lisa C., Thomas, Carolyn C., "Conceptual Design of a Lunar Base Thermal Control System", (1988) report prepared for NASA, Paper Number LBS-88-225.

7. Green, Steve T., "Models of Energy Transport System Components for Space Applications", (1991) Southwest Research Institute, San Antonio, SWRI Project 04-3083.

8. Incropera, Frank P., DeWitt, David P., Fundamentals of Heat and Mass Transfer, (John Wiley & Sons, New York, 1990).

9. Kreider, Jan F., Kreith, Frank, Solar Heating and Cooling, (McGraw Hill, New York, 1975).

10. Mattick, A., Hertzberg, A, "Liquid Droplet Radiators for Heat Rejection in Space", Journal of Energy, Volume 5, Number 6, pp 387-392, 1981.

11. Mattick, A.T., Hertzberg, A.,"The Liquid Droplet Radiator- an Ultralightweight Heat Rejection System for Efficient Energy Conversion in Space", Acta Astronautica, Volume 9, Number 3,

pp. 165-172, 1982.

12. Carrier Technical Development Program, Air Conditioning Fundamentals, 1974.

13. John Thornborrow, NASA Johnson Space Center, Houston, TX, Telephone Conversation, 10/27/91.

14. Connell, Richard B., Fieber, Joseph P., Paruleski, Kerry L., Torres, Hernan D., "Design of an Inflatable Habitat for NASA's Proposed Lunar Base", report prepared for NASA, August, 1990.

15. Carrier Systems Design Manual, Carrier Air-Conditioning Company, Syracuse, New York, 1974.

16. Kakac, Sadik, "Boilers, Evaporators, and Condensers", John Wiley and Sons, New York, 1991.

17. ASHRAE Handbook, Fundamentals 1989, SI Edition, Atlanta, GA.

18. Butterworth, D., "Film Condensation of Pure Vapor", Heat Exchanger Design Handbook, vol.2, Chapter 2.6.2, Hemisphere Publishing Corp., New York, 1983.

19. Rohsenhow, W.M., "Boiling", Handbook of Heat Transfer,

Chapter 13, McGraw-Hill, New York, 1973.

20. Chi, S.W., "Heat Pipe Theory and Practice", McGraw Hill Book Company, New York, 1976.

21. Webb, B.J, Antoniak, Z.I, Pauley, K.A., "Advanced Ceramic Fabric Body Mounted Radiator for Space Station Freedom Phase 0 Design", Heat Transfer in Space Systems, ASME, New York,1990.

22. Ewert, Michael K., Petete, Patricia A., Dzenitis, John, "Active Thermal Control Systems for Lunar and Martian Exploration", SAE Intersociety.

APPENDIX A1

SPECIFICATION SHEET

Geometry

a. Module – Diameter 16m
wall thickness
Wall material - kevlar
surface area burried - 2/3
surface area under regolith - 1/3
Thickness of regolith - 2m

b. Inhabitants/Equipment within module
No. of people - 12
Kevlar-thickness
- Thermal conductivity

c. Location: Equater

Lunar enviromental conditions

a. Maximum surface temperature: 384 K(111°c)
minimum surface temperature: 102 K(-171°c)

b. Lunar radius 1737.72 km

c. Lunar Solar Constant: 1370 W/m^2

d. Albedo from earth $\cong$ 0

Functional Requirements

Maintain temperature of 21°C (18-24°C)
Humidity controlled by LSS (Life support system)
Oxygen revitalized by LSS (Life support system)

Geometry for TCS

- Minimize weight, volume

Energy to drive TCS

- Electrical
- Nuclear waste heat
- Solar heat

Materials

Radiators - low α, high ε
Properties of working fluids: large c_p

Safety

- Each component must have a backup
- No toxic working fluids inside module.

Placement

- Outside the module
- minimize lunar dust
- Micro meteorite impacts.

Operation

- once installed, no human attention
- Humans cannot adjust temperature inside module.

Maintenance & life

- Maintained by 1 person
- Life of major components > 15 yrs

APPENDIX A2

PASSIVE CONTROL CALCULATIONS

The 2m of regolith around the module is modelled with the following assumptions.

1. Negligible thermal resistance offered by the modules outer surface.
2. Temperature inside module = 21°C
3. The module has 2m regolith around it, even though this is true for only half of the module.
4. Steady state conditions exist.
5. 1-D
6. No contact resistance
7. Analysis at lunar noon.

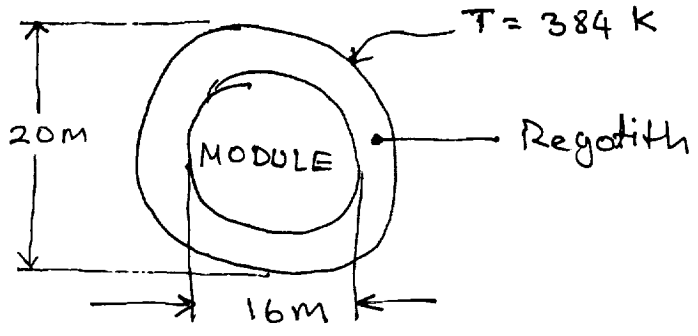

$K = .004\ W/m.K$

$$q = \frac{4\pi K \cdot \Delta T}{(1/r_1) - (1/r_2)}$$

$$\begin{pmatrix}\text{Heat input from} \\ \text{surrounding at noon}\end{pmatrix} = \frac{4\pi(.004)(384-294)}{1/8 - 1/10}$$

$$= .180\ KW$$

$$\begin{pmatrix}\text{Heat loss from} \\ \text{module at night}\end{pmatrix} = \frac{4\pi(.004)(294-102)}{1/8 - 1/10}$$

$$= .386\ KW$$

APPENDIX B1

ESTIMATE OF VAPOR COMPRESSION CYCLE PERFORMANCE

Assume: $T_{low} = 270\ K$

$T_{High} = 384\ K$

Cooling load = 50 kw

Single stage vapor compression cycle

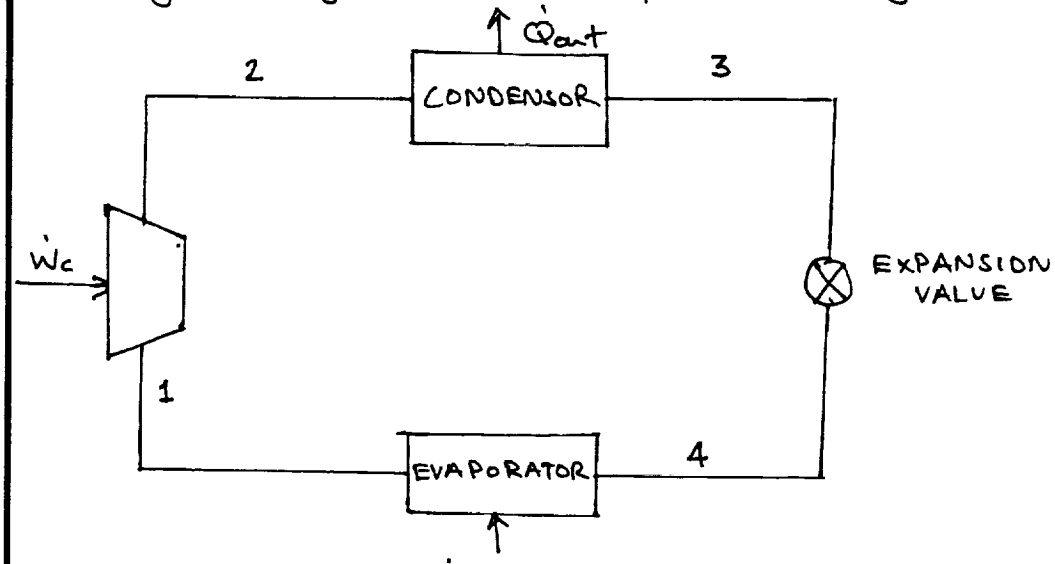

Working fluid : Refrigerant 11

An overall energy balance yields:

$$\dot{Q}_{out} = \dot{Q}_{in} + \dot{W}_c = 50\ kW + \dot{W}_c$$

Assume:

1. The compressor is isentropic and has an efficiency of 70%
2. Negligible pressure losses in the piping and heat exchanger.
3. Expansion valve is isenthalpic.
4. The refrigerant is saturated liquid at the condensor exit and saturated vapor at evaporator exit.
5. The refrigerant is always below its critical point.

State	Temerature	Pressure	Enthalpy
1 (satvap)	270 K	0.05 MPa	390 KJ/kg
2	384 K	1.1 MPa	450 KJ/kg
3 (satliq)	384 K	1.1 MPa	300 KJ/kg
4	270 K	0.05 MPa	300 KJ/kg

$\frac{\dot{W}}{\dot{m}} = h_2 - h_1 = 60 \text{ KJ/kg}.$

$\frac{\dot{Q}_{in}}{\dot{m}} = h_1 - h_4 = 90 \text{ KJ/kg}$

$\dot{m} = \frac{50 \text{ kW}}{90 \text{ KJ/kg}} = 0.555 \text{ kg/s}$

$\dot{W} = 60 \text{ KJ/kg} \times \dot{m} = 60 \times 0.555 = 33.3 \text{ kW}$

$\dot{Q}_{out} = \dot{m}(h_2 - h_3) = 0.555 \frac{\text{kg}}{\text{s}} \times \left(150 \frac{\text{KJ}}{\text{kg}}\right)$

$\dot{Q}_{out} = 83.3 \text{ kW}$

Two stage (cascaded) VCS

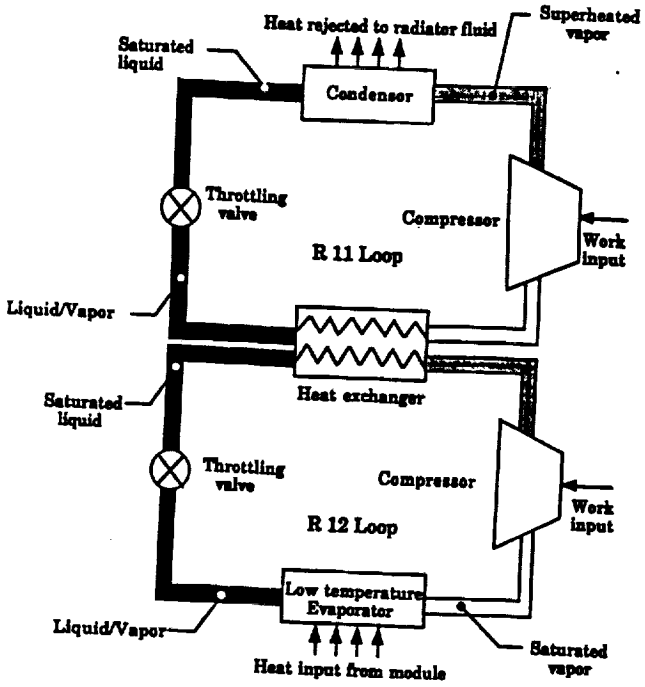

Known: $Q_{in} = 95$ kW

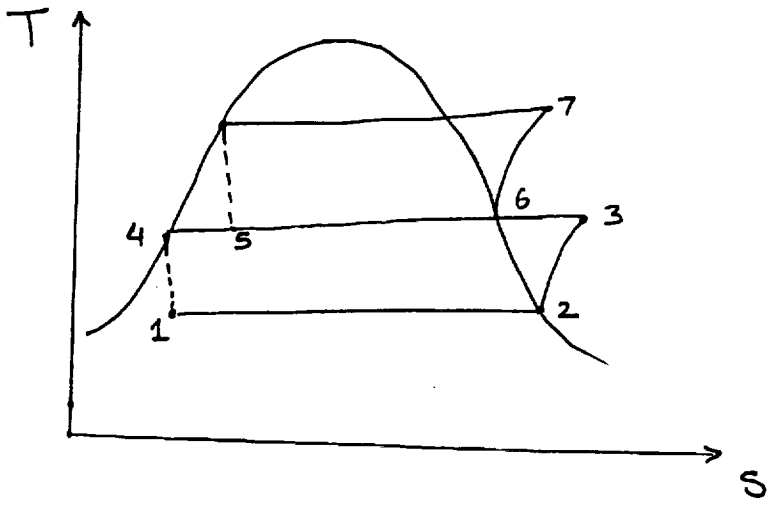

Refer: ASHRAE fundamental 1989

Operating Conditions

R12 Refrigeration Load temp: $-3^{\circ}C$

R11 Enviornment Temperature: $111^{\circ}C$

Heat load to be removed: 50 kW

Efficiency of Compressors: 70%

Refer to diagram on pg 54

$P_{high} = P_7 = P_8 = P_{sat}$ at $T = 111^{\circ}C$

$= 1.05$ MPa

$P_{low} = P_1 = P_2 = P_{sat}$ at $T = -3^{\circ}C$

$= 0.27$ MPa

P_{int} = Optimum interstage pressure

$= (P_H P_e)^{1/2} = P_4 = P_5 = P_6 = P_3$

$= 0.532$ MPa

Fluid	State	T °C	P (MPa)	h (KJ/kg)
R12	1	$-3^{\circ}C$	0.27	227
	2 SAT VAP	-3	0.27	351.5
	3 SUP VAP	60	0.5	385
	4 SAT LIQ	40	0.5	227
R11	5		0.5	300
	6 SAT VAP	60	0.5	430
	7 SUP VAP	111	1.1	450
	8 SAT LIQ	111	1.1	300

$$\dot{m}_A = \frac{Q_{in}}{h_2 - h_1} = \frac{50\,kW}{351.5 - 227}$$

$$= 0.4016\ kg/s$$

$$\dot{m}_B = \dot{m}_A \left(\frac{h_3 - h_4}{h_6 - h_5}\right) = 0.4016 \left(\frac{385 - 227}{430 - 300}\right)$$

$$= 0.4881\ kg/s$$

$$\dot{w}_A = \dot{m}_A (h_3 - h_2) = 0.4016\,(385 - 351.5)$$

$$\boxed{= 13.45\ kW}$$

$$\dot{w}_B = \dot{m}_B (h_7 - h_6) = 0.4881\,(450 - 430)$$

$$\boxed{= 9.76\ kW}$$

Total compressor Power $= 23.21\ kW$

$$\boxed{q_{rej} = 73.21\ kW}$$

Dimensioning of Condensor

Given: $\dot{Q} = 50 kw$

Condensing temperature $= 111^{\circ}C$

Condensing pressure =

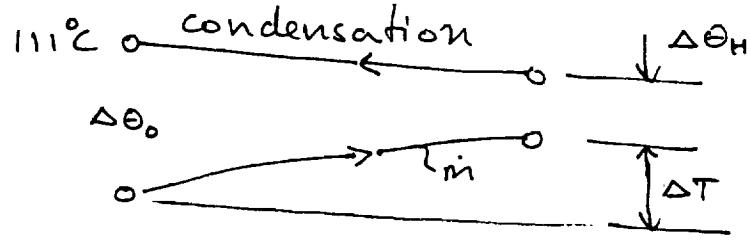

$$\Phi = \frac{\Delta T}{\Delta \theta_0}$$

$$x = \frac{UA}{\dot{m} C_p} = -\left[\ln(1-\Phi)\right]$$

$$UA = \frac{\dot{Q}}{\Delta \theta_0} = \frac{50 kw}{90 K} = 555.5 \ W/K$$

From fig 5.3 (8R1 paper)

$\tilde{M}$, specific mass parameter $= 2400 \ \frac{kg-k}{kw-m}$

$\tilde{M} = \frac{Mnx}{UA \, Dt}$ $\quad Dt$ = tube diameter

$$\frac{Mnx}{\dot{Q}} = \frac{\tilde{M}(UA) Dt}{\dot{Q}} = 2400 \frac{kg\,K}{kw\text{-}m} \times 0.555 \frac{kw}{K} \times 30$$

$= 39.96 kg$ per $50 kw$

$= .7992 \ kg/kw$

Dimensioning of Evaporator

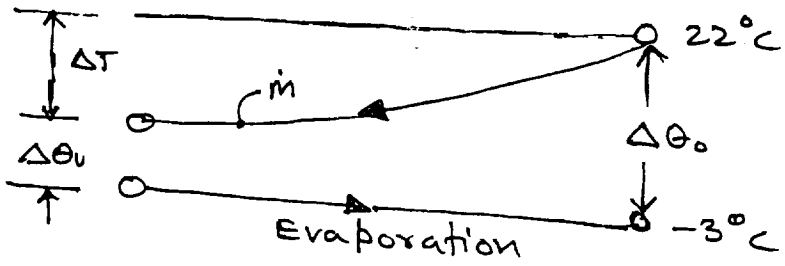

$$UA = \frac{\dot{Q}}{\Delta\Theta_0} = \frac{50\,kw}{22-(-3)} = 2000\ W/K$$

From fig 5.3, $\tilde{M} = 1600\ \frac{kg\,K}{kw\text{-}m}$

$$\tilde{M} = \frac{M_{hx}}{(UA)\,Dt} = \frac{M_{hx}}{\dot{Q}} = \frac{\tilde{M}\,(UA)\,Dt}{\dot{Q}}$$

$$\frac{M_{hx}}{\dot{Q}} = \tilde{M}\,\frac{UA}{\dot{Q}}\,Dt = 1600\ \frac{kg\,K}{kw\text{-}m} \times \frac{2000\ kw/K}{50\,kw} \times 30\times10^{-3}\,m$$

$$\boxed{\frac{M_{hx}}{\dot{Q}} = 1.92\ \frac{kg}{kw\ of\ heat}}$$

Mass of compressor

$$M_{cp} = 19 + 0.7(hp)$$

$$M_{cp(lb)} = 19 + 0.7\left(23.3 \times 10^{3} W \times \frac{1hp}{746W}\right)$$

$$= 50\,lb \times \frac{1\,kg}{2.2\,lb} = 22.78\,kg.$$

Mass of 2-stage VCS

Condenser : $0.7992 \frac{kg}{kW} \times 73.3\,kW = 58.58\,kg$

Compressors : 22.78 kg

Heat Exchanger : $1.92 \frac{kg}{kW} \times 50\,kW = 96\,kg$

Evaporator : $1.92 \frac{kg}{kW} \times 50\,kW = 96\,kg$

Total Mass = 273 kg

Mass of single stage VCS

Condensor : 58.58 kg

Compressor : $19 + 0.7\left(33.3 \times 10^{3} W \times \frac{1hp}{746}\right) \times \frac{1\,kg}{2.2\,lb} = 22.8\,kg.$

Evaporator : 96 kg

Total Mass = 176 kg

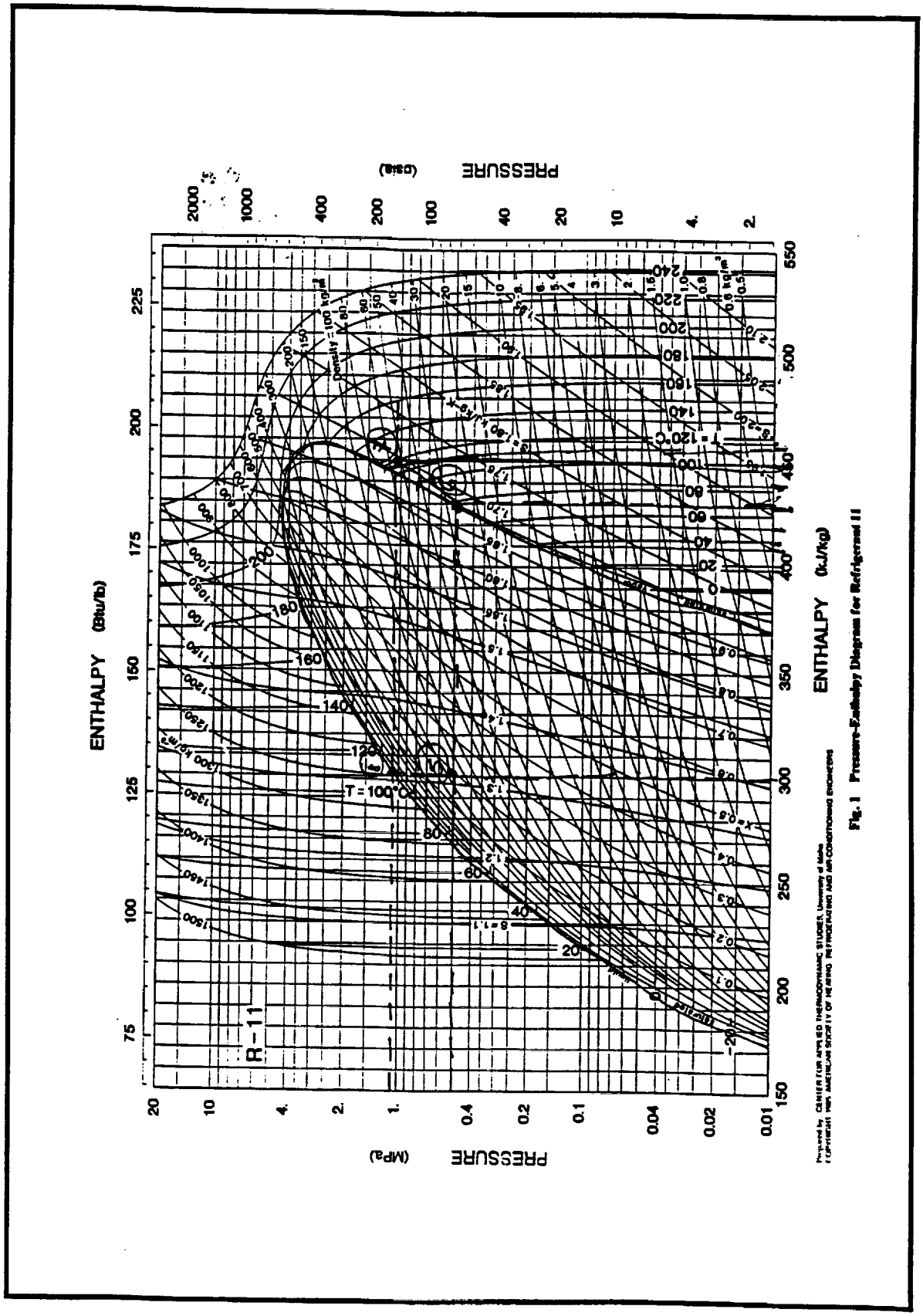

Fig. 1 Pressure-Enthalpy Diagram for Refrigerant 11

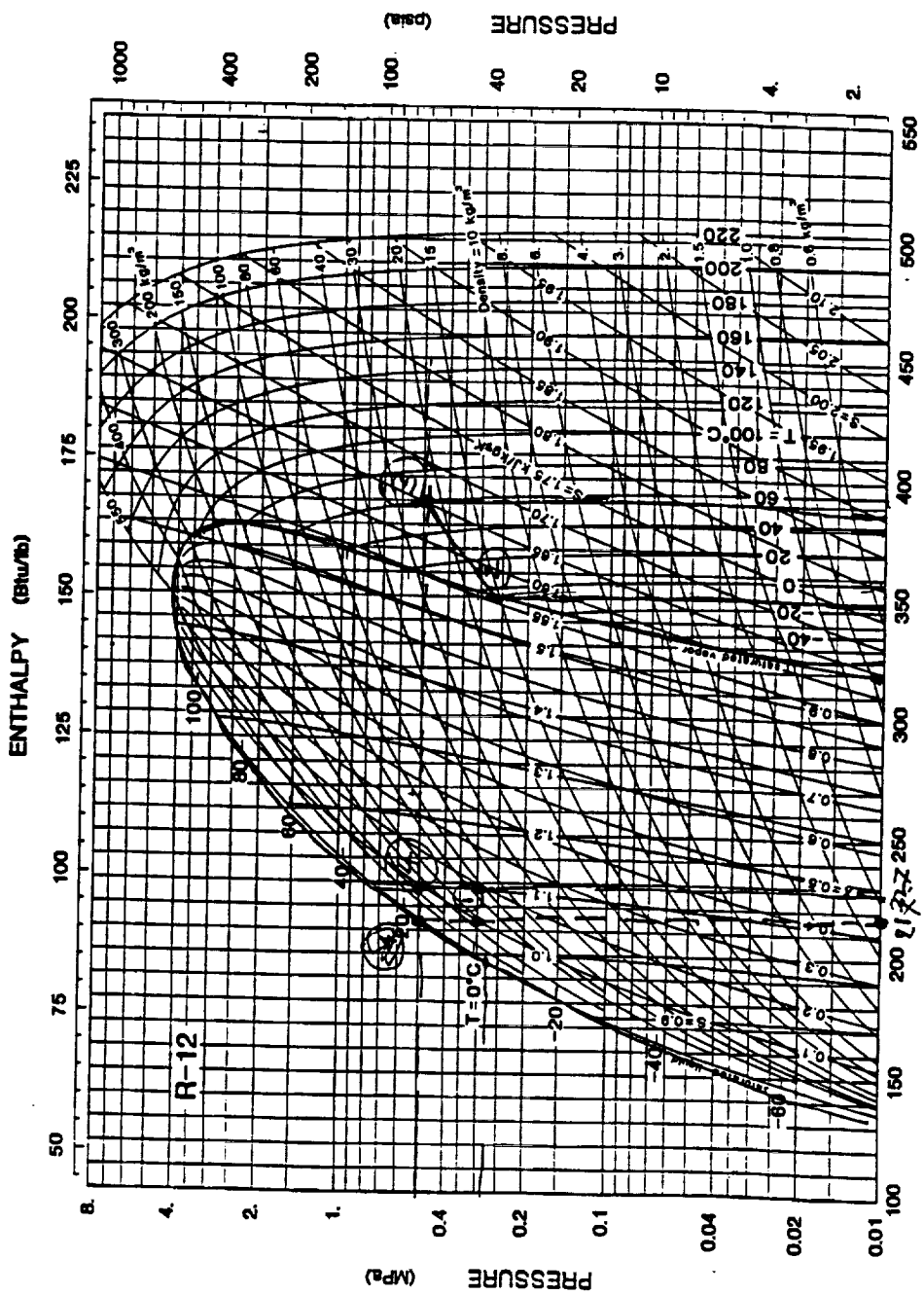

Fig. 2 Pressure-Enthalpy Diagram for Refrigerant 12

B10

Temp (K)	Qe (KJ/Kg)	Q'e(KW/Kg Hydrogen)	Q'e(KW/kg System)	Sp.Cooling kg/KW cool	System Mass for 50 KW coc
430	225.568	0.1879733	0.0939867	29.5	1475
400	251.968	0.2099733	0.1049867	29.5	1475
350	295.968	0.24664	0.12332	29.5	1475
300	339.968	0.2833067	0.1416533	29.5	1475
280	357.568	0.2979733	0.1489867	29.5	1475
275	361.968	0.30164	0.15082	29.5	1475
273	363.728	0.3031067	0.1515533	29.5	1475
271	365.488	0.3045733	0.1522867	29.5	1475
270	366.368	0.3053067	0.1526533	29.5	1475
268	368.128	0.3067733	0.1533867	29.5	1475

Qexternal h input (KW)	COP
277.26067	0.3610379
309.71067	0.3232101
363.794	0.2751602
417.87733	0.2395478
439.51067	0.227757
444.919	0.2249884
447.08233	0.2238997
449.24567	0.2228215
450.32733	0.2222863
452.49067	0.2212236

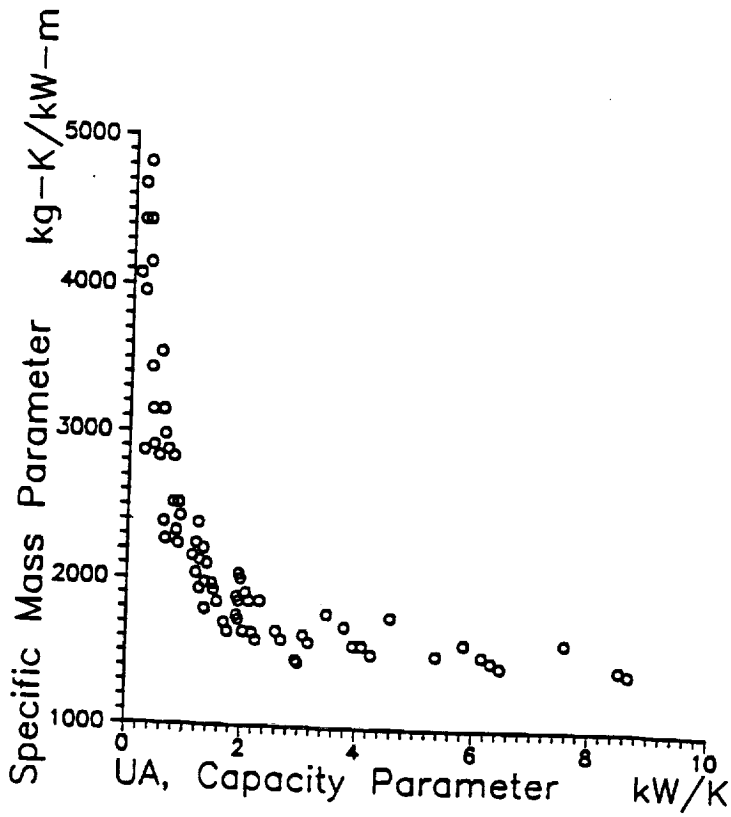
Specific Mass Parameter kg-K/kW-m
5000
4000
3000
2000
1000
0
2
4
6
8
10
UA, Capacity Parameter kW/K

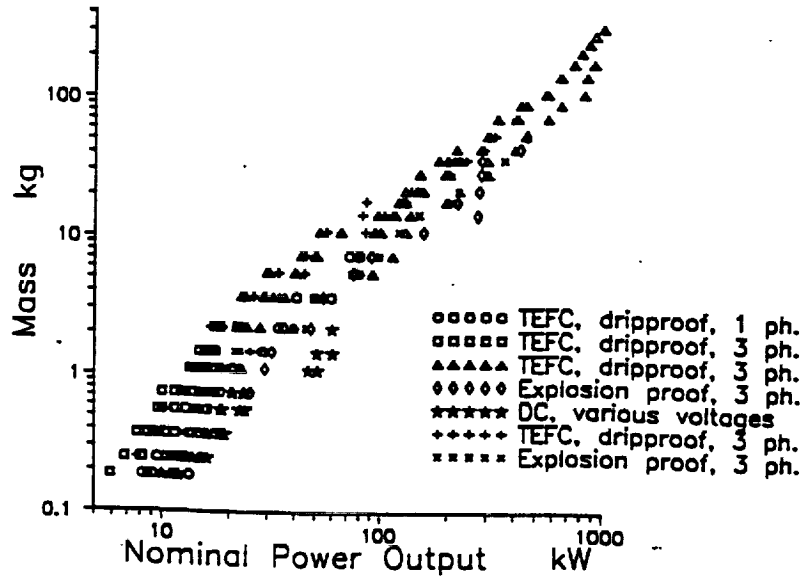
Mass kg
100
10
1
0.1
10
100
1000
Nominal Power Output kW
TEFC, dripproof, 1 ph.
TEFC, dripproof, 3 ph.
TEFC, dripproof, 3 ph.
Explosion proof, 3 ph.
DC, various voltages
TEFC, dripproof, 3 ph.
Explosion proof, 3 ph.

APPENDIX B 2

ESTIMATE OF VAPOR ABSORPTION CYCLE PERFORMANCE

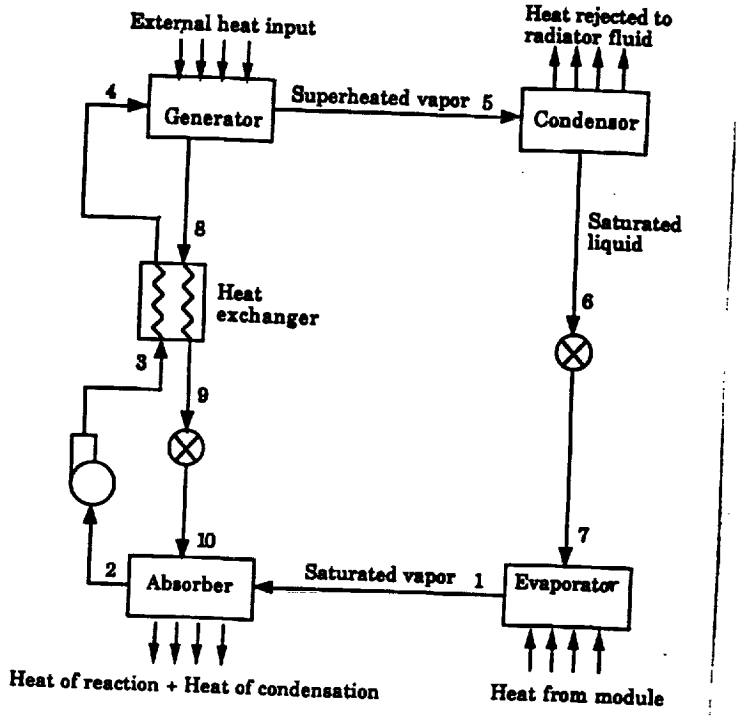

Working fluid: Water - Lithium Bromide.
Cooling load: 50 kw
Evaporator temperature: 0°C
Condensor temperature: 110°C.

State	T (°C)	P (kPa)	Wt %	h (kJ/kg)
1	167	140.9	0.6	359
2	88	140.9	0.6	191
3	80	0.603	0.6	191
4	29	0.603	0.55	72.6
5	29	140.9	0.55	72.6
6	100	140.9	0.55	218
7	167	140.9	0	2811
8	110	140.9	0	461
9	0	0.603	0	0
10	0	0.603	0	2373.9

This table specifies all the states in the cycle.

Evaporator:

The evaporator is operated at a temperature of 0°C. The saturation pressure at this temperature is 0.603 kPa. Since the evaporator and the absorber both operate at the same pressure,

$$P_9 = P_{10} = P_3 = P_4 = 0.603 \text{ kPa}.$$

Since the evaporator is operating at constant temperature, states 9 and 10 are at 0°C.

Absorber:

The operating temperature for the absorber is chosen such that at a concentration of 55 wt% LiBr the pressure will be 0.603 kpa. ~~The condensor~~

Condensor:

The operating temperature for the condensor was chosen to be 110°C. The saturation pressure at this temperature is 140.9 kpa. Since the generator and the condensor operate at the same pressure,

$$P_1 = P_2 = P_5 = P_6 = P_7 = P_8 = 140.9 \text{ kPa}$$

Generator

The generator temperature is chosen such that at a 60% Li-Br concentration, the pressure is 140.9 kpa.

Heat inputs and outputs

$\dot{m}_{ab}$ = mass flowrate of absorbant ($Li\text{-}Br$)

$\dot{m}_r$ = mass flowrate of refrigerant (H_2O)

$\dot{m}_s$ = mass flowrate of solution

X_{ab} = Concentration of $LiBr$ in absorbant

X_r = Concentration of $LiBr$ in refrigerant.

$$\frac{\dot{m}_{ab}}{\dot{m}_r} = \frac{X_r}{X_{ab} - X_r} = \frac{.55}{.6 - .55} = 11 \text{ kg/s}$$

$$\frac{\dot{m}_s}{\dot{m}_r} = \frac{\dot{m}_{ab} + \dot{m}_r}{\dot{m}_r} = \frac{\dot{m}_{ab}}{\dot{m}_r} + 1 = 12 \text{ kg/s}$$

The mass flow rate in the evaporator can then be found.

$$\dot{m}_r = \frac{Q_{ref}}{h_{10} - h_9} = \frac{50 kw}{2373.9 - 0} = 2.1 \times 10^{-2} \text{ kg/s}$$

$$\dot{m}_{ab} = \frac{\dot{m}_{ab}}{\dot{m}_r} \cdot \dot{m}_r = 11 (2.1 \times 10^{-2}) \text{ kg/s}$$

$$= .2308 \text{ kg/s}$$

$$\dot{m}_s = \dot{m}_r + \dot{m}_{ab} = .2308 + 2.1 \times 10^{-2}$$

$$= .2518 \text{ kg/s}$$

The heat input to the generator is

$$Q_{gen} = \dot{m}_r h_7 + \dot{m}_{ab} h_1 + \dot{m}_{ab} h_6$$

$$Q_{Gen} = 2.1\times10^{-2}(2811) + .2308(359) - .2578(218)$$

$$Q_{Gen} = 59 + 82 - 54$$

$$Q_{Gen} = 86.1\ kw$$

The COP of the system is

$$COP = \frac{Q_{ref}}{Q_{sup}} = \frac{50\ kw}{86.1\ kw} = .58$$

For the heat exchanger

$$q_{1-2} = \dot{m}_{ab}(h_1 - h_2)$$

$$= .2308(359 - 191) = 38\ kw$$

$$Q_{Heat\ Ex} = 38\ kw$$

For the condenser

$$Q_{cond} = \dot{m}_r(h_7 - h_8)$$

$$= 2.1\times10^{-2}(2811 - 461)$$

$$Q_{cond} = 49.35\ kw$$

For the Absorber

By an energy balance on the system we get $Q_A + Q_C = Q_G + Q_E$

$$Q_A = Q_G + Q_E - Q_C$$

$$= 86.1 + 50 - 49.35$$

$$Q_A = 86.75\ kw$$

Mass estimate for the Absorption cycle

According to Trane and Carrier catalogs the mass of an absorption system is abont 200 kg. Absorption systems genrally tend to weigh mor because of the extra heat exchanger surface area needed. The units ~~are~~ e manufactured for use on earth are not geared towards minimizing mass. There units have extra components that are not needed for proper system operation. Therefore a mass of 500 kg for the absorption cycle is a ~~reas~~ resonable estimate.

APPENDIX B3

ESTIMATE OF METAL HYDRIDE CYCLE PERFORMANCE

Assumptions:

a) M_{AT} = Total mass of vessel A

M_A = Mass of metal hydride

$M_{AT} = 2M_A$

b) A: CaNi$_5$

Net specific heat, $C_A = 0.44$ KJ/kg·K

Enthalpy of adsorption $\Delta H_{aA} = 15300 \frac{KJ}{kg}$

Storage Concentration, $\hat{x}_A = 0.01799 \frac{kg-H_2}{kg-CaNi_5}$

Active portion of vessel A, $\gamma_A = .9$

c) B: LaNi$_5$:

Net specific heat, $C_B = 0.44$ KJ/kg·K

Enthalpy of adsorption, $\Delta H_{ab} = 14550$ KJ/kg

Storage Concentration, $\hat{x}_B = 0.01388 \frac{kg-H_2}{kg-LaNi_5}$

Active portion of vessel B, $\gamma_B = 0.9$

d) Cycle time = 20 minutes

e) Cooling load = 50kW

T_{low} = 270K

T_{high} = $T_{rejection}$ = 384K

f) Initial temperature of Bed A is variable = T_1

Initial State:

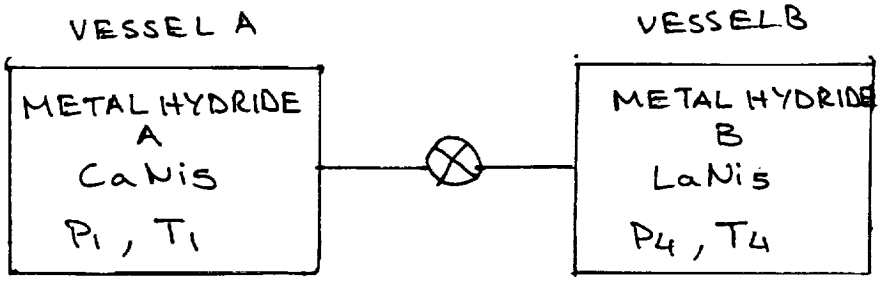

In stage 1, an external heat input of Q_{A1} is applied to the metal hydride in vessel A.

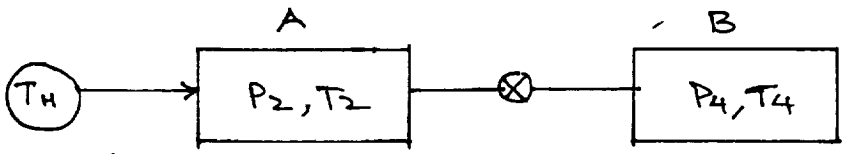

The energy delivered to vessel A in stage 1

$$Q_{A1} = M_{At}\, C_A\, (T_2 - T_1)$$

where T_1 = initial temperature of vessel A

T_2 = temperature of vessel A at end of stage 1

During stage 2, external heat of Q_{A2} is applied.

$$Q_{A2} = M_A \hat{x}_A \gamma_A \Delta H_{aA}$$

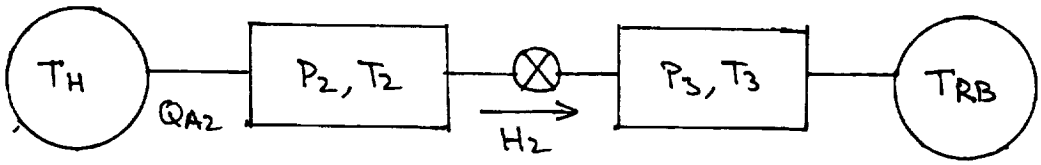

The energy removed (desorbed) from vessel B is Q_{B2}. In stage 3, an energy transfer of Q_{A3} takes place from vessel A to a heat sink. Vessel A is cooled back to T_1.

In step 4, the valve is open and H_2 desorbs from B to A, hence cooling B from T_3 to T_4 (since pressure equilibrium must be maintained) Energy is delivered to B from a low temperature space. This energy is the cooling load Q_{B4}

$$Q_{B4} = M_B \hat{x}_B \gamma_B \Delta H_{aB} - M_{Bt} C_B (T_3 - T_4)$$

$$= 50 \text{ kw of cooling load.}$$

Rejection temperature $= T_3 = 384$ K

Low temperature $= T_4 = 270$ K

Graph shows the cycle diagram relating the temperature and the pressure of each state. From the figure and knowledge of T_3, $T_2 = 438.6$ K

$$Q_{external} = Q_{A1} + Q_{A2} = M_{At} C_A (T_2 - T_1) + M_A \hat{x}_A \frac{M_A}{\Delta H}$$

$$\frac{Q_{ext}}{M_A} = \left[0.88\,(438.6 - T_1) + 217.99\right]$$

Hence, the specific external heat required decreases with increasing initial temperature of vessel A, as shown in figure

$$\text{The COP} = \frac{\text{cooling load}}{\text{energy required to drive process}}$$

The COP increases with an increase in the minimum temperature, as shown in figure

if $T_{initial} = 300K$, 417 kw of external heat is required.

The system mass is 29.5 $\frac{Kg}{Kw\,cooled}$ x 50 kw

The COP of the system is 0.24

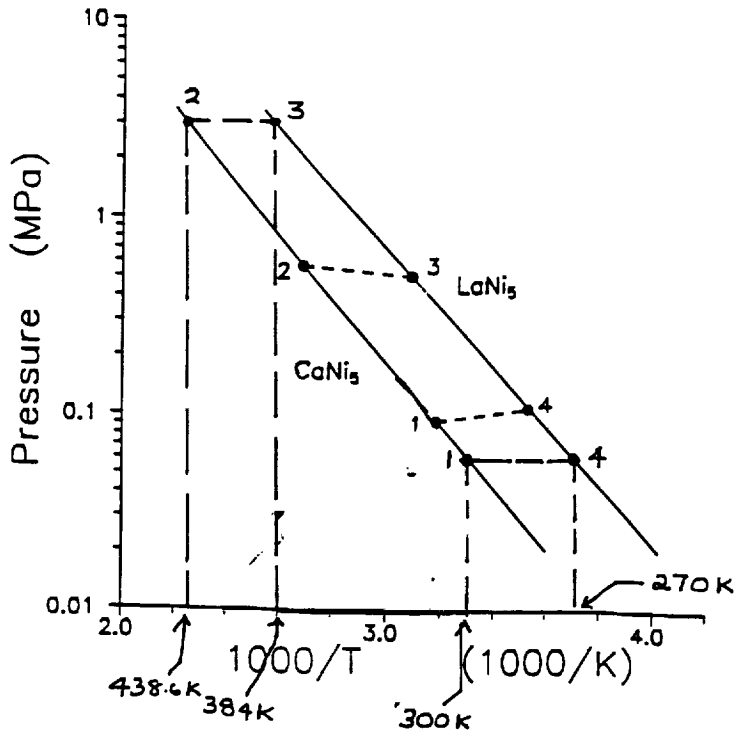

Figure 3-4. $LaNi_5/CaNi_5$ Hydride Heat Pump Cycle

Graph of minimum cycle temperature vs COP

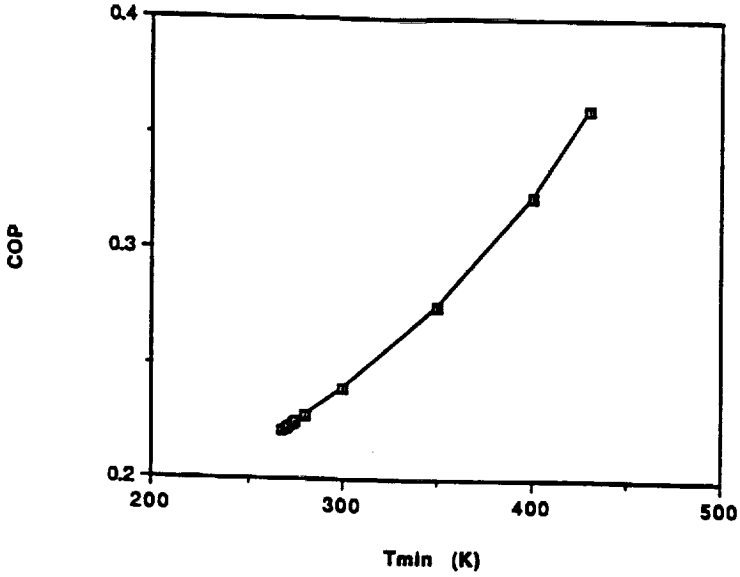

External Heat Input vs Initial Temperature of system (to remove a 50 KW load from T = 270 K to T = 384 K).

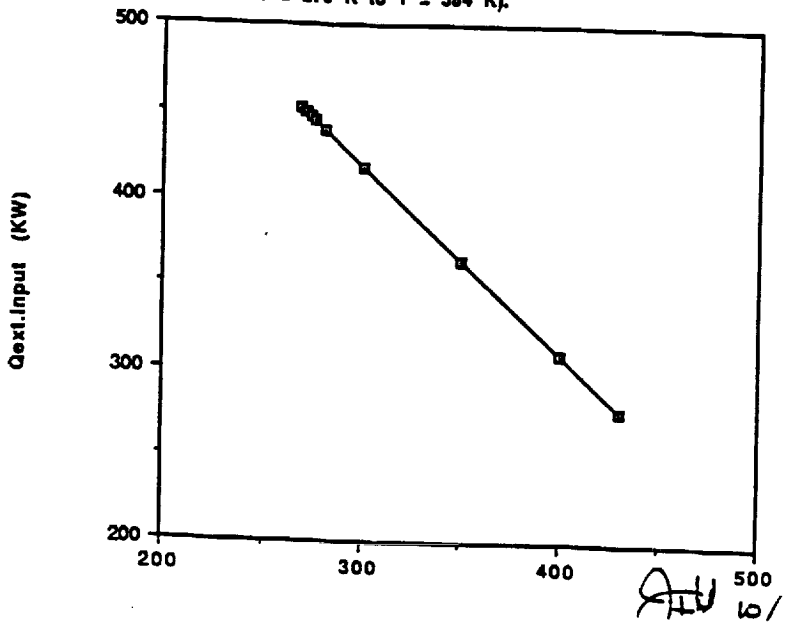

B23

APPENDIX C1

CALCULATIONS FOR FLAT PLATE RADIATORS

Horizontal radiator sink temperature and heatflux

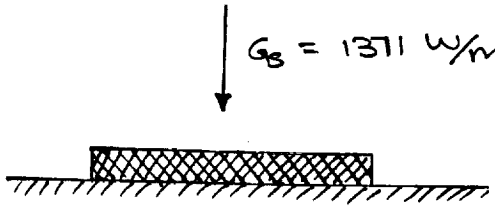

Assumptions:

G_s = Solar irradiation = $1371\ W/m^2$

α_s = Solar absorptivity of radiator surface = .2

ε_{moon} = emissivity of lunar surface = .96

ε = emissivity of radiator = .8

T_{moon} = Temperature of moon = 384 K (at noon)

θ = Sun angle

Energy balance on radiator

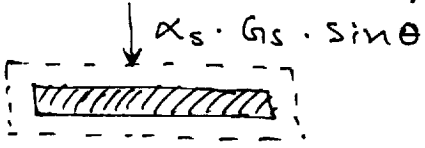

$$\varepsilon \cdot \sigma \cdot T_{sink}^4 = G_s \cdot \alpha_s \cdot \sin\theta$$

$$T_{sink}^4 = \frac{(1371)(-2)\sin\theta}{(.8)(5.6\times10^{-8})}$$

$$T_{sink} = 278.8(\sin\theta)^{1/4} \quad \text{—— (1)}$$

At lunar noon, $\theta = 1$

$$T_{sink} = 278.8\ K$$

Equation 1 is used to calculate the effective sink temperature of the horizontal radiator with varying time.

Heat flux when plate at $T_{rad} = 270K$ is given by:

$$q'' = \varepsilon \cdot \gamma \cdot (T_{rad}^4 - T_{sink}^4)$$

$$q''_{(T=270K)} = 4.536\times10^{-8}(270^4 - T_{sink}^4) \quad \text{—— (2)}$$

when $T_{rad} = 384K$

$$q''_{(T=384K)} = 4.536\times10^{-8}(384^4 - T_{sink}^4) \quad \text{—— (3)}$$

Vertical radiator

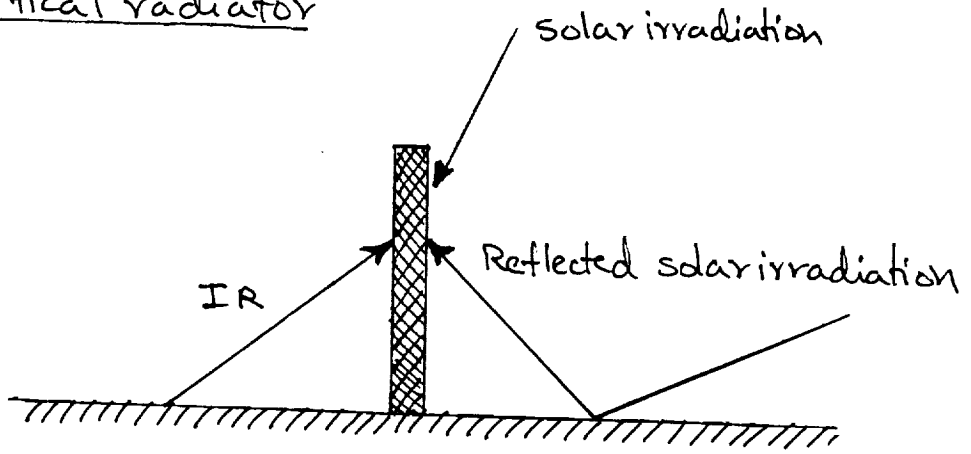

IR = infrared radiation from lunar surface

F = view factor of radiator to lunar surface = .5

ρ = albedo of lunar surface = 0.07

Energy balance on the radiator

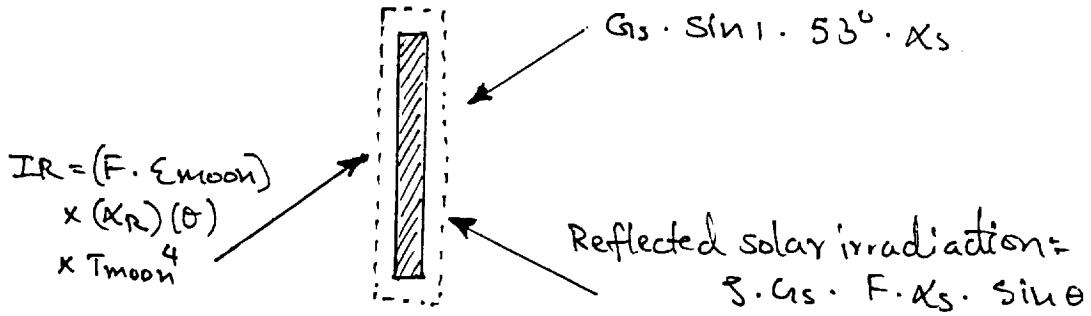

$$\varepsilon \cdot \sigma \cdot T_{sink}^4 = G_s \cdot \sin 1.83 \cdot \alpha_s \sin\theta + G_s \cdot \rho \cdot F \cdot \alpha_s \cdot \sin\theta + F \cdot \varepsilon_{moon} \cdot \alpha_R \cdot \sigma \cdot T_{moon}^4$$

$$(.8)(5.67\times10^{-8})(T_{sink})^4 = (1371)(\sin 1.53)(.2)\sin\theta + (1371)(.07)(.5)(.2)\cdot\sin\theta + (.5)(.96)(.8)(5.67\times10^{-8})(T_{moon})^4$$

$$T_{sink} = \left[1.614 \times 10^{8} \sin\theta + 2.115 \times 10^{8} \sin\theta + .48\, T_{moon}^{4}\right]^{1/4} \quad (4)$$

This equation is used to find the effective sink temperature of the vertical radiator with time.

At lunar noon,

T_{sink} = 322.44 K (Using the above equation)

Heat flux radiated at $T_{radiator}$ = 270 is given by

$$q'' = 4.536 \times 10^{-8} \left(270^{4} - T_{sink}^{4}\right) \quad (5)$$

At Trad = 384 K

$$q'' = 4.536 \times 10^{-8} \left(384^{4} - T_{sink}^{4}\right) \quad (6)$$

Mass Calculations

Assumptions

1. Heat load to be rejected = 50kw
2. Radiator temperature = 384 K
3. Conditions at lunar noon.
4. Fin efficiency = .7

Horizontal Radiator:

Using equation 3

$$q'' = (712\ W/m^2)(.7) = 500\ W/m^2$$

Radiator mass per unit area of radiating surface = 10 kg/m²

Mass of horizontal radiator = $\frac{50(15)}{\cdot 5}$

= 1000 kg

Mass per unit kW = 20 kg/kW

Vertical Radiator

using equation 6

$q'' = 496\ W/m^2\ (\cdot 7) = 347\ W/m^2$

Radiator mass per unit area of radiating surface = 5 kg/m²

∴ Mass of vertical radiator

$= \frac{(5)(50)(5)}{\cdot 347} = 720$ kg.

Mass per unit kW = 14·4 kg/kW

APPENDIX C2

CALCULATIONS FOR PARELLEL PLATE RADIATORS

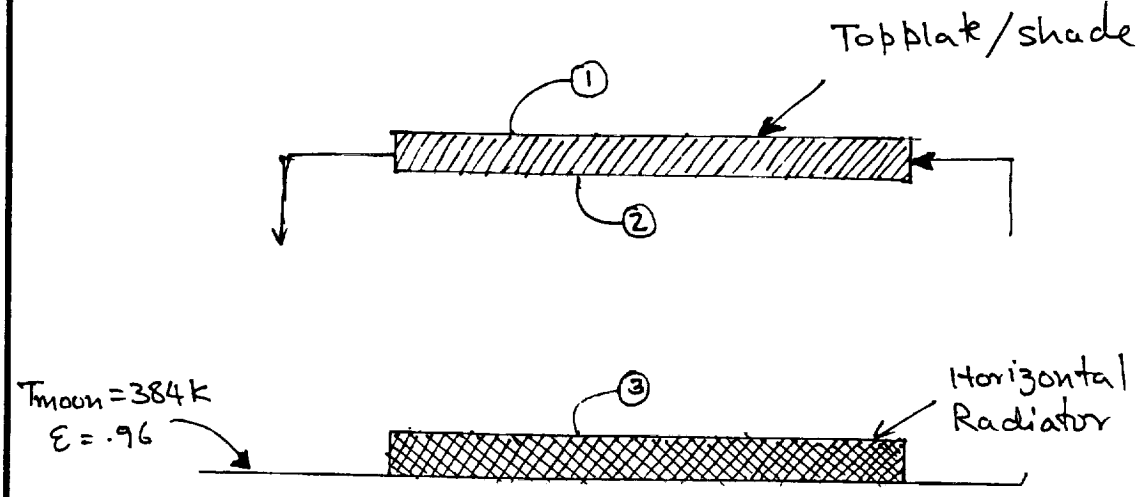

Assume, the collector and radiator are 10 m in length, .125m x .125m in c/s

Distance between ① and ③ = 1m

Surface properties

① surface – $(\alpha_s)_1 = .9$, $\varepsilon_1 = .9$

② surface – $(\alpha_s)_2 = .9$, $\varepsilon = .9$

③ surface – $\varepsilon_3 = .8$, $\alpha_{IR} = .8$

} Black Paint on Metallic Substrate

Energy balance on top plate/shade

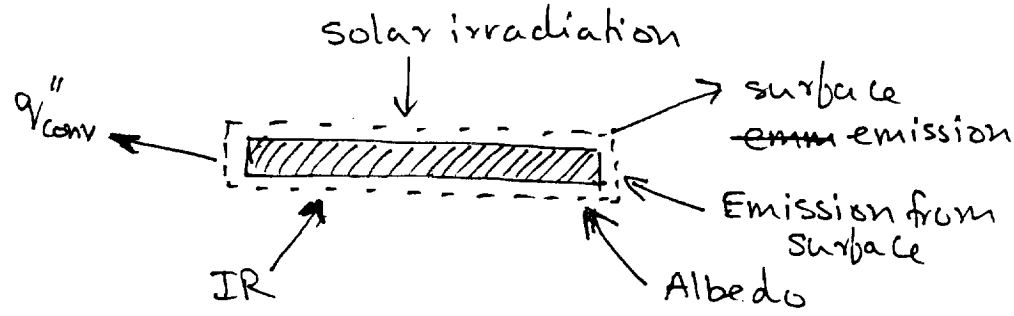

Solar irradiation = $G_s \cdot (\alpha_s)$

surface ① emission = $\varepsilon_1 \cdot \sigma \cdot (T_{shade})^4$

surface ② emission = $\varepsilon_2 \cdot \sigma \cdot (T_{shade})^4$

Emission from surface ③ = $\alpha_2 \cdot \varepsilon_3 \cdot \sigma \cdot T_{rad}^4 \cdot F_{r-s}$

Albedo = $(albedo)(G_s)(1 - F_{r\to s})(\alpha_s)_2$

IR = $\varepsilon_{moon} \cdot \sigma \cdot (T_{moon})^4 \cdot (1 - F_{r\to s}) \cdot (\alpha_2)$

$q''_s = h(T_{shade} - T_m)$

where $T_{shade} = \dfrac{T_{s,o} + T_{si}}{2}$

$G_r(\alpha_s)_1 - \varepsilon_1 \cdot \sigma \cdot (T_{shade})^4 - \varepsilon_2 \cdot \sigma \cdot (T_{shade})^4 - \alpha_2 \varepsilon_3 \cdot \sigma \cdot T_{rad}^4 \cdot F_{r-s} + (albedo)(G_s)(1 - F_{r-s})(\alpha_s)_2 + \varepsilon_{moon} \cdot \sigma \cdot T_{moon}^4 (1 - F_{r\to s}) \cdot \alpha_2 = q''_s$

$\Rightarrow (1371)(.9) - (.9)(5.67 \times 10^{-8})(300)^4 - (.9)(5.67 \times 10^{-8})(300)^4 + .9(.8)(5.67 \times 10^{-8})(384)^4(.06) + (.07)(1371)(.94)(.9) + (.96)(5.67 \times 10^{-8})(384)^4(1 - .06)(.9)$

$q_s'' = 1566\ W/m^2$

Fluid Ammonia: (NH_3) at 300k

$\rho = .6894\ kg/m^3$, $C_p = 2.158\ kJ/kg\cdot k$

$\mu = 101.5 \times 10^{-7}$, $\nu = 14.7 \times 10^{-6}$

$k = 24.7 \times 10^{-3}$, $Pr = .88$

$$D_h = \frac{4A_c}{P} = \frac{4(.125)(.125)}{4(.125)} = .125$$

$$Re_D = \frac{(.6894)(5)(.125)}{101.5 \times 10^{-7}} = 42{,}450$$

Entry length $= 1.25\ m$

$\therefore$ flow is turbulent and fully developed.

we can use the correlation

$$Nu_D = (.023)(Re_D)^{4/5} Pr^{4}$$

$L/D = 80$, $\therefore Re_D \geq 10{,}000$

$L/D \geq 10$

$Pr \geq .7$

$$Nu_D = 110.45 = \frac{hD_h}{R}$$

$$\boxed{h = 21.83\ W/m^2\cdot k}$$

$q_s'' \cdot P \cdot L = \dot{m} c_p (T_{m,o} - T_{mi})$ ——— (1)

Also $q_s'' = h (T_6 - T_m)$ ——— (2)

using equation 2

$$T_s - T_m = \frac{1566}{21.83} = 71.736$$

$$T_s = T_m + 71.736$$

Also,

$$T_{m,o} - T_{m,i} = \frac{q_s'' \cdot P \cdot L}{\dot{m} c_p}$$

$$= \frac{(1566)(.5)(10)}{(.054)(2158)} = 67.2$$

$$T_{s,i} - T_{m,i} = 71.736$$

$$T_{s,o} - T_{m,o} = 71.736$$

$$T_{m,o} - T_{m,i} = 67.2$$

$$\frac{T_{s,o} + T_{si}}{2} = 300$$

$T_{m,i} = 230\,K$

$T_{m,o} = 297.2\,K$

$T_{s,i} = 301.736$

$T_{s,o} = 368.9$

Therefore the equation has to be solved iteratively, Assuming that $T_{shade} = 335$

$$\boxed{q_s'' = 1108\ W/m^2}$$

Using equation ②

$$T_s - T_m = \frac{1108}{21.83} = 50.75$$

using equation ①

$$T_{m,o} - T_{m,i} = \frac{(1108)(.5)(10)}{(.054)(2158)} = 47.54$$

Say $T_{m,i} = 270\,K$

$T_{m,o} = 317.54$

$T_{s,i} = 320.75$

$T_{s,o} = 368.3$

$T_{shade} = T_{s,i} + T_{s,o} \approx 335\,K$

Calculations for worst case sink temperature

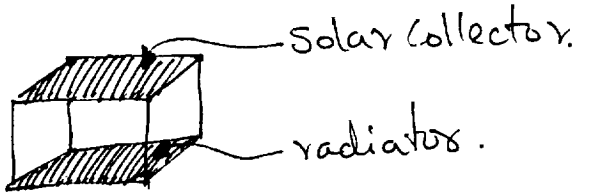

The radiator sees the shade with a view factor of .06. Using enclosure rule, the view factor of the radiator to the hypothetical vertical walls is .94 if the radiators are alligned such that the longer vertical walls (10m) are alligned east-west, the maximum solar irradiation on the walls will be:

$(1371)(\sin 1.53^\circ) = 36.6\ W/m^2$.

The view factor of the radiator to the vertical walls will be .9.

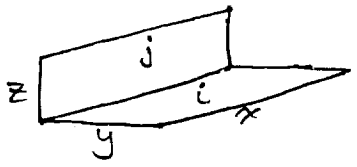

$x = 10cm$
$y = .125$
$z = 1m$

$\frac{z}{x} = .1 \quad \frac{y}{x} = .0125$

$F_{ij} = .45$

∴ the radiator sees the long vertical walls and the view factor of the radiators to the vertical walls aligned North-south is negligible. Therefore the effect of sun angle changing during the course of the day will not affect the effective sink temperature that much.

∴ effective sink temperature (worst case)

$(.8)(5.67\times10^{-8})(T_{sink})^4 = .9(5.67\times10^{-8})(335)^4 \times(.8)(.06) + (1371)\sin 1.53(.94)(.2)$

$\boxed{T_{sink} = 170K}$

$q''_{rad} = \varepsilon \cdot \gamma \cdot (T_{rad}^4 - T_{sink}^4)$

$= .8\,(5.67\times10^{-8})(384^4 - 170^4)$

$\boxed{q''_{rad} = 948.4\ W/m^2}$

Mass calculations for parallel plate radiator

Heat to be rejected = 50 kW

$$q'' = (948.4\ W/m^2)(.7) = 664\ W/m^2$$

Weight of radiator = $10\ kg/m^2$

Weight of top plate = $10\ kg/m^2$

$$\text{total mass} = \frac{(50)(10)(2)}{(.948)(.7)} \simeq 1500\ kg$$

$$\therefore \text{specific mass} = \frac{1500}{50} = \boxed{30\ kg/kW}$$

APPENDIX C3

CALCULATIONS FOR REFLUX BOILER RADIATOR

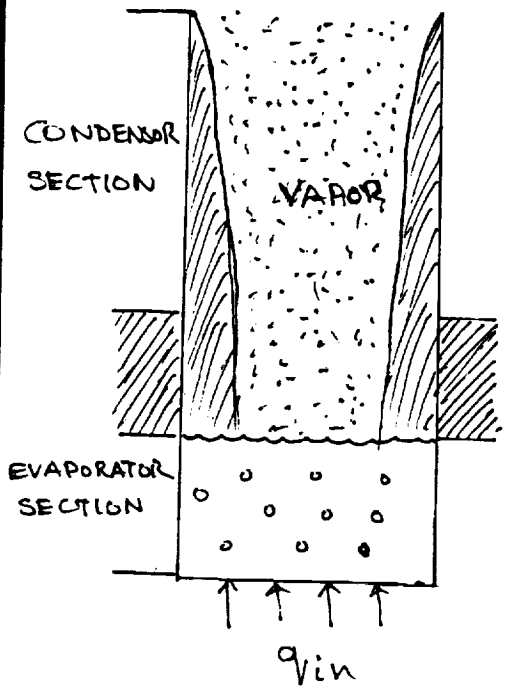

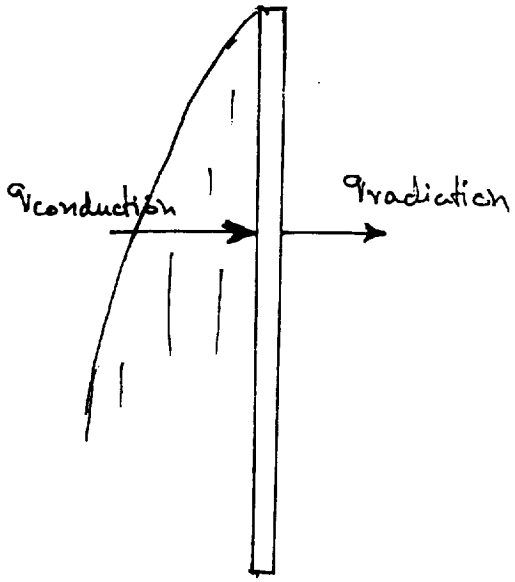

Assume that the liquid will be heated to 384 K by using a 2 stage vapor compression cycle. As calculated earlier, for a 50 kw load, 73.3 kw of power will be input to the fluid. Hence 73.3 kw

will have to be rejected. A constant temperature of the vapor is assumed across the entire condenser section.

Working fluid: Water

Properties:

Saturated water, liquid (100°C)

density $\rho_l = 957.9\ kg/m^3$

specific heat $C_{p,l} = 4.217\ kJ/kg \cdot K$

Viscosity: $\mu_L = 279 \times 10^{-6}\ Ns/m^2$

Prandtl No. $Pr_l = 1.76$

heat of vaporization: $h_{fg} = 2257\ kJ/kg$

surface tension of liquid vapor interface.

Assumptions:

1. Steady state conditions - all the heat added at the evaporator is removed at the condensor.
2. Water is at standard ~~atm~~ atmospheric pressure 1.01 bar
3. Axial conduction through the tube wall is negligible.
4. Wall temperature of the condenser section is constant along its length.

5. Heat is supplied uniformly to the evaporator section
6. change of liquid pool level in the evaporator is negligible.
7. surface of radiator is made up of copper.

Analysis of Evaporator

excess temperature $\Delta T_e = T_{surface} - T_{sat}$

$= 384\ K - 373\ K$

$\Delta T_e = 11\ K$

for water at 1 atm, nucleate pool boiling will occur at $5K < \Delta T_E < 30^\circ C$

Hence the correlation for estimating the heat transfer rate per unit area of plate surface is given by

$$q_s'' = \mu_l h_{fg} \left[\frac{g(\rho_L - \rho_v)}{\sigma}\right]^{1/2} \left(\frac{C_{p,l}\,\Delta T_e}{C_{sf}, h_{fg} Pr^n}\right)^3$$

The values of $C_{s,f}$ and n corresponding to the polished copper surface-water combination are

$C_{s,f} = 0.013$ and $n = 1.0$

Hence, the boiling heat flux is

$$q_s'' = 279 \times 10^{-6} \frac{N s}{m^2} \times 2257 \times 10^3 \frac{J}{kg} \times$$

$$\times \left[\frac{1.633 \, m/s^2 (957.9 - 0.595) \frac{kg}{m^3}}{55.9 \times 10^{-3} N/m} \right]^{1/2}$$

$$\times \left(\frac{4.217 \times 10^3 \, J/kg \cdot K \times 11^0 C}{0.013 \times 2257 \times 10^3 \times 1.76} \right)^3$$

$$q_s'' = 74.4 \frac{kw}{m^2}$$

$$A = \text{area reqd for evaporation} = \frac{q_s}{q_s''} = \frac{73.3 kw}{74.4 kw/m^2}$$

$$= .985 m^2$$

$$A_e = \pi D L_e = 0.985 m^2$$

$$L_e = \frac{0.985 m^2}{\pi D} = \frac{0.988 m^2}{\pi \times 0.1 m} = 3.135$$

Analysis of the condensor

$$q_{cond} = 73.3 kw$$

if $T_{s,cond}$ is required to be $95^\circ C = 368 K$

and $T_{sat} = 100^\circ C$

$$T_f = \frac{T_{sat} + T_{surf}}{2} = 97.5^\circ C = 370.5 K$$

at $T_f = 370.5K$, water has the following properties:

$$\rho_\ell = \frac{1}{V_f} = \frac{1}{1.042 \times 10^{-3}} = 959.7 \text{ kg/m}^3$$

$$\mu_\ell = 289 \times 10^{-6} \text{ Ns/m}^2$$

$$k_\ell = 0.679 \frac{W}{m.K}$$

$$C_{p,\ell} = 4214 \text{ J/kg.K}$$

The condensation heat transfer rate is given by

$$q = h_L (\pi D L_{cond}) (T_{sat} - T_s)$$

$$L_{cond} = \frac{q}{h_L \pi D (T_{sat} - T_s)}$$

$$DL_{cond} = \frac{73.3 \times 10^3 W}{h_L \pi \times (5K)} = \frac{4606.42}{h_L}$$

Assuming laminar film condensation on a vertical surface

$$h_L = 0.943 \left[\frac{g \rho_\ell (\rho_\ell - \rho_v) k_\ell^3 h_{fg}}{\mu_\ell (T_{sat} - T_s) L} \right]^{1/4}$$

$$Ja = \frac{C_{p,\ell} (T_{sat} - T_{surf})}{h_{fg}}$$

$$= \frac{4214 \text{ J/kg K} (100 - 95)^\circ C}{2257 \times 10^3 \text{ J/kg}} = 9.335 \times 10^{-3}$$

$$h'_{fg} = h_{fg}(1 + .68\,Ja) = 2257 \frac{kJ}{kg \cdot K}(1.00634)$$

$$h'_{fg} = 2271.3\ kJ/kg$$

Hence

$$L^{1/4}\bar{h}_L = 0.943\left[\left\{1.635 \frac{m}{s^2} \times 959.7 \frac{kg}{m^3}(959.7 - .596) \times (0.674)^3 \times 2.271 \times 10^6 \frac{J}{kg}\right\} \Big/ \left(289 \times 10^{-6} \frac{kg}{s\,m} \times 5K\right)\right]^{1/4}$$

$$L_{cond}^{1/4}\bar{h}_L = 4919.04$$

$$\bar{h}_L = \frac{4919.04}{L_{cond}^{1/4}}$$

$$D L_{cond} = \frac{4666.4\,25}{\bar{h}_L} = \frac{4666.4.23}{\frac{4919.04}{L^{1/4}}}$$

$$D L^{3/4} = \frac{4666.4 - 23}{4919.04} = .9486$$

if $D = 1$, $L_{cond} = 20.88m \Rightarrow A_{cond} = 6.3m^2$

∴ the area required for condensation heat transfer of 73.3 kW is $6.3\,m^2$.

However the area required to radiate 73.3 kW is much larger.

$$q_{rad} = \sigma A (T_s^4 - T_{sink}^4)$$

$$\frac{73.3 \times 10^3 W}{5.67 \times 10^{-8} \frac{W}{m^2 K^4} (368^4 - 322^4) K^4} = A$$

$$\therefore A = 170 m^2$$

Hence No of reflux boilers =

$$= \frac{\text{required radiation area}}{\text{heat pipe area}}$$

$$= \frac{170 m^2}{6.3 m^2} = 26.98$$

Hence 27 reflux boilers are required. each has a diameter of 10cm and a length of 20m.

Radiator Mass

A typical mass estimate for a radiator is 5.2 kg/m^2.

Mass of radiator surface $= 5.2 \times A_s$

$= 5.2 \times 170 m^2$

$= 884$ kg.

Liquid Mass

$m_{H_2O} = \rho_{H_2O} \times V_{H_2O}$ $\quad V_{H_2O} = V_{evap}$

$V_{evap} = L_{evap} \times \frac{\pi}{4} D^2$

$= 3.139m \times \frac{\pi}{4} D^2 = 0.025 m^3$

$M_{H_2O} = 998 \frac{kg}{m^3} \times .025 m^3 = 24.95 kg$

Total mass of reflux Boiler = ~~[illegible]~~ 709 kg

Power Estimate :

External heat required = 0

for 50 kW cooling, 23.3 kW of work will be required (assuming a 2 stage vapor compression cycle is used).

External work required = 23.3 kW

Total cooling load = 73.3 kW

Mass Estimate : same as vertical plate, but $\eta = .95$

Total mass = $\frac{50\,(5)}{(.496)(.95)} = 530 kg$

∴ specific mass = 10.6 kg/kW.

APPENDIX C4

CALCULATIONS FOR LIQUID DROPLET RADIATOR

Definition of terms

ε_0 = individual droplet emissivity

τ = optical depth normal to its surface

n = # of droplets per unit volume

θ = c/s of a droplet = λa^2

r = Droplet radius

s = Sheet thickness

ε = effective emissivity of sheet.

T_i = Droplet initial temperature

T_f = final temperature

T = instantaneous temperature

Specific mass of sheet = $\frac{\text{sheet mass}}{\text{area}}$

$= 2\lambda \cdot \rho_d$

where $\rho_d = \frac{8 \cdot a}{3}$

Overall energy balance on liquid sheet

Assume: No temperature variation within the sheet.

$$-E_{out} = E_{stored}$$

$$-\varepsilon \cdot \sigma \left(T^4 - T_{sink}^4\right) = 2\tau \cdot P_d \cdot C_p \frac{dT}{dt}$$

integrating

$$\int \frac{dt}{2\tau P_d C_p} = \int \frac{dT}{-\varepsilon \sigma T^4 + \varepsilon \sigma T_{sink}^4}$$

$$t = 2\tau P_d C_p \int \frac{dT}{-\varepsilon \cdot \sigma \cdot T^4 + \varepsilon \cdot \sigma \cdot T_{sink}^4}$$

where t = transit time

Assuming $T_i = 384\,k$

$T_{sink} = 322\,k$ [The liquid sheet acts as a vertical radiator alligned eastwest]

$\varepsilon = .1$

$\tau = 1$ (mean optical depth)

ε = effective emissivity of sheet = .17

$$\frac{\text{sheet mass}}{\text{Area}} = \frac{\varepsilon}{2\tau} = \frac{.17}{2(1)} = .085\ kg/m^2$$

For 7055, which can be used for this application

$\varepsilon_0 = .5$

$\tau = 1$, $\varepsilon = .5$

$$\frac{\text{sheet mass}}{\text{Area}} = \frac{.5}{2} = .25 \text{ kg/m}^2$$

$\rho = 1 \text{ g/cm}^3$

$C_p = 1.67 \text{ J/g·K}$

Using equation ①

$$t = 2\lambda \rho d \cdot C_p \int_{T_f}^{T_i} \frac{dT}{-\varepsilon \cdot \sigma \cdot T^4 + \varepsilon \cdot \sigma \cdot T_{sink}^4}$$

$$= 2(1)\left(\frac{.000125}{3}\right)(1000)(1670)\int_{360}^{384} \frac{dt}{(5)\,5.67\times10^{-8}(T^4 - 322^4)}$$

$$t = 27.8 \int_{360}^{384} \frac{dT}{2.8\times10^{-8}T^4 - 304.8}$$

$= .10640288$ (integral was solved using mathview)

$= 2.96$ seconds

A typical value for initial velocity $= 17.1 \text{ m/s}$

Length of sheet $= (17.1)(2.96)$

$= 50 \text{ m}$

Required Area for radiator

Assuming: $T_f = 360$, $T_i = 384$

T_e = effective radiating temperature

$$T_e^4 = 3T_i^4/(f^3 + f^2 + f)$$

where $f = T_i/T_f$

$$f = 1.066$$

$$\boxed{T_e = 371.7}$$

$$\therefore q''_{rad} = (.5)(371.7^4 - 322^4)(5.67 \times 10^{-8})$$

$$q''_{rad} = 236.4 \text{ watts/m}^2$$

∴ to reject 50 kw

radiator area $= 211.5 \text{ m}^2$

$$\boxed{\text{Area} = 211.5 \text{ m}^2}$$

Choosing collector diameter = .25m

Choosing generator diameter = 4m

sheet length = 50m

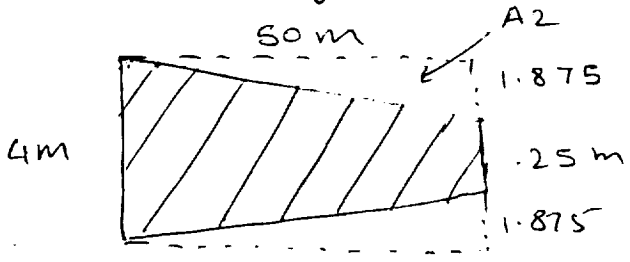

Radiating area = $[A_1 - A_2 - A_3]2$

$= \left[4(50) - \frac{1}{2}(1.875)(50) - \frac{1}{2}(1.875)(50)\right]2$

Radiating Area = 212 m^2

Mass Calculations

A compared to a solid radiator for mass, the liquid droplet radiator has the additional mass of the collector, generator and the radiating liquid. The rest of the equipment such as pumps, piping and power requirements are comparable.

Generator Mass: 245 kg for 24 m diameter generator

$\therefore$ for 8.5 m, mass = 150 kg

$\therefore$ **generator mass = 150kg**

Collector mass = 300 kg for 1 m of Collector

$\therefore$ for .25m Collector, mass = 150 Kg

Collector mass = 150kg

Mass of liquid sheet:

$\tau = n s \sigma$

where s = sheet thickness

for, 50 μm droplets, a typical spanning of droplets results in

$s = 3.2$ cm

$$n = \frac{\lambda}{s\sigma} = \frac{1}{(3.2)(\pi)(r^2)}$$

$$n = \frac{1}{(.032)(\pi)(25\times10^{-6})^2}$$

$= 1.6 \times 10^{10}$ droplets/m^3 of sheet

Volume of one droplet $= \frac{4}{3}\pi r^3$

$= \frac{4}{3}(\pi)(25\times10^{-6})^3$

$= 6.52 \times 10^{-14}$

Volume occupied by the liquid material per m^3 of sheet volume

$= (6.52\times10^{-14})(1.6\times10^{10})$

$= .001044\ m^3$ of DOW 705

Total volume of liquid sheet $= (212)(.032)$

$= 6.784\ m^3$

Volume of DOW 705 in the whole sheet $= (6.784)(.001044)$

$= .0071\ m^3$

Density of Dow 705 $= 1000 \text{ kg/m}^3$

Mass of liquid sheet $= .0071 \times 1000$

$= 7.1 \text{ kg}$.

$\therefore$ Total mass of LDR for 50 kW rejection = Generator mass + Collector Mass + liquid sheet mass

$M_{LDR} = 150 + 150 + 7.1$

$\boxed{M_{LDR} = 307.1 \text{ kg}}$

$\therefore$ Mass per unit kW rejection $= \frac{307.1}{50}$

$\boxed{= 6.14 \text{ kg/kW}}$

APPENDIX D

DECISION MATRICES

Rating	Description
100	Completely satisfies all design criteria
90	Satisfies all the primary criteria
80	Satisfies most of the primary criteria and all secondary
70	Satisifes most primary and most secondary
60	Satisfies some primary and most secondary
50	Satisfies some primary and some secondary
40	Satisfies few primary and some secondary
30	Satisfies few primary and few secondary
20	Satisfies no primary and few secondary
10	Satisfies no primary and one secondary
0	Satisfies no primary and no secondary

Criteria / Weighting Factor / Alternative design	Mass	Volume	Power requirement	Redundancy	Total
	.40	.30	.15	.15	1.0
Air loop	70 / 28	65 / 19.5	50 / 7.5	60 / 9	64.0
Single water loop	90 / 36	85 / 25.5	75 / 11.25	80 / 12	**84.75**
Double water loop	75 / 30	75 / 22.5	80 / 12	80 / 12	76.5

Decision matrix for heat acqusition system

Alternative design \ Criteria / Weighting Factor		Mass	Volume	Power	Additional radiator load	Temperature control	Redundancy	Reliability	Ease of Design	**Total**
		.30	.16	.14	.13	.11	.06	.05	.05	1.0
Vapor compression	Single stage	100 / 30	100 / 11	50 / 7	80 / 10.4	80 / 8.8	90 / 5.4	90 / 4.5	90 / 4.5	86.6
	Two stage	90 / 27	90 / 14.4	70 / 9.8	100 / 13	100 / 11	90 / 5.4	80 / 4.0	80 / 4	**88.6**
Vapor absorbtion		70 / 21	60 / 9.6	100 / 14	70 / 9.1	70 / 7.7	70 / 4.2	70 / 3.5	70 / 3.5	72.6
Metal hydride		50 / 15	60 / 9.6	90 / 12.6	50 / 6.5	50 / 5.5	70 / 4.2	60 / 3.0	50 / 2.5	58.4

Decision matrix for transport system

Alternative design / Criteria / Weighting Factor		Mass	Adaptability to lunar environment	Volume	Reliability	Redundancy	Ease of design	Total
		.3	.19	.18	.14	.13	.06	
Flat plate	Horizontal	60 / 18	80 / 15.2	60 / 10.8	80 / 11.2	80 / 10.4	90 / 5.4	71.0
	Vertical	70 / 21	80 / 15.2	70 / 12.6	80 / 11.2	80 / 10.4	90 / 5.4	75.8
Parallel plate		50 / 15	80 / 15.2	50 / 9	80 / 11.2	80 / 10.4	70 / 4.2	65.0
Reflux boiler		90 / 27	80 / 15.2	70 / 12.6	80 / 11.2	70 / 9.1	70 / 4.2	**79.3**
Liquid droplet		100 / 30	60 / 11.4	90 / 16.2	60 / 8.4	50 / 6.5	50 / 3	75.5

Decision matrix for heat rejection system

APPENDIX E1

Heat load calculations

Heat load calculations were done for the maximum and the minimum cases. For the maximum case the breakdown of the total heat load is as follows.

53 KW	Science experiments.
15 KW	Thermal control system.
10.7 KW	Life support system
5.45 KW	lightning.
3.29 KW	people (crew).
1.5 KW	Comunications.
0.18 KW	external heat load

Therefore the total heatload was calculated to be 89 KW.

The maximum heat gain from the crew was calculated as follows.

Assume a crew size of 12

Assume crew is performing moderately strenuous work.

From Carrier system design manual at a temperature of 75°F

Sensible heat = 325 Btu/hr/person.

latent heat = 525 Btu/hr/person.

Therefore total sensible heat is

$12 \times 325 \text{ Btu/hr/person} = ~~6300~~ 3900 \frac{\text{Btu}}{\text{hr}}$

$= 1.1429 \text{ kW}$

Total latent heat is.

$12 \times 525 \text{ Btu/hr/person} = 6300 \text{ Btu/hr}$

$= 1.846 \text{ kW}$

The latent heat gain from other sources is accounted for as follows

Hygiene water	.44 kg/man day.
Food preparation	.03 kg/man day.
Experiment water	.45 kg/man day.
laundry water	.06 kg/man day.
Total	.98 kg/man day.

$.98 \frac{\text{kg}}{\text{man·day}} \times 12 \text{ men} \times \frac{1 \text{ day}}{24 \text{ hrs}} \times \frac{1 \text{ hr}}{3600 \text{ s}} = 1.361 \times 10^{-4} \frac{\text{kg}}{\text{s}}$

By multiplying this number by the heat of evaporation of water we get:

$1.361 \times 10^{-4} \frac{kg}{s} \times 2257 \, kJ/kg = .307 \, kW.$

∴ the maximum heat load from equipment as well as people is

$1.846 \, kW + .307 \, kW = 2.153 \, kW$

Minimum heat load

For the minimum heat load calculation it was assume that only the life support system and the communication system would be operational.

Therefore the total heat load for the minimum case is 12 kW.

APPENDIX E2

HEAT LOAD DISTRIBUTION CALCULATIONS

To determine what part of the total heat load should be on the water loop and what part of it should be on the air loop the following calculations were made.

Ventilation requirement of 5 airchanges/hr are adequate. If the load is distributed evenly, 37 kW on the water loop and 37 kW on the airloop then the number of air changes can be calculated.

$$37\ kW \times 3412.14 \frac{Btu/hr}{kW} = 126249\ Btu/hr$$

The temperature of the Module is to be maintained at $73\ ^\circ F = 22.7\ ^\circ C$

$T_{supply} = 12.7^\circ C = 55^\circ F$.

$$CFM = \frac{126249\ Btu/hr}{1.08(73-55)} = 6494\ Cfm$$

$$= 3.06\ m^3/s$$

Volume of the module = $\frac{4}{3}\pi r^3$ where $r = 8m$

$$V_{module} = 2144.6\ m^3$$

$$3.06\ \frac{m^3}{s} \times 3600\ \frac{s}{hr} = 11016\ m^3/hr$$

$$\therefore \#\text{ of air changes} = \frac{11016\ m^3/hr}{2144.6\ m^3} = 5.13$$

Since the number of air changes is more than 5, adequate ventilation will be provided.

It was therefore decided that 37 kW would be collected by the air loop and the remaining 37 kW would be collected by the water loop.

APPENDIX E3

DESIGN CALCULATIONS FOR WATER LOOPS

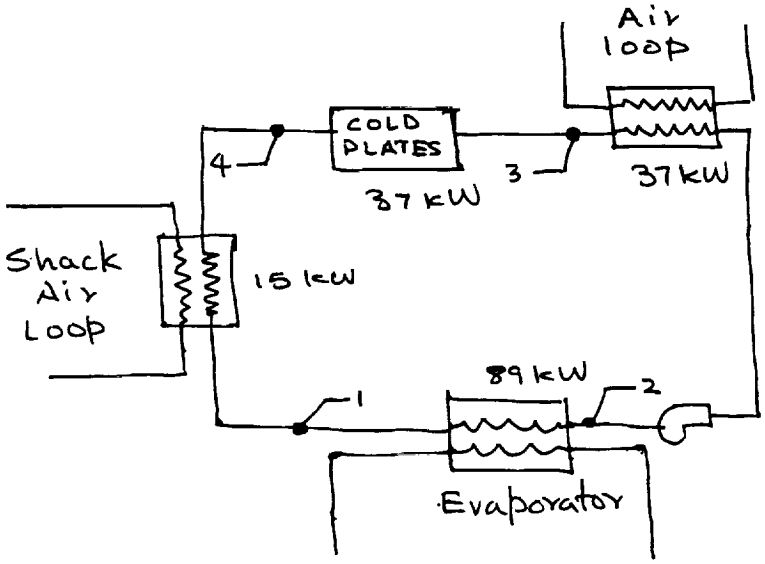

The total heat load to be rejected at the evaporator is 89 kW.

Knowing the temperatures at 1 and 2 are 25°C and 7°C respectively, the mass flow rate of the loop can be calculated.

$$q = \dot{m} C_p (T_2 - T_1)$$

$$\therefore \dot{m} = \frac{q}{C_p (T_2 - T_1)} = \frac{89\ kW}{4.18\ (18)} = 1.18\ \frac{kg}{s}$$

37 kW is to be acquired by the water loop from the air.

Knowing the mass flow rate in the loop, and the inlet temperature, the water temperature at state 3 can be determined.

$$T_3 = \frac{q}{\dot{m} C_p} + T_1$$

$$T_3 = \frac{37}{1.18(4.18)} + 7 = 14.5^\circ C$$

$$\boxed{T_3 = 14.5^\circ C}$$

Similarly q from the cold plates is 37 kW.

$$\therefore T_4 = \frac{q}{\dot{m} C_p} + T_3$$

$$T_3 = \frac{37}{1.18(4.18)} + 14.5 = 22^\circ C$$

$$\boxed{T_3 = 22^\circ C}$$

q generated by the TCS is 15 kW

$$T_1 = \frac{15}{1.18(4.18)} + 22.0$$

$$\boxed{T_1 = 25^\circ C}$$

∴ The system is balanced.

An average cold plate size of 30cm x 50cm was assumed.

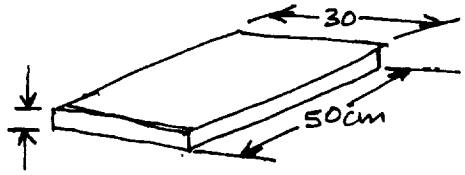

Cold plate area = 30cm x 50cm = 1500 cm^2

The heat flux from the electronics equipment is at the rate of 1 W/cm^2.

∴ each cold plate collects 1500 W.

To collect a total heat load of 37 kW 25 cold plates would be required.

$$\#\text{ of cold plates} = \frac{37\text{ kW}}{1.5\text{ kW}} = 24.6 \approx \underline{25}$$

The mass flow rate through each cold plate will be

$$\frac{1.18\text{ kg/s}}{25\text{ cold plates}} = 0.0472\text{ kg/s per cold plate.}$$

Piping dimensions.

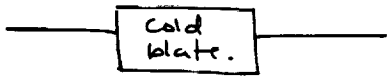

The tubes that connect to the cold plates are .635 cm Diameter

$$\dot{m} = \rho V A = .0472 \text{ kg/s}$$

$$A = \frac{\pi D^2}{4} = \frac{\pi(.00635)^2}{4} = 3.166 \times 10^{-5} \text{ m}^2$$

$$V = \frac{\dot{m}}{\rho A} = \frac{.0472}{1000(3.166 \times 10^{-5})} = 1.49 \text{ m/s}$$

For the pipes that run on floors 1, 3 and 4.

$\dot{m} = (.0472 \text{ kg/s})\, 9 = .4248$.
since there are 9 coldplates on levels 3 & 4.

$$A = \frac{.4248}{\rho V} = \frac{.4248}{1.49(1000)} = 2.85 \times 10^{-4} \text{ m}^2$$

$\boxed{D_h = 1.9 \text{ cm}}$

For the pipes that run vertically

$\dot{m} = 1.18 \text{ kg/s}$

$$A = \frac{1.18}{1000(1.49)} = 7.919 \times 10^{-4} \text{ m}^2$$

$\boxed{D_v = 3.17 \text{ cm}}$

The individual floor loops are 20 m long.

the vertical pipes are 17 m long.

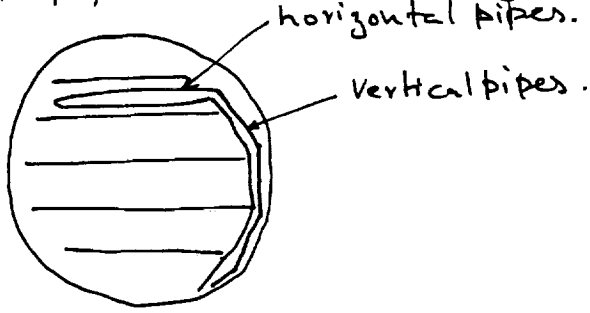

Pump power required

The pump has to overcome the head loss due to friction

For the cold plate pipes: $V = 1.49\ m/s$

$D = .00635\ m$.

$$Re = \frac{1.49(.00635)}{1\times10^{-6}\ m^2/s} = 9486.5$$

$$\varepsilon = .046 \quad \therefore \quad \frac{\varepsilon}{D} = \frac{.046}{.635} = 7.244\times10^{-3}$$

From the moody charts we get $f = .08$

$$h_L = \left(f\frac{L}{Dn} + \Sigma K\right)\frac{V^2}{2g}$$

$$\text{Power} = \dot{m}\,\Delta P = .0472\,\rho g h_L$$

$$= 38\ W.$$

In a similar manner the power requirements for the all the piping network was found.

$$\boxed{\text{Power}_{total} = .33\ kW}$$

APPENDIX E4

CALCULATIONS FOR DUCTING

To calculate the dimensions of the air ducts, the mass flow requirements for every level were considered.
The total ~~m~~ volumetric flow rate is $3.06 m^3/s$
it is divided as follows

level	Area m^2	$\dot{m}$ (m^3/s)	Each duct
0	53	.213	.071
1	83.5	.335	.111
2	153.0	.615	.205
3	183.2	.736	.245
4	171.3	.688	.2292
5	171.7	.473	.1576

Since there are 3 main supply ducts, each main duct carries $1.02\ m^3/s$.
As the main supply ducts rise from level 0 to level 5, they have to decrease in size to keep the speed of the air constant.

The velocity for the main duct is 7.62 m/s and for the supply duct is 6.1 m/s knowing the volumetric flowrate and the velocity, the diameter of the duct can be calculated by the equation:

$$\dot{M} = VA$$

$$\therefore A = \frac{\dot{M}}{V} = \frac{1.02\ m^3/s}{7.62\ m/s} = .134\ m^2$$

$$\therefore D = 42\ cm$$

in a similar manner the diameters for the ducts as they rise from level 0 to level 5 are calculated. The table below sumarizes these calculations.

level	Q	Diameter (m)	Pressure loss (Pa/m)
0 – 1	1.02	.42	1.6
1 – 2	.949	0.40	1.8
2 – 3	.838	0.37	2.0
3 – 4	0.633	0.33	2.0
4 – 5	0.3878	0.26	3.0
5 – top	0.1586	0.20	1.9

These pressure losses and the duct diameters were calculated using the Trane companys duct calculator device.

There are 2 branch ducts on each main duct at every floor. For the branch ducts velocities of 6.1 m/s was assumed. The table below sumarizes the flow rates and the duct diameters for every level.

level	$\dot{m}$ m^3/s	diameter (m)	Ploss ($\frac{Pa}{m}$)
0	0.0359	0.085	7.5
1	0.0558	0.11	5.1
2	0.1025	0.15	3.81
3	0.1226	0.16	3.0
4	0.1146	0.16	3.0
5	0.0788	0.13	4.0

Fan power requirements

The fan power required to supply the needed flow rate can be found by calculating the static pressure loss in the duct. From Trane company's duct calculator we get the following results.

level	Pressure loss ('in/100 ft of duct)
0 - 1	.195
1 - 2	.220
2 - 3	.244
3 - 4	.244
4 - 5	.366
5 - Top	.232

For the main ducts the pressure loss is 1.5 in of H_2O/100ft of duct.

For the 3 main ducts the pressure loss is .37 in of water.

For branch ducts we get the following figures

level	Pressure loss in w/100ft	length(ft)
0	.917	15
1	.623	21.12
2	.466	25
3	.366	25.28
4	.366	23
5	.489	18

∴ Adding the losses for each duct and multiplying by 6 (No. of ducts) we get a pressure loss of 3.03 in of water.

We also know the total cfm = 6494.29

∴ from a figure of fan curves we can find the horse power needed.

The pressure loss is 3.4 + .2 (3.4) for bends and passing the air through the coil.

∴ The pressure loss is 4.08 in of water.

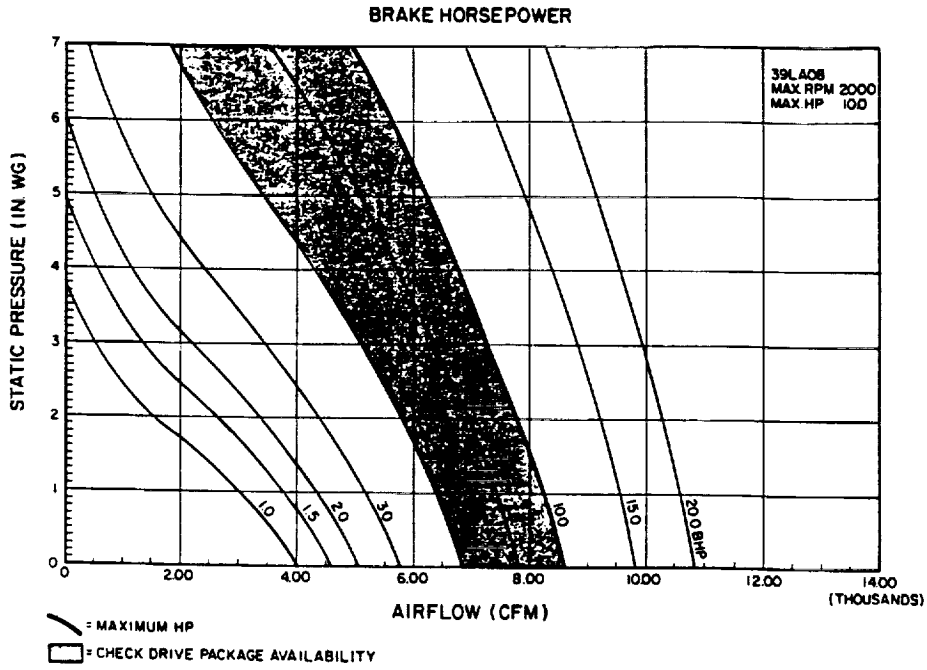

From the above figure at a pressure loss of 4.0 in.wg, and at a CFM of 6494.29 we can find the horsepower needed.

$$hp = 8.75$$

$$\boxed{\text{Power} = 6.5 \text{ kW}}$$

PSYCHROMETRIC CHART

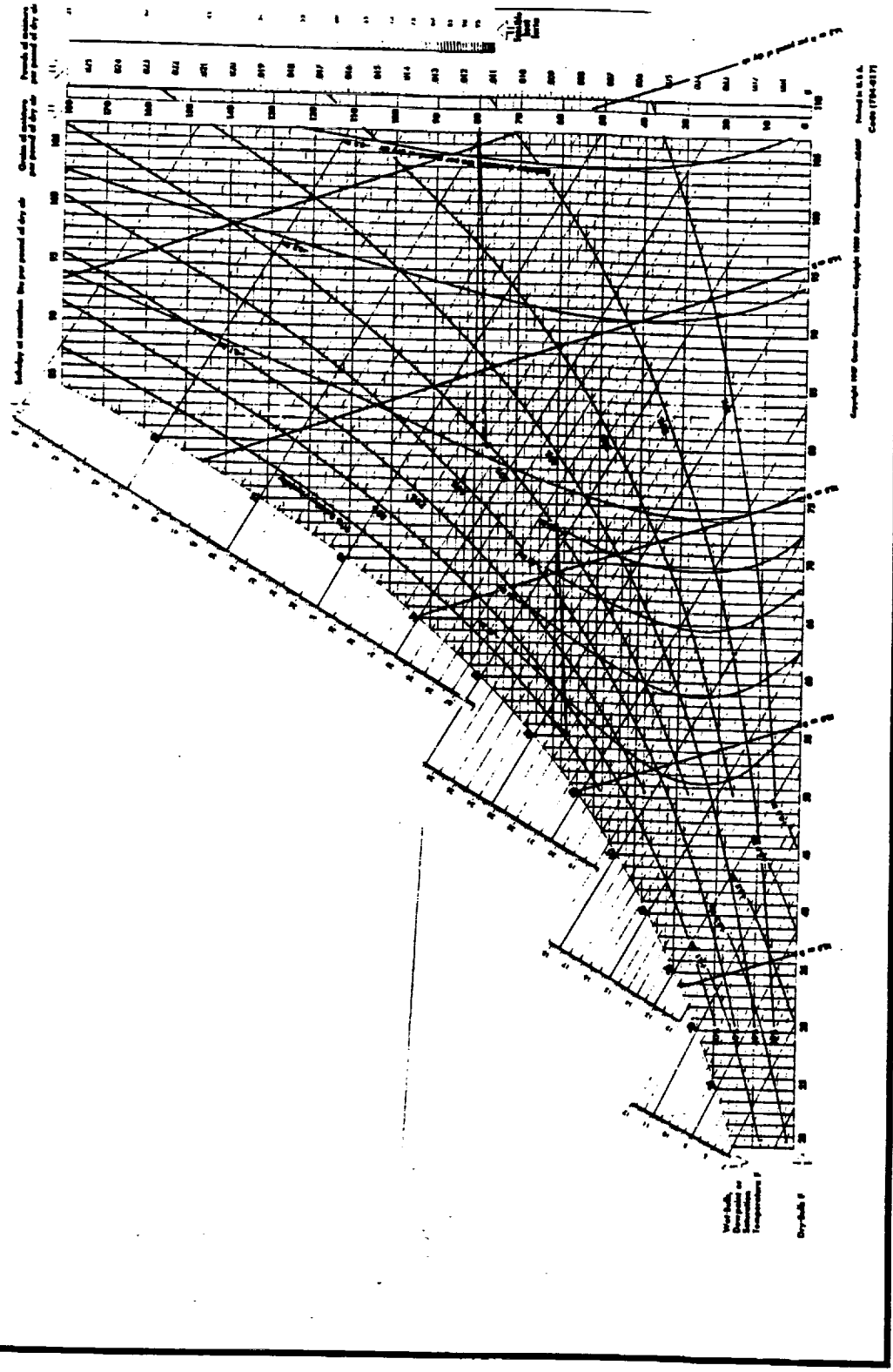

APPENDIX E5

OPERATION CALCULATIONS
REDUCED LOAD

To operate the system at a reduced load the ~~te~~ bypass valve is adjusted. for a minimum heat load of 12 kW

$$12 \times 3412.14 = 40945 \text{ Btu/hr}$$

$$cfm = \frac{40945}{1.08(18)} = 2106 = 1.07 \text{ m}^3/\text{s}$$

$$q = \dot{m} c_p \Delta T$$

$$\dot{m} = \frac{q}{c_p \Delta T} = \frac{12 \text{ kW}}{4.18(25-7)} = .16 \text{ kg/s}$$

The supply air temperature is

$$T_{supply} = \frac{(1.07)12.7 + (1.95)22.7}{3.02} = \underline{19.15^\circ C}$$

APPENDIX E 6

MASS CALCULATIONS

Mass of Ducting:

Assume ducts are made out of aluminum.

$\rho = 2700 kg/m^3$.

Average diameter for main ducts = .33m

length = 15.6m

$\pi d = 1.03 \times 15.6 = 16.17$

Assume thickness of $3 \times 10^{-3} m$

$V = \pi d L t = 4.85 \times 10^{-2}$

$V_{TOT} = 3 \times (4.85 \times 10^{-2}) = 1.455 \times 10^{-1} m^3$

For branch ducts, for level 0

$D = .089 m$ length = $4.95^{-} m$.

$V = \pi d L t = 3.96 \times 10^{-3} m^3$

For 3 ducts $V_{TOT} = 1.189 \times 10^{-2} m^3$

By similar calculations the volumes of all other ducts were calculated.

Mass of piping

The pipes that run vertially are 3 cm diameter.

assume thickness of 3×10^{-3} m.

assume pipes are made of a Titanium alloy.

$\rho = 4420 \text{ kg/m}^3$.

$\pi D l(t) = \pi(3\times10^{-2})(20)(3\times10^{-3}) = 5.654\times10^{-4} \text{ m}^3$

where l the length of the pipe is 20 m.

$m = \rho V$, where $\rho = 4420 \text{ kg/m}^3$ $\therefore$ $m = 25 \text{ kg}$

for horizontal running pipes.

assume length of 60 m. and $D = 2\times10^{-2}$ m

$$\pi D l(t) = \pi(2\times10^{-2})(60)(3\times10^{-3}) = 1.13\times10^{-2}$$

$$m = \rho V = 4420\,(1.13\times10^{-2})$$

$$m = 50.8 \text{ kg}.$$

$$m_{TOT} = 50.8 + 25 = 75.8 \approx 76 \text{ kg}.$$

These calculations are sumarized in the table below.

level	V_{TOT} m^3
0	1.189×10^{-2}
1	4.1×10^{-2}
2	6.57×10^{-2}
3	7.147×10^{-2}
4	6.5×10^{-2}
5	4.26×10^{-2}

The total Volume of both the branch ducts and the main ducts is

$$V_{TOT} = .443 m^3.$$

For $t = 2 \times 10^{-3}$, $V = 2.95 \times 10^{-1} m^3$.

$$Mass = \rho V = 2700 \times (2.95 \times 10^{-1} m^3)$$

$$Mass = 797.41 kg.$$

Mass of cold plates

$$V = .50 \times .3 \times .006 = 9 \times 10^{-4} m^3$$

$$\rho = 7800 \, kg/m^3$$

$$M = \rho V = 7.02 kg$$

$$M_{TOT} = 7.02 \times 25 = 175.5$$

Mass volume of tube inside coldplate $= 6.33 \times 10^{-5} m^3$

$= .5 kg.$

$\therefore$ $7.02 - .5 = 6.52$

6.52×25 plates $= 163 kg$

APPENDIX F1

OPERATING CONDITIONS OF THE TRANSPORT SYSTEM

1. During lunar night, the vapor compression system will be bypassed.
2. Maximum heatload at night = 74 kW.
3. Temperature of fluid in the transport system = 0°C.
4. Temperature drop between transport system and rejection system = 10°C.

From the above data if the vapor compression system is bypassed, the radiator temperature will be

$$T_{rad} = -10^{\circ}C = 263K$$

Using Equation

$$q = \varepsilon \cdot \sigma \cdot A \left(T_{rad}^4 - T_{sink}^4\right)$$

$T_{sink} = 88^{\circ}K$ at lunar night for a vertical radiator.

The area required to reject the maximum load was ~~74 kW~~ determined.

$$74 \times 10^3 = (.8)(5.67 \times 10^{-8})(A)(263^4 - 85^4)$$

$$\boxed{A = 345 \text{ m}^2}$$

This area is the minimum area required to reject 74 kW at lunar night if the vapor compression system is ~~sh~~ switched off.

As area of the radiator had to be minimized and also the power consumption, this area was chosen for the radiators.
As the radiator area was fixed, it was possible to calculate the operating parameters of the vapor compression system.
As the sink temperature is the highest at lunar noon (323) both stages of the compression system will operate.

Max heat load at lunar noon to be rejected = Heat from module + heat from TCS + work done on the fluid. [$\eta = .7$]

Max load = $74 + 15 + (51)(.7) = 126$ kW

The work done and the heat generated were calculated for a number of exiting temperatures.

∴ A temperature lift of the vapor compression system was determined.

A temperature lift of 0°C to 110°C was required.

From the analysis shown in Appendix F2, The inner stage temperature was determined to be 60°C

APPENDIX F2

DESIGN OF VAPOR COMPRESSION SYSTEM

This appendix presents a thermodynamic analysis of the two stage vapor compression system design solution.

The operating limits of the system were determined in Appendix F1.

The transport system must operate at a temperature lift of 110°C.

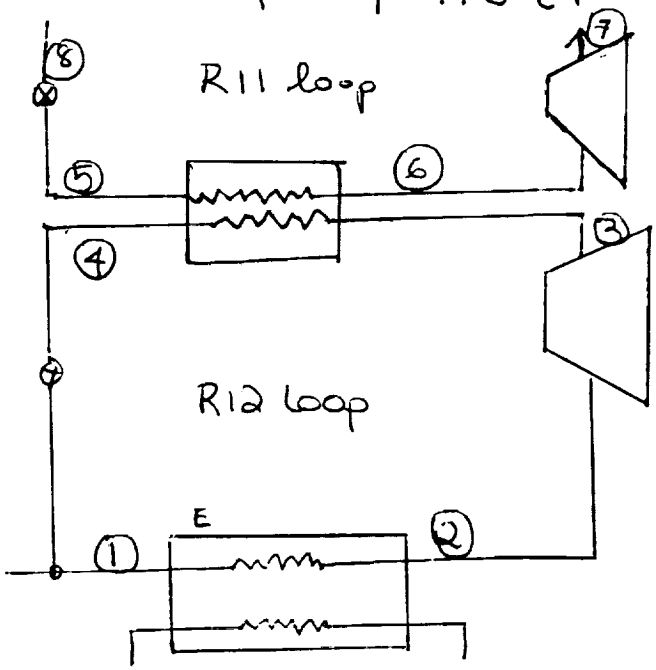

Behavior of working fluid in Loop 2 (R11

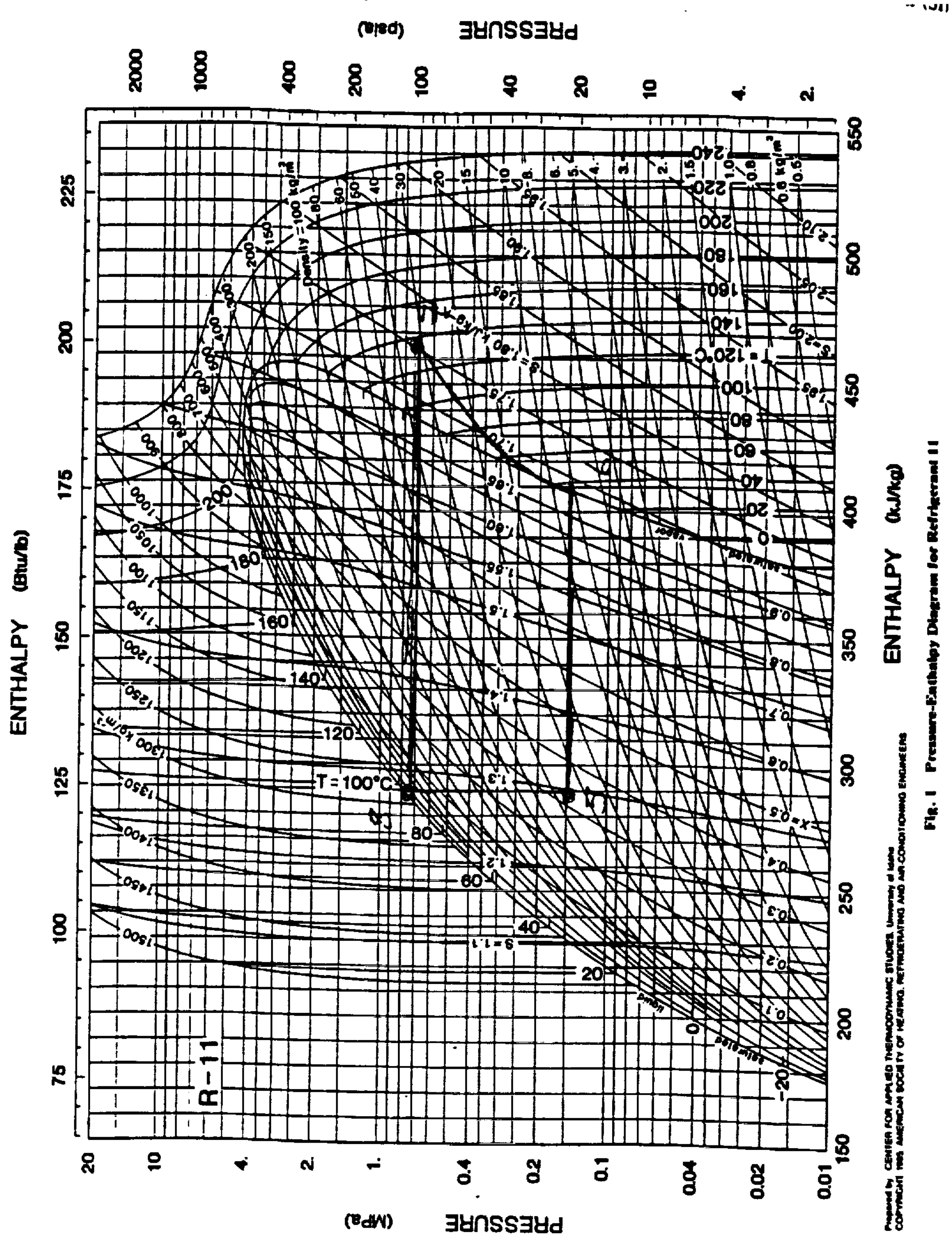

Figure F2:2

PRECEDING PAGE BLANK NOT FILMED

Based on analysis in Appendix F1, the operating conditions are as follows; (see fig F2:1, F2:2.

State	Temp (°C)	Pressure (MPa)	Enthalpy (KJ/Kg)
1	0	0.3	240
2	0	0.3	352
3	60	1.0	377.7
4	42	1.0	240
5	40	0.2	290
6	40	0.2	411
7	110	0.8	452
8	100	0.8	290

States 1-4 (1st stage) is R12.

States 5-8 (2nd stage) is R11.

Assumptions: 1. Compressors are 70% efficient
This is assumed when finding enthalpies

Worst Case Analysis: Max heat Load

The worst case for a stage operation is when 89 KW enters the 1st stage evaporator. This load consists of 74 KW of internal heat and 15 KW of heat generated by the TCS.

$$\dot{Q} = \dot{m}_{R12}(h_2 - h_1)$$

$$\dot{m}_{R12} = \frac{\dot{Q}}{h_2 - h_1} = \frac{89\ KW}{112\ KJ/kg} = 0.794\ kg/s$$

$$\dot{W}_{R12} = \dot{m}_{R12}(h_3 - h_2)$$

$$= 0.794 \frac{kg}{s}(377.7 - 352)\ KJ/kg$$

$$\boxed{\dot{W}_{R12} = 20.4\ KW}$$

Hence, the heat transported into the 2nd stage $= \dot{Q} + \dot{W}_{R12} = (89 + 20.4)\ KW$

$= 109.4\ KW.$

Based on this heat transfer and the mass flow rate in the 1st Stage, the mass flow through the 2nd stage is found.

$$\dot{m}_{R11} = \dot{m}_{R12}\left[\frac{h_3 - h_4}{h_6 - h_5}\right]$$

$$\dot{m}_{R11} = 0.794\ kg/s\left[\frac{377.7 - 240}{411 - 290}\right]$$

$$\dot{m}_{R11} = 0.903\ kg/s$$

$$\dot{W}_{R11} = \dot{m}_{R11}[h_7 - h_6]$$

$$= 0.903\ kg/s[447.14 - 411.17]$$

$$\boxed{\dot{W}_{R11} = 32.5\ KW.}$$

Total compressor work = **52.9 KW**
(Maximum load)

Total heat to be rejected = 74 KW + 52 kW
= 126 KW

The 52. KW accounts for both the heat generated + the work done on the fluid.

ANALYSIS FOR MINIMUM HEAT LOAD.

Internal heat = 12 KW

assuming 70% compressor efficiency, 30% is given off as heat.

$$\dot{q} + 0.3\dot{W} = \frac{1}{0.24}\dot{W}$$

$$12 = 4.047\dot{W} \Rightarrow \dot{W} = 2.965 \text{ KW}$$

$$Q_{\substack{\text{MODULE} \\ \text{TTCs}}} = Q_M + Q_{TCS} = Q + 0.3W$$

$$\doteq 12 + 0.868 = 12.9 \text{ KW}$$

$$\simeq \boxed{13 \text{ KW}}$$

Dimensioning of Components: EVAPORATOR

$C_h = C_{max} = \infty$, since working fluid is changing phase.

$C_{min} = \dot{m}_c C_{p,c}$

The cold fluid is water, at a mass flow rate of 1.08 kg/s (see Acquisition system analysis)

$C_{min} = 1.08 \text{ kg/s} \times 4.177 \frac{\text{kJ}}{\text{kg K}}$

$C_{min} = 4.511 \text{ kW/K}.$

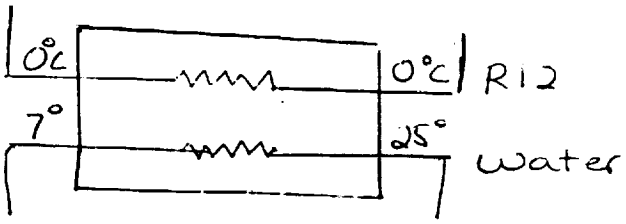

$$q = \varepsilon C_{min} [T_{hi} - T_{ci}] \quad \text{——— (1)}$$

$$NTU = \frac{UA}{C_{min}} \quad \text{——— (2)}$$

(1) $\Rightarrow$ $89 \text{ kW} = 4.511 \frac{\text{kW}}{\text{K}} [298 - T_{ci}]$

(2) $\Rightarrow NTU = \frac{UA}{4.511 \frac{\text{kW}}{\text{K}}}$

$T_{ci} = 273 \text{ K}$

U = overall heat transfer coefficient

A = effective area for heat exchange (m^2)

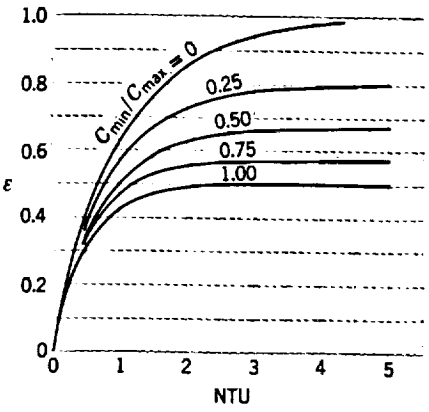

Reference:
'Fundamentals of Heat & Mass Transfer'
Incropera & DeWitt
(J. W ley & Sons)

$C_{min}/C_{max} = 0$. For $\varepsilon = 0.9$, NTU = 2.25

(2) $\Rightarrow$ UA = 10.15 KW/K.

Compressors

1st stage: Work done = 20.4 KW

2nd Stage: Work done = 32.5 KW

Compressor Efficiency = 70%.

Dimensioning of Interstage Evaporator Condenser

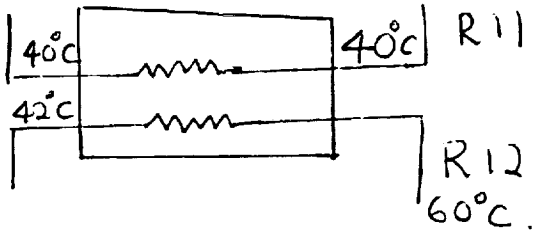

$q = UA(T_{cond} - T_{evap})$

$q = 89\ KW + 20.4 = 109.4\ KW$

$$UA = \frac{109\ KW}{20\ K} = 5.45\ KW/K.$$

Dimensioning of Evaporator Condensers (in rejection system).

(1)

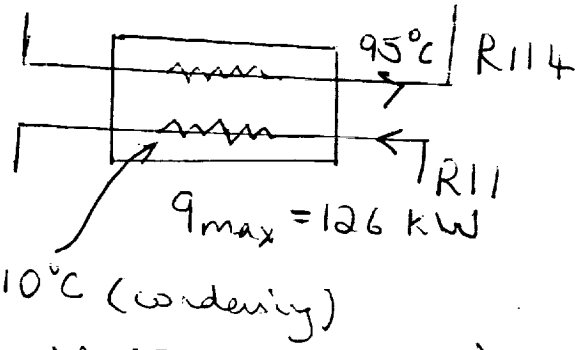

$$q = UA\,(T_{cond} - T_{evap})$$

$$\Rightarrow UA = q/\Delta T = \frac{126\ KW}{15\ K} = 8.4\ \frac{KW}{K}.$$

(2)

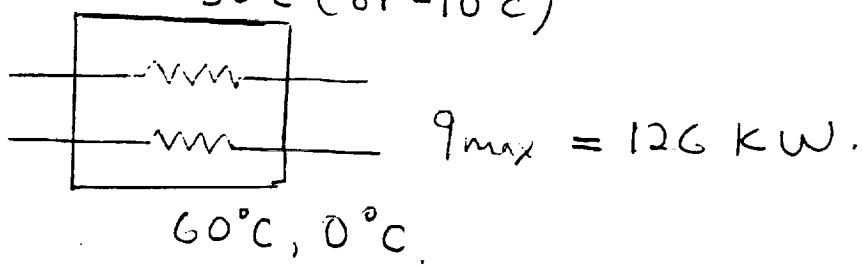

$$q = UA\,(T_{cond} - T_{evap})$$

$$UA = \frac{q}{\Delta T} = \frac{126\ KW}{10\ K} = 12.6\ \frac{KW}{K}.$$

APPENDIX F3

SELECTION OF WORKING FLUID

The performance of various working Fluids was determined for two cases

1) Evaporator temp = 0°C
   Condenser temp = 50°C.
2) Evaporator temp = 50°C
   Condenser temp = 110°C.

$$\frac{\dot{W}}{\dot{m}} = h_2 - h_1 \quad \text{(across evaporator)}$$

$$\frac{\dot{Q}_c}{\dot{m}} = h_2 - h_3 \quad \text{(across compressor}$$

Power input $$\frac{\dot{W}}{\dot{Q}_c} = \frac{h_2 - h_1}{h_2 - h_3}$$

1) Evaporator temperature = 0°C
Condenser temperature = 50°C

Working Fluid	Power input / cooling load
R 11	0.22
R 12	0.25
R 21	0.23
R 22	0.26

2) Evaporator temperature = 50°C
Condenser temperature = 100°C

Working Fluid	Power input / cooling load
R 11	0.17
R 12	0.21
R 21	0.19
R 22	0.27

APPENDIX F4

CALCULATIONS FOR CONTROL DEVICES AND PIPING

Control of the vapor compression is required when the heat load drops from its maximum value of 89 kW (internal + TCS) The worst case analysis is performed here. Namely; when the heat load drops from 89 kW to a minimum 12 kW (internal) As calculated in Appendix F2,

$$q_{into_{1st\ compressor}} = 12.89\ kW$$

Please see fig. on following page.

$$\dot{m}_{loop_1} = \frac{12.89\ kW}{112\ kJ/kg} \quad \left(\text{since } \dot{m} = \frac{q_{in}}{h_2 - h_1}\right)$$

$$= 0.1151\ kg/s$$

$$\dot{W}_{comp} = \dot{m}_1(h_3 - h_2) = .1151\ \frac{kJ}{s}\left[25.685\right]\frac{kJ}{kg}$$

$$= 2.96\ kW$$

$$\dot{m}_{loop_2} = \dot{m}_{loop_1}\left[\frac{h_3 - h_4}{h_6 - h_5}\right]$$

$$= 0.241\ \frac{kg}{s}\left[\frac{377.7 - 240}{411 - 290}\right] = 0.131\ kg/s$$

$$\dot{W}_{comp2} = \dot{m}_{loop2}\,(h_7 - h_6)$$

$$= 0.131\ \frac{kg}{s}\left[447.14 - 411\right]\frac{kJ}{kg}$$

$$= 4.73\ kW$$

$$Q_{\substack{into\\radiators}} = 19.69\ kW$$

(Both stage operation - max internal load)

REFRIGERANT PIPE SIZING

Assume: Copper Pipe

for 32 mm OD; 55 KW capacity

for 40 mm OD; 115 KW capacity

$$\rho_l = 1395.6\ kg/m^3$$

$$\rho_v = \frac{1}{0.05571} = 17.95\ kg/m^3.$$

$$\dot{m} = \rho A V \Rightarrow V = \frac{\dot{m}}{\rho A}$$

$$= \frac{0.794\ kg/s}{1395\ kg/m^3 \times \frac{\pi}{4}(40\times10^{-3})^2}$$

$$V = 35\ m/s$$

for O.D of 50 mm, $V = 22.6\ m/s$

Distance of piping $\simeq 10\ m$.

(to circulate one loop completely)

$$\text{time} = \frac{10\ m}{22.6\ m/s} = 0.445\ s.$$

worst case time:

$$V = \frac{0.794}{1395 \frac{kg}{m^2} \times \frac{\pi}{4} \times (20 \times 10^{-3})^2}$$

$$= 1.8 \text{ m/s}$$

$$\text{time} = \frac{10 \text{ m}}{1.8 \text{ m/s}} = 5.52 \text{ seconds}$$

Accumulator for Loop 1.

An accumulator is required to vary the mass flow rate when the heat load drops from maximum. The accumulator must store maximum mass when heat load drops to a minimum from maximum.

$$\dot{m}_{low} = 0.1151 \text{ Kg/s}$$

$$\dot{m}_{max} = 0.794 \text{ Kg/s}$$

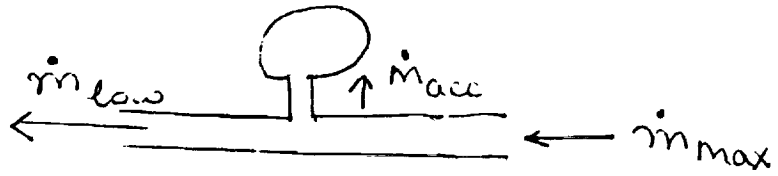

$$\dot{m}_{acc} = \dot{m}_{max} - \dot{m}_{low}$$

$$= 0.794 - 0.1151 = 0.679 \text{ Kg/s}$$

time to open accumulator = 5.52 sec.

Maximum mass reqd to be stored by accumulator $= 5.52 \text{s} \times 0.679 \frac{kg}{s} =$ **3.74 kg**

Accumulator for Loop 2

assume time to open accumulator is once again 5.52 s (assuming loop has a length of 10 m).

$\dot{m}_{max} = 0.903$ kg/s

$\dot{m}_{min} = 0.131$ kg/s

Maximum mass stored by accumulator $= 5.52 \text{ sec} \left(\dot{m}_{old} - \dot{m}_{new}\right)$

$= 5.52 \text{ s} (.903 - .131) \frac{\text{kg}}{\text{s}}$

maximum mass req'd to be stored by loop 2 accumulator $= 4.26$ kg.

Design of Pump for Outer Loop.

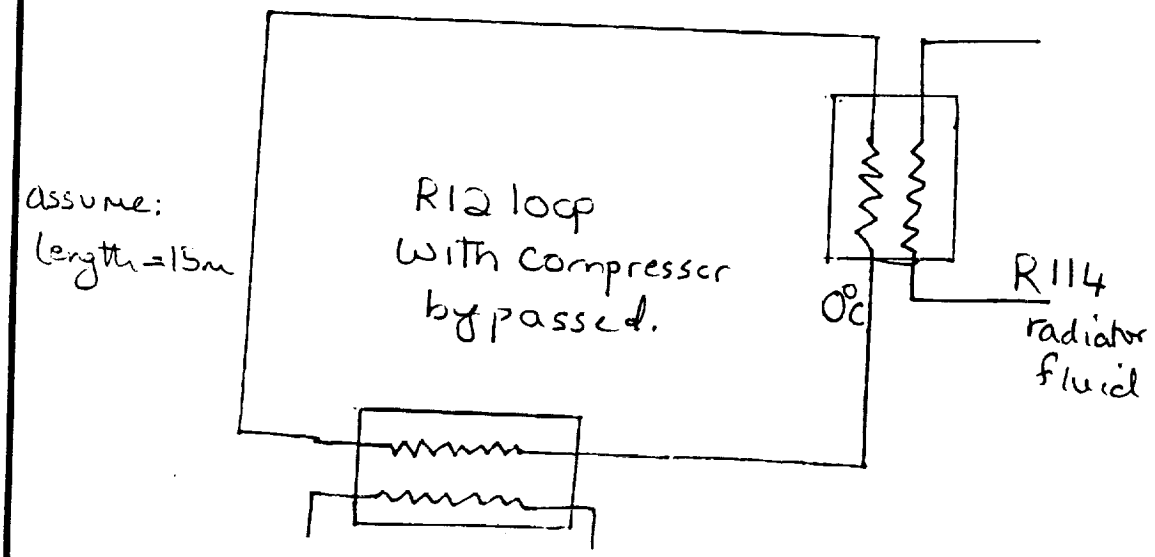

$q_{max} \Rightarrow \dot{m}_{max} = 0.794\ kg/s$

$q_{min} = 27\ KW \Rightarrow \dot{m}_{min} = 0.115\ kg/s$

Require: a pump to maintain circulation at this ranges of flow rates.

Case I: $q_{internal} = 89\ KW$

$q_{internal} = 12.9\ KW$

If we used a pump to vary the mass flow rate, the pressure will change.

The head loss due to friction is

$$h_f = f \frac{L}{D} \frac{V^2}{2g}.$$

Commercial steel pipe: $\varepsilon/D = 0.0009$

$\varepsilon = .00015\ ft$ $D = 50\ mm$

$\Rightarrow f = .019$

$$h_f = 0.019 \times \frac{15m}{50 \times 10^{-3} m} \times \frac{U^2\ (m^2/s^2)}{2 \times 1.635\ m/s^2}$$

$= 43.58\ m$ of $V = 5\ m/s$.

Pressure drop due to friction $= \rho g h_f = 99\ KPa$.

$$V = \frac{\dot{m}}{\rho A} = \frac{\dot{m}}{1315\ \frac{kg}{m^3} \times \frac{\pi}{4} (20 \times 10^{-3})^2}$$

$$V = \frac{\dot{m}}{0.4382}$$

$\dot{m}_{max} = 0.794$ kg/s $\Rightarrow V_{liq} = 1.81$ m/s

$\dot{m}_{min} = 0.115$ kg/s $\Rightarrow V_{liq} = 0.263$ m/s

hence $h_{f_{max}} = 5.71$m or $h_{f_{min}} = 0.12$ m

$P_{loss\ due\ to\ friction\ max} =$ **13.02 KPa**

$P_{loss\ due\ to\ fricton\ min} =$ **0.264 KPa**

$H_T = 313$ KPa. or 300.2 KPa

for a centrifugal pump,

N = speed, H = head.

$$\frac{H_2}{H_1} = \left(\frac{N_2}{N_1}\right)^2 \Rightarrow \frac{N_2}{N_1} = \sqrt{\frac{313}{301.6}} = 1.021$$

$$\frac{\dot{m}_2}{\dot{m}_1} = \frac{N_2}{N_1} \Rightarrow \frac{N_2}{N_1} = \frac{0.794}{0.115} = 6.9$$

so $\frac{H_2}{H_1} = 49.3$

at 2, want $H = 300$ KPa $+ H_f$.

$H_2 = 313$ KPa.

$$\frac{3.9}{H_1} = 49.3$$

$$\Rightarrow H_1 = 6.4 \text{ KPa}.$$

The process of using a pump to both overcome friction and adjust mass flow is not feasible, This is because for the the low flow rate to high flow rate change, the speed of the pump is high. Conseq, the pressure increase is very high, Therefore, a pump is required to overcome friction and accumulator to vary flow.

$$\text{Pumping Power} = \frac{\dot{m}\,\Delta P_{pump}}{\eta \rho}$$

$$= \frac{0.794 \text{ kg/s} \times 13.00 \times 10^3 \text{ N/m}^2}{(0.7)\, 1395.6 \text{ kg/m}^3}$$

at 70% efficiency, $P_{max} = 10$ W.

Design of Accumulator for outer Loop 3

Can use same accumulator as for Loop 1.

$$\dot{m}_{accumulator} = 0.679 \text{ kg/s}$$

$$\text{time} = \frac{15 \text{ m}}{1.8 \text{ m/s}} = 8.33 \text{ sec.}$$

$$m_{stored} = 0.679 \text{ kg/s} \times 8.33$$

$$= 5.66 \text{ kg of fluid}$$

Design of Loop 4

Loop 4 does not require a pump because of the compressor. No extra accumulator is required, since the same one for Loop 1, 3 can be used.

APPENDIX F5

STAGEWISE OPERATION OF THE TRANSPORT SYSTEM

To minimize power consumption, stagewise operation of the transport system was used. From appendix F1 and F2

① For both stages switched off, the temperature of the working fluid of the transport system $= 0^{\circ}C$, $T_{rad} = -10^{\circ}C$

② For single stage operation, $T_{fluid} = 60^{\circ}C$, $T_{rad} = 50^{\circ}C$

③ For both stages operating

$T_{fluid} = 110^{\circ}C$

$T_{rad} = 98^{\circ}C$

Since the area of the radiators was known, and the sink temperatures for different times of the day, it was possible to determine the stagewise operation as a function of time of day. using equation

$$q = \varepsilon A \sigma (T_{rad}^4 - T_{sink}^4)$$

The maximum heat load for the 3 possible stagewise operation are

night operation - 74 kW
single stage - 94 kW
2 stage - 126 kW

For night operation

$$74 \times 10^3 = (.8)(5.67 \times 10^{-8})(345)(263^4 - T_{sink}^4)$$

$$\boxed{T_{sink} = 85\,K}$$

When sink temperature is 85 K, both stages can be bypassed.

For single stage operation

$$94 \times 10^3 = (.8)(5.67 \times 10^{-8})(345)(323^4 - T_{sink}^4)$$

$$T_{sink} = 264.3\,K$$

∴ for any sink temperature between 264.3 K and 85 K, only the 1st stage is operated.

For two stage operation

$$126 \times 10^3 = (.8)(5.67 \times 10^{-8})(345)(374^4 - T_{sink}^4)$$

$$T_{sink} = 323\,K$$

For sink temperature between 323 K and 264.3 K, both stages of the compression system are operated.

Using the equation derived in appendix C, for the sink temperatures of the vertical radiator as a function of sun angle, the sun angle at which Tsink = 264.3K was found. It was found that at a sun angle of ± 41.5°, the sink temperature is 264.3 K

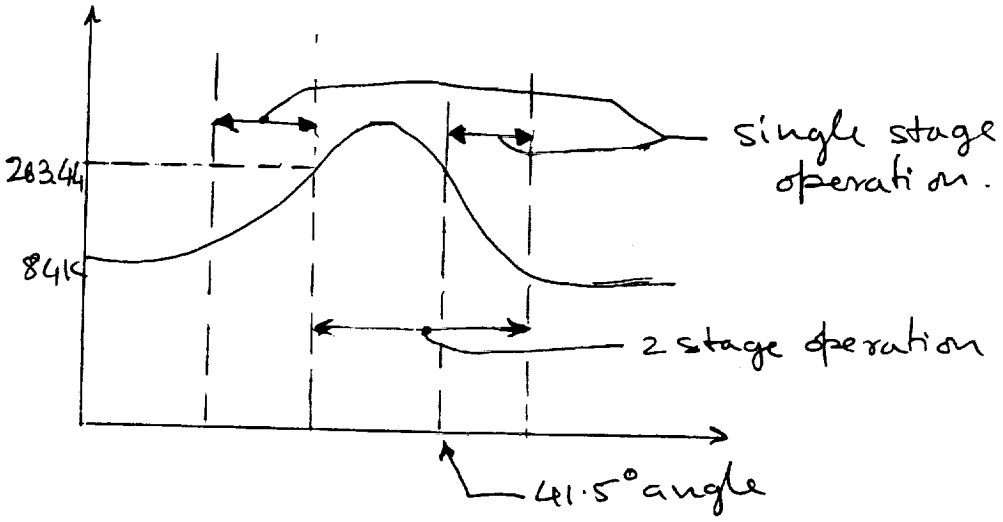

APPENDIX F6

MASS AND POWER CALCULATIONS FOR TRANSPORT SYSTEM.

The mass estimate for the transport system shown in Figure 27 of the report is given below.

EVAPORATOR

The mass of the heat exchanger can be related to the UA parameter and the tube diameter. A typical tube diameter used here is 0.025m. The graph relating the mass of the heat exchanger to the UA parameter of the heat exchanger is shown below [ ] in Figure F6-1

$$M_{hx} = \tilde{M} UA D_t.$$

In Appendix F2, UA was found.

$$UA = 10.15$$

From graph, $\tilde{M} = 1400 \frac{kgK}{KWm}$

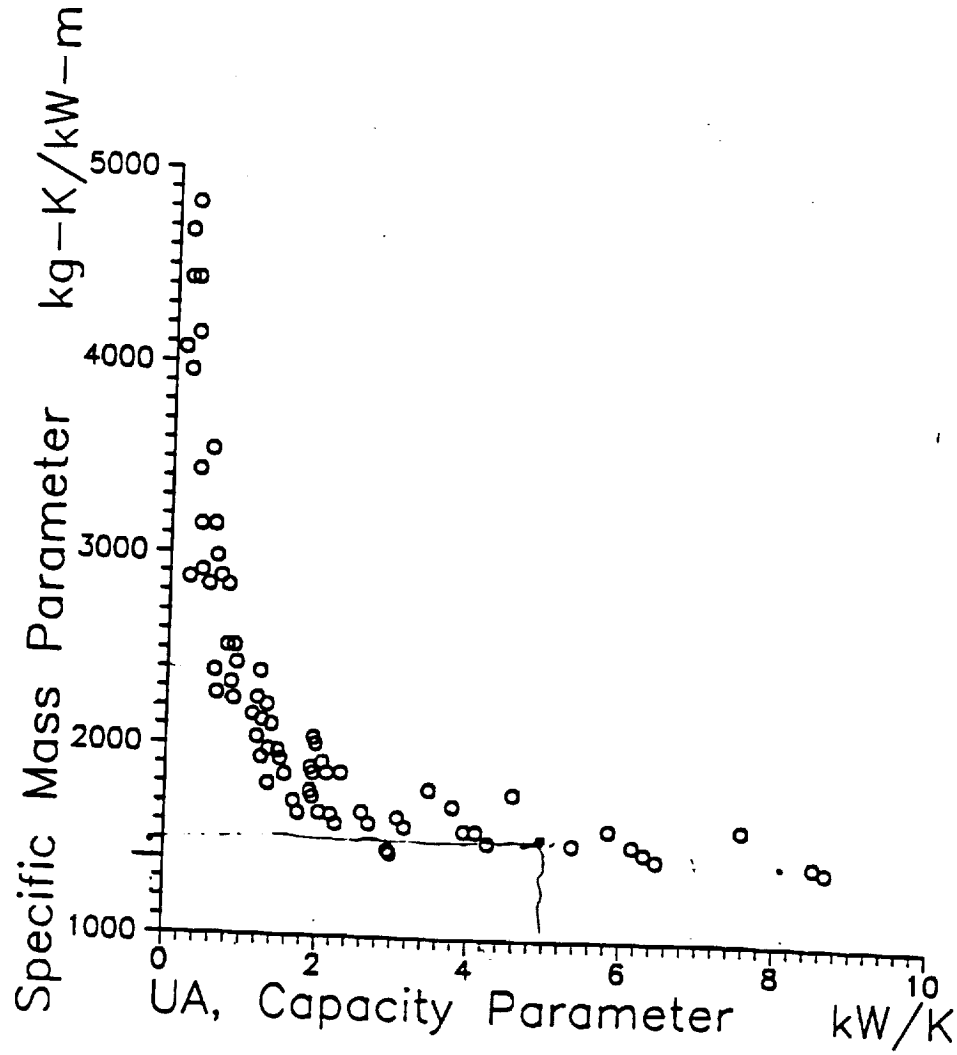
Specific Mass Parameter kg-K/kW-m
5000
4000
3000
2000
1000
0
2
4
6
8
10
UA, Capacity Parameter kW/K

Figure F6-1 [6]

$$M_{hx} = \tilde{M} UA D_t = 14209.7 \times 0.025\,m$$

$$\boxed{M_{evap} = 355\ kg}$$

1st Stage COMPRESSOR

$$M_{cp} = 19 + 0.7(hp) \quad \text{(from ref.)}$$

$$M_{(lb)} = 19 + 0.7\left(20.4 \times 10^3\ W \times \frac{1\ hp}{746\ W}\right)$$

$$= 36.6\ lb \times \frac{1\ kg}{2.2\ lb}$$

$$\boxed{M_{Comp} = 17.34\ kg}$$

INTERSTAGE EVAPORATOR CONDENSER

$$UA = 5.145\ \frac{KW}{K} \quad \text{(as calc. in App. F2)}$$

From figure F6-1, $\tilde{M} = 1500\ \frac{kg\,K}{KW\,m}$

$$M_{hx} = \tilde{M} UA D_t = 1500\ \frac{kg\,k}{KW\text{-}m} \times 5.165\ \frac{KW}{K} \times 0.025\,m$$

$$\boxed{M_{hx} = 193.7\ kg.}$$

2nd Stage COMPRESSOR

$$M_{cp} = \left[19 + 0.7\left(32.5 \times 10^3\ W \times \frac{1\ hp}{3746\ W}\right)\right] \frac{1}{2.2}$$

$$\boxed{M_{comp} = 22.5\ kg}$$

RADIATOR EVAPORATOR/CONDENSER 1

$UA = 8.1 \frac{kW}{K} \Rightarrow \tilde{M} = 1400 \frac{kg\text{-}K}{kW\text{-}m}$

$M_{hx} = 1400 \frac{kg\,K}{kW\,m} \times 8.4 \times 0.025 m$

$\boxed{M_{evap/cond} = 294 \text{ kg}}$

RADIATOR EVAPORATOR CONDENSER 2

$UA = 12.6 \frac{kW}{K}$ (see App. F2)

$\tilde{M}$ = 1400 $\frac{kg\,K}{kW\,m}$, from fig F6-1

$M_{hx} = 1400 \frac{kg\text{-}K}{kW\text{-}m} \times 12.6 \frac{kW}{K} \times 0.025 m$

$\boxed{M_{hx} = 441 \text{ kg}}$

MASS OF PIPING

estimated length of pipes = 60 m.

volume = 0.042 m^3 (assume D_t = 30mm)

assume titanium pipes, 30mm Diam

$m = \frac{8}{17} \times 60 m =$

$= \boxed{28 \text{ kg}}$

MASS OF WORKING FLUID

estimated pipe length = 60 m

volume = 0.042 m^3

$m = \rho V = 1350 \frac{kg}{m^3} \times .042 m^3 \approx 60 kg$

MASS OF PUMPS + ACCUMULATORS

estimated = 20 kg

MASS OF TRANSPORT SYSTEM

Evaporator	355 kg
1st Stage Compressor	17 kg
Evap / Condenser	193 kg
Accumulator (Loop1)	4 kg
Compressor (2nd)	23 kg
Radiator Evap. 1	294 kg.
Accumulator (Loop2)	5 kg.
Radiator Evap 2	441 kg
Pump (Outer Loop)	3 kg
Working Fluid	60 kg
Piping	28
Total Mass	1423 kg

APPENDIX G1

DESIGN OF REFLUX BOILERS

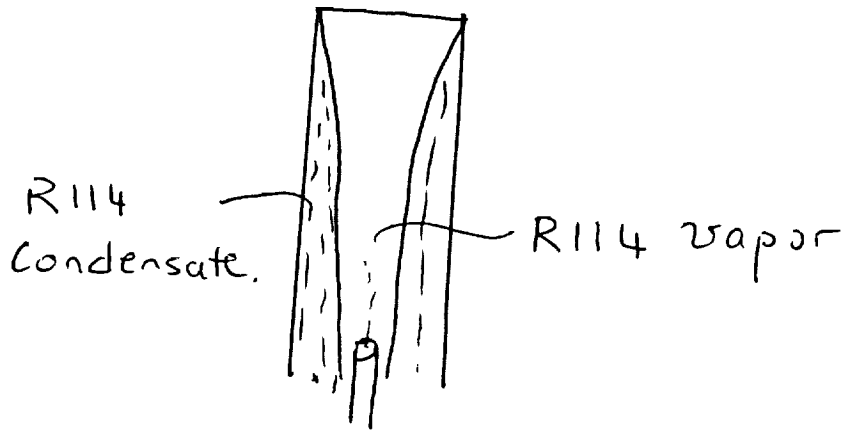

Maximum heat load at night = 74 KW

heat flux radiated = heat flux Condensed

$$\varepsilon\sigma\left(T_{rad}^4 - T_{sink}^4\right) = \bar{h}_L\left(T_{sat} - T_{rad}\right)$$

where

$$\bar{h}_L = .943\left[\frac{g\rho_l(\rho_l-\rho_v)k_l^3 h'_{fg}}{\mu_l(T_{sat}-T_{rad})L}\right]^{1/4}$$

where

$\bar{h}_L$ is the condensation heat transfer coefficient.

ρ_l = density of liquid

K_l = thermal conductivity of liquid

$h'_{fg} = h_{fg}$ (assumed) = latent heat of vaporization

μ_l = viscosity of liquid

$$\varepsilon \sigma (T_{rad}^4 - T_{sink}^4) = \bar{h}_L (T_{sat} - T_{rad})$$

$\Rightarrow$

$$0.8(5.67\times10^{-8})(T_{rad}^4 - T_{sink}^4)$$

$$\doteq .943 \left[\frac{g\rho_l(\rho_l-\rho_v)k_l^3 h_{fg}}{\mu_l (T_{sat}-T_{rad})L}\right]^{1/4}(T_{sat}-T_{rad})$$

$$\Rightarrow \frac{g\rho_l(\rho_l-\rho_v)k_l^3 h_{fg}}{\mu_l (T_{sat}-T_{rad})L} = \left[\frac{(0.8)(5.67)(10^{-8})(T_{rad}^4 - T_{sink}^4)}{(.943)(T_{sat}-T_{rad})}\right]^4$$

$$\Rightarrow L = \left[\frac{(g\rho_l(\rho_l-\rho_v)k_l^3 h_{fg})(T_{sat}-T_{rad})^3}{\mu_l[(4.8\times10^{-8})(T_{rad}^4 - T_{sink}^4)]^4}\right]$$

$$L = \frac{1.63[\rho_l(\rho_l-\rho_v)]k_l^3 h_{fg}(T_{sat}-T_{rad})^3}{\mu_l[(4.8\times10^{-8})(T_{rad}^4 - T_{sink}^4)]^4} \quad \text{—(1)}$$

T_{sat} = Saturation temperature of vapor

T_{rad} = surface temperature of radiator.

L = length of condensate film.

Evaluate all properties at saturation temperature (3 radiator temps)

$T_{sat} = -10°C$: $\rho_v = 4.68\ kg/m^3$

$\rho_\ell = 1521.4\ kg/m^3$

$\mu_\ell = 566.3 \times 10^{-6}\ Pa \cdot s$

$h_{fg} = 129.3 \times 10^3\ J/kg$

$K_\ell = 74.5 \times 10^{-3}\ W/mK$

$c_{p,\ell} = 0.923 \times 10^3\ J/kg\,K$

$T_{sat} = 50°C$: $\rho_v = 32.57\ kg/m^3$

$\rho_\ell = 1373.4\ kg/m^3$

$\mu_\ell = 265 \times 10^{-6}\ Pa \cdot s$

$K_\ell = 57 \times 10^{-3}\ W/mK$

$h_{fg} = 158.78\ J/kg$

$c_{p\ell} = 1.064 \times 10^3\ J/kg\,K$

$T_{sat} = 100°C$: $\rho_v = 108.48\ kg/m^3$

$\rho_\ell = 1167.5\ kg/m^3$

$h_{fg} = 183.36 \times 10^3\ J/kg$

$\mu_\ell = 170 \times 10^{-6}\ Pa \cdot s$

$K_\ell = 43 \times 10^{-3}\ \frac{W}{mK}$

$c_{p,\ell} = 1.19 \times 10^3\ J/kg\,K$

The radiator area is found using eqn below:

$$A_{radiator} = \frac{q\ [88, 109, \text{or } 126]}{4.531 \times 10^{-8} (T_{rad}^4 - T_{sink}^4)}$$

Find width of radiator 'b'

$$b = \frac{A}{l}$$

Using eqn 1, the length was varied in order to find the variation of temperature difference (between vapor and wall) with radiator length.

The mass flow rate of the condensate can be related to condensate film by

$$\frac{\dot{m}_l}{b_{\text{width}}} = \frac{g \rho_l (\rho_l - \rho_v)}{3 \mu_l} \left[\frac{4 k_l \mu_l (T_{sat} - T_s) \chi}{g \rho_l (\rho_l - \rho_v) h_{fg}} \right]^{3/4}$$

Radiator temp (K)	Length (m)
263	0
262.95	0.017
262.9	0.134
262.85	0.454
262.6	8.75
262.5	17.196

Checking For Sonic Flow Limitations:

The sonic flow limit occurs when the heat load transported up the reflux boiler is greater than or equal to $Q_{s,max}$, where

$$Q_{smax} = A_v \rho_o h_{fg} \left[\frac{\gamma_v R T_o}{2(\gamma_v + 1)} \right]^{1/2}$$

where

γ_v = ratio of specific heats

T_o is stagnation temp (temperature of vapor at velocity of 0 = temp at liquid-vapor interface.

ρ_o = vapor density.

Since the vapor is R114, and since the equation assumes a perfect gas, the following equation is used. This equation accounts for nonideal gases.

$$q'' = 0.5 h_{fg} (\rho_o P_o)^{1/2}$$

$\rho_o = \rho_v$

$P_o = P_{sat}$

q'' is evaluated for three different radiator temperatures.

T_{sat} (°C)	ρ_v (kg/m^3)	h_{fg} (J/kg)	C_p	R	P(MPa)
-10	4.68	129.3×10^3	.69	48.6	.058
50	32.57	158.8×10^3	.76	48.6	.448
100	108.5	183.4×10^3	.8	48.6	1.419

$$q'' = 0.5\, h_{fg} (\rho_v P_v)^{1/2}$$

CASE I :

$$q'' = 0.5 \times 129.3 \times 10^3 \frac{J}{kg} \times (4.68 \times .058 \times 10^6)^{1/2}$$

$$= 33.68 \frac{MW}{m^2}$$

CASE II :

$$q'' = 0.5 \times 158.8 \times 10^3 (32.57 \times .448 \times 10^6)^{1/2}$$

$$= 303.4\ MW/m^2$$

CASE 3

$$q'' = 0.5 \times 183.4 \times 10^3 \times (108.5 \times 1.419 \times 10^6)^{1/2}$$

$$= 1138\ MW/m^2.$$

minimum area reqd = $\frac{\text{max ht load}}{q''}$

$$= \frac{90 \times 10^3\ W}{33.68 \times 10^6\ W/m^2}$$

$$A_{min} = 2.67 \times 10^{-2}\ m^2.$$

Cross sectional area must be greater than this value.

Checking for Entrainment Limit

The vapor velocity is limited by a critical point at which the vapor shear causes such a high drag force that the condensate does not return down the tube. The critical vapor velocity is

$$v_g = \frac{C^2 \left[g D_H \left(\rho_l / \rho_g - 1 \right) \right]^{1/2}}{\left[1 + \left(\dot{m}_l / \dot{m}_g \right)^{1/2} \left(\rho_g / \rho_l \right)^{1/4} \right]^2} \quad \rightarrow (1)$$

$$C^2 = 0.53 F_1 F_2$$

$F_2 = 1$ for square ended tubes

$$F_1 = \left(\frac{\sigma}{\sigma_w} \right)^{0.5} = \left(\frac{\sigma}{0.072\ N/m} \right)^{0.5}$$

$$\sigma_{R114} = 12 \times 10^{-3}\ N/m.$$

$$F_1 = \left(\frac{12 \times 10^{-3}\ N/m}{0.072\ N/m} \right)^{0.5} = 0.1666$$

$C^2 = 0.0883$

$g = 1.635\ m/s^2$

$D_H = \frac{4A_c}{P}$

Cross sectional area

(based on sonic limits)

Assume: 20 modular radiators.

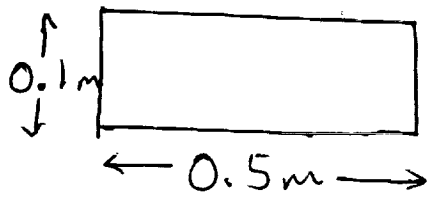

overall.

$A_c = 0.05\ m^2$ $P = 1.2\ m$

length, $L = 17.25\ m$

$\rho_g = 108.5\ kg/m^3$

$A_J = 0.05m \times 0.5m = .025m \times 20_{rad}$

$A_{TOT} = .5m^2$.

$\dot{m}_{TOT} = \rho_v A_{TOT} v_g = 0.687\ kg/s$

$v_{g\,actual} = \frac{0.687\ kg/s}{108.48\ \frac{kg}{m^3} \times 0.5m^2} = .0126\ \frac{m}{s}$

$v_{g\,flooding} = \frac{.0833\left[1.635 \times .166 \times 9.8\right]^{1/2}}{\left[1 + \left(\frac{\dot{m}_L}{.0343}\right)^{1/2} 0.55\right]^2}$

↑ on a per radiator basis

$$\frac{\dot{m}_{l\,per\,rad}}{b} = 6.6425 \times 10^{-3} \times^{3/4}$$

$$\dot{m}_l = 0.5 \times 6.6425 \times 10^{-3} \times (17.25)^{3/4}$$

$$\dot{m}_l = 0.02811$$

put back into ①,

$$v_{g_{flood}} = 0.046\ m/s$$

So flooding <u>limit is NOT reached.</u>

$$\delta(x) = \left[\frac{4 \times 43 \times 10^{-3} \times 170 \times 10^{-6} \times 1 \times 17.25}{2019462.9 \times 183.4 \times 10^{3}}\right]^{1/4}$$

$$= 0.2\ mm.$$

$Re_L = 658.8$ => wavy flow

APPENDIX G2

TEMPERATURE CONTROL ANALYSIS FOR HEAT REJECTION SYSTEM

The heat rejection capability of radiators for stagewise operation is shown below.

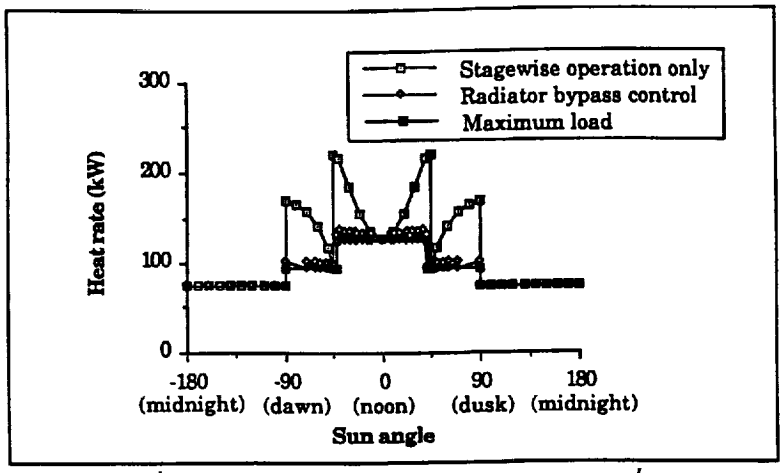

The radiators over reject heat even at maximum heat load. The bypass radiator concept is suggested.

Radiator bypass Concept

Radiator area = $345\ m^2$

# of radiators = 20

$\therefore$ area per radiator = $17.25\ m^2$

Max. heat loads – night operation = 74 kW
single stage operation - 94 kW
two stage operation - 126 kW

Night operation

The sink temperature does not vary at night. also from the graph, it can be seen that the radiators do not over reject heat. Therefore radiators need not be by passed at night.

Single stage operation

The sink temperature varies between 85 K and 264.3 K

From By passing radiators, areas available for heat rejection are from 0 to 345 m^2 in steps of 17.25 m^2

using equation

$$q = \varepsilon \cdot \sigma \cdot A \left(T_{rad}^4 - T_{sink}^4\right)$$

The sink temperature at which the radiator can reject the maximum load for various areas available was determined.

$$T_{sink} = \left[T_{rad}^4 - \frac{q}{\varepsilon \cdot \sigma \cdot A}\right]^{1/4} \quad \text{——— (1)}$$

$A = [345 - (17.25)(n)]$ where $n = 1 - 20$

Using equations ① and ②

the number of radiators to be ~~determined~~ operated at different times of the single stage operation and two stage operation were determined.

The results of this analysis are presented below.

# of radiators in operation		sink temperature Range
20	night operation	85 K
12	single stage operation	89 – 172
13		172 – 201
14		201 – 219
15		219 – 231.5
16		231.5 – 241
17		241 – 248.6
18		248.6 – 254.9
19		254.7 – 259.9
20		259.9 – 264.3
12	two stage operation	264.3 – 272.6
13		272.6 – 284.6
14		284.6 – 293.7
15		293.7 – 301
16		301 – 306.98
17		306.9 – 312.0
18		312 – 316
19		316 – 319
20		319 – 323

Using this information the heat rejection capability of the radiator was determined.

The sun angle corresponding to a sink temperature was calculated by using equation

$$T_{sink} = \left[1.614\times10^{8}\sin\theta + 2.18\times10^{8}\sin\theta + .48\,T_{moon}^{4}\right]^{1/4}$$

This equation is derived in appendix C1

The graph of heat rejection Vs. sun angle is shown below. the data to plot this curve is also given.

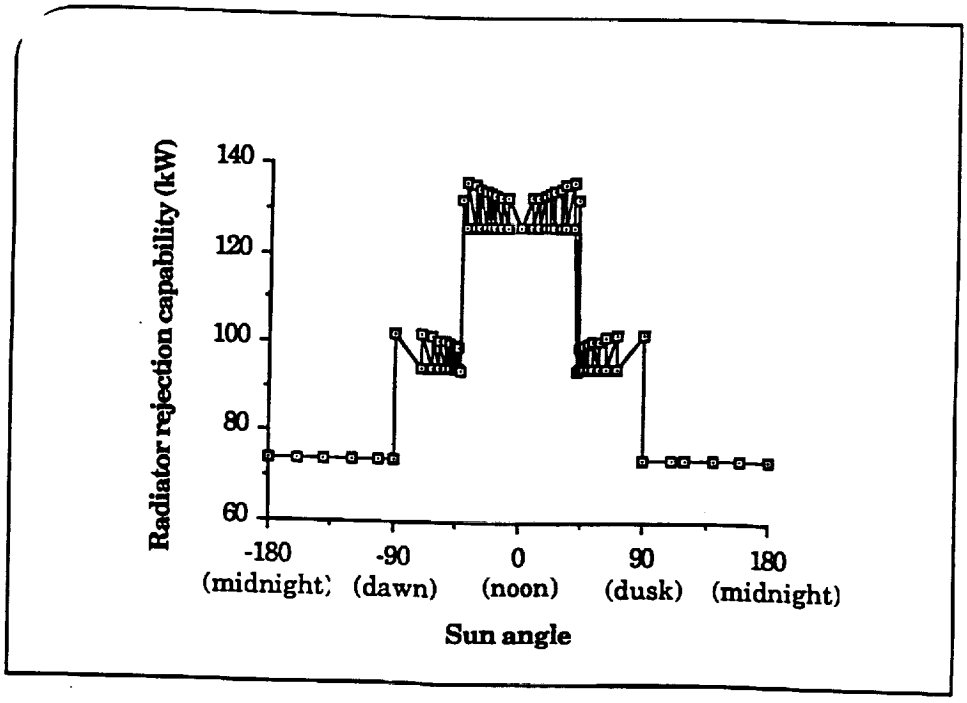

rejected (	sun angle
74.058	-180.000
74.058	-170.000
74.058	-160.000
74.058	-150.000
74.058	-140.000
74.058	-130.000
74.058	-120.000
74.058	-110.000
74.058	-100.000
74.058	-90.000
101.713	-90.000
99.253	-80.000
94.020	-70.000
101.833	-70.000
94.000	-62.000
101.231	-62.000
98.878	-60.000
94.000	-57.500
100.714	-57.500
94.000	-52.500
100.267	-52.500
94.620	-50.000
94.000	-49.500
99.875	-49.500
94.000	-47.000
99.530	-47.000
94.001	-45.000
99.223	-45.000
94.000	-43.000
98.948	-43.000
93.972	-41.500
132.067	-41.500
129.150	-40.000
125.997	-38.500
136.345	-38.500
125.860	-33.000
135.693	-33.000
128.511	-30.000
126.000	-29.000
134.908	-29.000
125.914	-24.500
134.414	-24.500
126.001	-21.500
133.762	-21.500
131.500	-20.000
125.892	-18.000
133.411	-18.000
125.998	-13.000
132.998	-13.000
127.894	-10.000
125.998	-8.500
132.629	-8.500
126.140	0.000
74.058	180.000
74.058	170.000
74.058	160.000

heat rejected (	sun angle
74.058	150.000
74.058	140.000
74.058	130.000
74.058	120.000
74.058	110.000
74.058	100.000
74.058	90.000
101.713	90.000
99.253	80.000
94.020	70.000
101.833	70.000
94.000	62.000
101.231	62.000
98.878	60.000
94.000	57.500
100.714	57.500
94.000	52.500
100.267	52.500
94.620	50.000
94.000	49.500
99.875	49.500
94.000	47.000
99.530	47.000
94.001	45.000
99.223	45.000
94.000	43.000
98.948	43.000
93.972	41.500
132.067	41.500
129.150	40.000
125.997	38.500
136.345	38.500
125.860	33.000
135.693	33.000
128.511	30.000
126.000	29.000
134.908	29.000
125.914	24.500
134.414	24.500
126.001	21.500
133.762	21.500
131.500	20.000
125.892	18.000
133.411	18.000
125.998	13.000
132.998	13.000
127.894	10.000
125.998	8.500
132.629	8.500

Inert gas requirement : Worst cases for inert gas requirement are considered.

1. when heat load is minimum at night

$q = 12\,kW$

Radiator area required $= \frac{12 \times 10^3}{\varepsilon \cdot \sigma \cdot (T_{rad}^4 - T_{sink}^4)}$

$= 60\,m^2$

As each radiator provides $17.25\,m^2$ of area

no. of radiators needed $= 4$.

only 4 radiators should be capable of providing any intermediat area between 0 and $17.25\,m^2$

area reduction for each radiator $= 4.3125\,m^2$

to get any required area for any heat load inbetween the maximum and minimum heat.

There should be enough inert gas which is capable to reduce the area of each radiator by $4.3\,m^2$.

Single stage operation

Minimum heat load = 15kW

$T_{sink} = 85\,K$

$$A = \frac{15 \times 10^3}{(.8)(5.67 \times 10^{-8})(325^4 - 85^4)}$$

$A = 30.5$

∴ two radiators are required.

the two radiators provide an area of $34.5\ m^2$.

∴ $4\ m^2$ reduction in area is required by the radiators.

The worst case occurs when a heatload that requires an area of just above $34.5\ m^2$, 3 radiators will be required. Therefore, 3 radiators must be able to provide an area just above $34.5\ m^2$ therefore, each radiator must be able to reduce its area to $\frac{34.5}{3}$

$= 11.5\ m^2$.

Two stage operation

$q_{min} = 20 \times 10^3$ watts, $T_{sink} = 264.3$ K.

Area required $= \frac{20 \times 10^3}{\cdot 8 (5.67 \times 10^{-8})(371^4 - 284.3^4)}$

$= 31.32 \text{ m}^2$

∴ the worst case is the same as for single stage operation.

From this analysis - the amount of inert gas to be stored in each radiator should be enough to reduce the area of each radiator from $17.25^- + 11.25 \text{m}^2$

Analysis for proving the advantage of Bypassing radiators.

If radiators not bypassed, at worst case, $q_{min} = 15 \times 10^3$, $T_{sink} = 85$ K

required area $= 30.5^- \text{m}^2$

As 20 radiators will be operation.

Each radiator must reduce to 1.725^-m^2

An area reduction of $18^-.25^- \text{m}^2$ as opposed in air of $5^-.75^-$ when radiators are bypassed.

APPENDIX G3

MASS AND POWER CALCULATIONS FOR HEAT REJECTION SYSTEM

The major components the constitute the mass of the rejection system are

1. Radiators

   specific mass = 3kg/m² of radiating area.

   surface area = (5)(345) = 1725 kg.

2. Piping

   As shown in appendix E6,

   specific mass of piping = .471 g/m.

   length of piping = 30 meters

   total mass of piping = 14 kg.

3. Working fluid.

   Density of R114 = 1480 kg/m³

Volume of working fluid = Volume in pipes + volume along the walls of the radiator.

$$= \frac{\pi}{4} D^2 l + l(b)(h)$$

$$= \frac{\pi}{4} (.03)^2 (30) + (345)(.2 \times 10^{-4})$$

$$= .021 + .069$$

Total mass of working fluid

$$= (1450)(.021 + .069)$$

$$= 130 \text{ kg}.$$

∴ total mass of 186.9 kg.

The power required to run the pump is about .3 kW.